

เอกซเรย์ดิฟแฟรกชันของสารประกอบเชิงซ้อนบาราคอล



นางสาวปิติพร ฉิมสุข

สถาบันวิทยบริการ

จุฬาลงกรณ์มหาวิทยาลัย

วิทยานิพนธ์นี้เป็นส่วนหนึ่งของการศึกษาตามหลักสูตรปริญญาวิทยาศาสตรมหาบัณฑิต

สาขาวิชาเคมี ภาควิชาเคมี


คณะวิทยาศาสตร์ จุฬาลงกรณ์มหาวิทยาลัย

ปีการศึกษา 2546

ISBN 974-17-3934-6

ลิขสิทธิ์ของจุฬาลงกรณ์มหาวิทยาลัย

X-RAY DIFFRACTION OF BARAKOL COMPLEXES



Miss. Pitiporn Chimsook

สถาบันวิทยบริการ  
จุฬาลงกรณ์มหาวิทยาลัย

A Thesis Submitted in Partial Fulfillment of the Requirements  
for the Degree of Master of Science in Chemistry

Department of Chemistry

Faculty of Science

Chulalongkorn University

Academic Year 2003

ISBN 974-17-3934-6

Thesis Title X-ray diffraction of barakol complexes  
By Miss. Pitiporn Chimsook  
Field of Study Chemistry  
Thesis Advisor Assistant Professor Nongnuj Muangsin, Ph.D.  
Thesis Co-advisor Assistant Professor Nattaya Ngamrojnavanich, Ph.D.

---

Accepted by the Faculty of Science, Chulalongkorn University in Partial  
Fulfillment of the Requirement for the Master's Degree

..... Dean of Faculty of Science  
(Professor Piamsak Menasveta, Ph.D.)

Thesis Committee

..... Chairman  
(Professor Sophon Roengsumran, Ph.D.)

..... Thesis Advisor  
(Assistant Professor Nongnuj Muangsin, Ph.D.)

..... Thesis Co-advisor  
(Assistant Professor Nattaya Ngamrojnavanich, Ph.D.)

..... Member  
(Associate Professor Amorn Petsom, Ph.D.)

..... Member  
(Assistant Professor Thawatchai Tuntulani, Ph.D.)

ปิติพร นิมสุข : เอกซเรย์ดิฟแฟรคชันของสารประกอบเชิงซ้อนบาราคอล

(X-RAY DIFFRACTION OF BARAKOL COMPLEXES) อ. ที่ปรึกษา : ผศ. ดร. นงนุช

เหมืองสิน, อ.ที่ปรึกษาร่วม : ผศ. ดร. นาดยา งามโรจนวณิชย์; 84 หน้า ISBN 974-17-3934-6

วิทยานิพนธ์นี้นำเสนอการหาโครงสร้างผลึกของสารประกอบแอนไฮโดรบาราคอลและแอนไฮโดรบาราคอลคลอไรด์ที่ไม่เคยมีการรายงานมาก่อน แอนไฮโดรบาราคอลและแอนไฮโดรบาราคอลคลอไรด์ตกผลึกในระบบโมโนคลินิก สเปซกรุ๊ป  $P2_1/c$  และ  $P2_1/n$ ,  $Z = 4$  ที่มีขนาดยูนิตเซลล์เท่ากับ  $a = 13.2280(7)$ ,  $b = 6.8738(2)$ ,  $c = 19.7879(9)$  Å,  $\beta = 127.013(2)^\circ$  และ  $a = 12.2547(2)$ ,  $b = 8.051(2)$ ,  $c = 12.8133(2)$  Å,  $\beta = 99.514(1)^\circ$  ตามลำดับ สารประกอบเชิงซ้อนชนิดใหม่ของบาราคอล กับกรดคาร์บอกซิลิก (กรดพธาลิกและกรด3-ไฮดรอกซีเบนโซอิก) ได้เตรียมขึ้นและพิสูจน์เอกลักษณ์ด้วยเทคนิคสเปกโตรสโคปี และเอกซเรย์คริสตัลโลกราฟี และได้ศึกษาผลของอิเล็กโตรสแตติก, การเคลื่อนที่ของอิเล็กตรอน และอันตรกิริยาระหว่างโมเลกุลในระบบภายในวงของบาราคอล จากการศึกษาด้วยเทคนิคเอกซเรย์คริสตัลโลกราฟีแสดงให้เห็นว่าสารประกอบเชิงซ้อนของบาราคอล-กรดพธาลิกเป็นสารประกอบเชิงซ้อนแบบคู่ออออน (ion-pair complex) การรวมตัวของสารประกอบเชิงซ้อนแบบคู่ออออนระหว่างบาราคอล-กรดพธาลิก ถูกทำให้เสถียรได้ด้วยแรงระหว่างไอออน อันตรกิริยาแบบ  $\pi-\pi$  และพันธะไฮโดรเจน สารประกอบเชิงซ้อนของบาราคอล-กรด 3-ไฮดรอกซีเบนโซอิกเป็นสารประกอบเชิงซ้อนแบบ  $\pi-\pi$  การตกผลึกรวมของบาราคอลกับกรด3-ไฮดรอกซีเบนโซอิก ถูกทำให้เสถียรโดยอันตรกิริยาแบบ  $\pi-\pi$  จากการศึกษาด้วยเทคนิคสเปกโตรสโคปี ได้แก่ IR,  $^1\text{H-NMR}$  และ UV-vis, พบว่าให้ผลการทดลองที่สอดคล้องกับผลการทดลองที่ได้จากเทคนิคเอกซเรย์คริสตัลโลกราฟี จากสเปกตรัม  $^1\text{H-NMR}$  ของสารประกอบเชิงซ้อนของบาราคอล-กรดพธาลิกในของผสม  $\text{CDCl}_3\text{-CD}_3\text{OD}$  แสดงให้เห็นถึงการเปลี่ยนแปลงสเปกตรัมอย่างชัดเจนโดย ออร์โธ-โปรตอนของกรดพธาลิก ( $\Delta\delta_{\text{H}}(\text{ppm}) = 0.37$ ) และโปรตอนของบาราคอลเคลื่อนที่แบบควาน์ฟิลด์ ( $\Delta\delta_{\text{H}}(\text{ppm}) = 0.31$  สำหรับโปรตอน H3, 0.53 สำหรับโปรตอน H4, 0.57 สำหรับโปรตอน H6 และ 0.33 สำหรับโปรตอน H9)

ภาควิชา.....เคมี..... ลายมือชื่อนิสิต.....

สาขาวิชา.....เคมี..... ลายมือชื่ออาจารย์ที่ปรึกษา.....

ปีการศึกษา.....2546.....ลายมือชื่ออาจารย์ที่ปรึกษาร่วม.....

# # 4472330423 : MAJOR CHEMISTRY

KEY WORD: X-RAY DIFFRACTION/ BARAKOL/ SPECTROSCOPIC METHOD.

PITIPORN CHIMSOOK : X-RAY DIFFRACTION OF BARAKOL  
COMPLEXES. THESIS ADVISOR : ASSIST. PROF. NONGNUJ  
MUANGSIN, Ph.D. THESIS COADVISOR : ASSIST. PROF.  
NATTAYA NGAMROJNAVANICH, Ph.D. 84 pp.ISBN 974-17-3934-6.

This thesis presents the first successful crystal structure determination of anhydrobarakol and anhydrobarakol hydrochloride. Anhydrobarakol and anhydrobarakol hydrochloride were crystallized in a monoclinic system, space group  $P2_1/c$  and  $P2_1/n$ ,  $Z = 4$  with unit cell parameters  $a = 13.2280(7)$ ,  $b = 6.8738(2)$ ,  $c = 19.7879(9)$  Å,  $\beta = 127.013(2)^\circ$  and  $a = 12.2547(2)$ ,  $b = 8.051(2)$ ,  $c = 12.8133(2)$  Å,  $\beta = 99.514(1)^\circ$ , respectively. The novel 1:1 molecular complexes of barakol and carboxylic acid (phthalic acid and 3-hydroxybenzoic acid) were synthesized and characterized by spectroscopic and X-ray crystallographic techniques. Electrostatic effects, electron delocalization, and intermolecular interactions in the barakol ring system were investigated. The X-ray crystallographic studies revealed that the barakol-phthalate complex exists in an ion-pair complex. The formation of barakol-phthalate ion-pair complex is stabilized by the complementary of ion-ion interaction,  $\pi$ - $\pi$  interaction and hydrogen bonding. The barakol-3-hydroxybenzoic acid complex is a  $\pi$ - $\pi$  molecular complex. The co-crystallization of barakol-3-hydroxybenzoic acid complex is solely stabilized by  $\pi$ - $\pi$  interactions. The spectroscopic studies including IR,  $^1\text{H-NMR}$  and UV-visible are consistent with the results from the X-ray analysis. The  $^1\text{H-NMR}$  spectrum of the barakol and phthalic acid complex in a mixture of  $\text{CDCl}_3$ - $\text{CD}_3\text{OD}$  showed a dramatic spectral changes with downfield shifts of the *ortho*-protons of phthalic acid ( $\Delta\delta_{\text{H}}(\text{ppm}) = 0.37$ ), and the proton resonances of barakol ( $\Delta\delta_{\text{H}}(\text{ppm}) = 0.31$  for proton H3, 0.53 for proton H4, 0.57 for proton H6 and 0.33 for proton H9).

Department.....CHEMISTRY.....Student's signature.....

Field of study..... CHEMISTRY.....Advisor's signature.....

Academic year.....2003.....Co-advisor's signature.....

## ACKNOWLEDGEMENTS

I wish to express highest appreciation to my thesis advisor, Assist. Prof. Dr. Nongnuj Muangsin and my thesis co-advisor, Assist. Prof. Dr. Nattaya Ngamrojnavanich For their invaluable guidance, kind supervision, profound assistance, encouragement and Suggestions the way to be good in study, research and chemistry. In addition, I would like To thank and pay my respect to Prof. Dr. Sophon Roengsumran, Assoc. Prof. Dr. Amorn Petsom and Assist. Prof. Dr. Thawatchai Tuntulani for their valuable suggestions and comments as committee members and thesis examiners.

Moreover, I would like to thank Assoc. Prof. Dr. Narongsak Chaichit, (Thammasart University), Assist. Prof. Dr. Chavang pakavatchai (Prince Songkla University) and Assist. Prof. Dr. Palangpol Kongsaree (Mahidol University) for X-ray Diffraction data collections. The supramolecular Chemistry Research Unit for UV-visible Spectrophotometer and Assist. Prof. Dr. Sanong Ekgasit for IR spectrophotometer.

My appreciation would be expressed to all of my friends and colleagues for their Helps and encouragement throughout my study. Finally, I would like to express my Deepest gratitude to my parents and family for their love kindness, encouragement, and Financial support throughout my life.

I also thank to Chulalongkorn University and the Development and Promotion of Science and Technology Talents Project of Thailand (DPST) and Research Centre for Bioorganic Chemistry (RCBC) for financial supports and giving the opportunity to study, laboratory facilities, chemicals and equipments.

# CONTENTS

	page
Abstract in Thai.....	iv
Abstract in English.....	v
Acknowledgement.....	vi
List of Figures.....	ix
List of Tables.....	xi
List of Schemes.....	xiii
List of Abbreviation and Symbols.....	xiii
<b>CHAPTER 1 INTRODUCTION.....</b>	<b>1</b>
1.1 Barakol.....	1
1.2 The chemical nature of barakol and its derivatives.....	2
1.3 Intermolecular interaction.....	2
1.4 Barakol complexes.....	5
1.5 Objective .....	6
<b>CHAPTER 2 INTRODUCTION TO X-RAY CRYSTALLOGRAPHY.....</b>	<b>7</b>
<b>CHAPTER 3 EXPERIMENTS.....</b>	<b>16</b>
3.1 General Procedures.....	16
3.1.1 Analytical Instrument.....	16
3.1.2 Materials.....	17
3.2 Extraction of barakol.....	17
3.3 Preparation of barakol complexes.....	19

	<b>page</b>
3.3.2 barakol-salicylic acid complex.....	19
3.3.4 barakol – phthalic acid complex.....	19
3.3.5 barakol – 3-hydroxybenzoic acid complex.....	19
<b>CHAPTER 4 RESULTS AND DISCUSSION.....</b>	<b>20</b>
4.1 Barakol.....	20
4.2 Barakol-salicylic acid (BA).....	22
4.3 Anhydrobarakol hydrochloride(BC).....	30
4.4 Barakol-Phthalic acid (BP).....	38
4.5 Barakol-3-hydroxybenzoic acid (BH).....	48
<b>CHAPTER 5</b>	
<b>CONCLUSION.....</b>	<b>58</b>
<b>REFERENCES.....</b>	<b>63</b>
<b>APPENDIX.....</b>	<b>67</b>
<b>VITA.....</b>	<b>84</b>

สถาบันวิทยบริการ  
จุฬาลงกรณ์มหาวิทยาลัย



## LIST OF FIGURES

<b>Figures</b>	<b>Page</b>
1.1 The feature of Khi-lek tree.....	2
1.2 Chemical structures of barakol, anhydrobarakol and anhydrobarakol Hydrochloride.....	2
3.1 Barakol extraction and purification procedures.....	18
4.1 Chemical structure of barakol and anhydrobarakol with atomic numbering.....	21
4.2 Chemical structure of anhydrobarakol (BA) with atomic numbering.....	24
4.3 An ORTEP drawing of BA, showing 50% probability displace ellipsoids.....	27
4.4 (a) Crystal packing of anhydrobarakol (BA), view along <i>a</i> -axis, hydrogen atoms were omitted for clarity (b) hydrogen bonding of BA with water.....	27
4.5 Keto-enol form of anhydrobarakol.....	28
4.6 <sup>1</sup> H-NMR spectra of barakol, salicylic acid and barakol-salicylic acid mixture...30	30
4.7 Chemical structure of anhydrobarakol hydrochloride(BC) • H <sub>2</sub> O with atomic numbering.....	32
4.8 An ORTEP drawing of BC, showing 50% probability displace ellipsoids.....	35
4.9 Crystal packing of anhydrobarakol hydrochloride(BC), view along <i>a</i> -axis, hydrogen atoms were omitted for clarity.....	35
4.10 Infinite chain of hydrogen bonding in anhydrobarakol hydrochloride.....	36
4.11 Chemical structure of barakol cation and phthalate, with atomic numbering ...	40
4.12 An ORTEP drawing of BP, showing 50% probability displace ellipsoids.....	43
4.13 Crystal packing of barakol phthalate(BP), view along <i>a</i> -axis, hydrogen atoms were omitted for clarity.....	43
4.14 $\pi$ - $\pi$ interaction of barakol-phthalate (BP).....	44
4.15 UV-spectrum of anhydrobarakol, phthalic acid and BP complex.....	45
4.16 <sup>1</sup> H-NMR spectra of barakol, phthalic acid and BP complex.....	46
4.17 <sup>1</sup> H-NMR titration of the mixture of barakol and phthalic acid at various ratios.....	47
4.18 Chemical structure of anhydrobarakol and 3-hydroxybenzoic acid, with atomic numbering.....	50
4.19 An ORTEP drawing of BH, showing 50% probability displace ellipsoids.....	53

<b>Figures</b>	<b>Page</b>
4.20 Crystal packing of barakol -3-hydroxybenzoic acid(BH), view along <i>a</i> -axis, hydrogen atoms were omitted for clarity .....	54
4.21 $\pi$ - $\pi$ interaction of barakol-3-hydroxybenzoic acid (BH).....	54
4.22 UV-spectrum of barakol, 3-hydroxybenzoic acid and BH.....	55
4.23 Compared $^1\text{H}$ -NMR spectra of anhydrobarakol, 3-hydroxybenzoic acid and BH.....	57
5.10 ORTEP structure of (a) anhydrobarakol (b) anhydrobarakol hydrochloride (c) barakol-phthalic Acid (BP) (d) barakol-3-hydroxybenzoic acid (BH).....	59
A.1 The UV spectrum of extracted barakol in ethanol.....	75
A.2 The IR spectrum of barakol in KBr.....	75
A.3 The $^1\text{H}$ -NMR spectrum of extracted barakol in $\text{CDCl}_3$ .....	76
A.4 The $^{13}\text{C}$ -NMR of extracted barakol in $\text{CDCl}_3$ .....	76
A.5 The Mass spectrum of extracted barakol in $\text{CDCl}_3$ .....	77
B.1 The UV spectrum of anhydrobarakol in ethanol.....	77
B.2 The IR spectrum of anhydrobarakol in KBr.....	78
B.3 The $^1\text{H}$ -NMR spectrum of anhydrobarakol in $\text{CDCl}_3+\text{CD}_3\text{OD}$ .....	78
C.1 The UV spectrum of anhydrobarakol hydrochloride (BC) in ethanol.....	79
C.2 The IR spectrum of anhydrobarakol hydrochloride (BC) in KBr.....	79
C.3 The $^1\text{H}$ -NMR spectrum of anhydrobarakol hydrochloride in $\text{CDCl}_3$ .....	80
C.4 The $^{13}\text{C}$ -NMR of anhydrobarakol hydrochloride in $\text{CDCl}_3$ .....	80
D.1 The IR spectrum of barakol-phthalic acid (BP) in KBr.....	81
D.2 The $^1\text{H}$ -NMR spectrum of phthalic acid in $\text{CDCl}_3+\text{CD}_3\text{OD}$ .....	81
D.3 The $^1\text{H}$ -NMR spectrum of barakol-phthalic acid (BP) in $\text{CDCl}_3+\text{CD}_3\text{OD}$ .....	82
E.1 The IR spectrum of barakol-3-hydroxybenzoic acid in KBr.....	82
E.2 The $^1\text{H}$ -NMR spectrum of 3-hydroxybenzoic acid (BH) in $\text{CDCl}_3+\text{CD}_3\text{OD}$ ....	83
E.3 The $^1\text{H}$ -NMR spectrum of barakol-3-hydroxybenzoic acid (BH) in $\text{CDCl}_3+\text{CD}_3\text{OD}$ .....	83

## LIST OF TABLES

Tables	Page
4.1 IR absorption bands of extracted barakol.....	20
4.2 NMR chemicalshifts(ppm) of barakol(1) and barakol(2) (Bycroft) <sup>6</sup> .....	21
4.3 Mass spectrum data of extracted barakol and barakol reported by Bycroft <sup>6</sup> .....	22
4.4 Crystal and experimental data of BA.....	25
4.5 Bond lengths (Å) and angles (°) of BA.....	26
4.6 IR data of anhydrobarakol (BA).....	29
4.7 <sup>1</sup> H-NMR spectra data (δ ppm) for anhydrobarakol (BA).....	30
4.8 Crystal and experimental data of BC.....	33
4.9 Bond lengths (Å) and angles (°) of BC.....	34
4.10 UV-vis data of anhydrobarakol hydrochloride (BC) in ethanol and Anhydrobarakol hydrochloride (Bycroft) <sup>6</sup> in ethanol.....	37
4.11 IR data of anhydrobarakol hydrochloride (BC) and anhydrobarakol hydrochloride (Bycroft) <sup>6</sup> .....	37
4.12 <sup>1</sup> H-NMR chemical shift (ppm) of anhydrobarakol hydrochloride(BC) and barakol hydrochloride (Bycroft) <sup>6</sup> .....	38
4.13 Crystal and experimental data of BP.....	41
4.14 Bond lengths (Å) and angles (°) of BP.....	42
4.15 UV-vis data of barakol, 3-hydroxybenzoic acid and BH in ethanol.....	44
4.16 Selected IR and <sup>1</sup> H-NMR data for barakol, phthalic acid and BP complex.....	45
4.17 Crystal and experimental data of BH.....	51
4.18 Bond lengths (Å) and angles (°) of BH.....	52
4.19 UV-vis data of barakol, 3-hydroxybenzoid acid and BH.in ethanol.....	55
4.20 Selected IR and <sup>1</sup> H-NMR data for barakol, 3-hydroxybenzoic acid BH complex .....	56
5.1 Comparison of acid strength (pK <sub>a</sub> ) barakol complexes and types of barakol of barakol ring.....	60
5.2 Summarized X-ray crystallographic results of anhydrobarakol Barakol hydrochloride , the complexes of barakol with pthalic acid and 3-hydroxybenzoic acid.....	61

<b>Tables</b>	<b>Page</b>
A.1 Fractional atomic coordinates ( $\times 10^4$ ) and equivalent isotropic displacement Parameters ( $\text{\AA}^2 \times 10^3$ ) for anhydrobarakol. $U_{eq}$ is defined as one third of the Trace of the orthogonalized $U_{ij}$ .....	68
A.2 Hydrogen-bond lengths ( $\text{\AA}$ ) for anhydrobarakol (BA).....	69
B.1 Fractional atomic coordinates ( $\times 10^4$ ) and equivalent isotropic displacement Parameters ( $\text{\AA}^2 \times 10^3$ ) for anhydrobarakol hydrochloride. $U_{eq}$ is defined as one third of the Trace of the orthogonalized $U_{ij}$ .....	70
B.2 Hydrogen-bond lengths ( $\text{\AA}$ ) for anhydrobarakol hydrochloride (BC).....	70
C.1 Fractional atomic coordinates ( $\times 10^4$ ) and equivalent isotropic displacement Parameters ( $\text{\AA}^2 \times 10^3$ ) for barakol-phthalate (BP). $U_{eq}$ is defined as one third of the Trace of the orthogonalized $U_{ij}$ .....	71
C.2 Hydrogen-bond lengths ( $\text{\AA}$ ) for barakol-phthalate (BP).....	72
D.1 Fractional atomic coordinates ( $\times 10^4$ ) and equivalent isotropic displacement Parameters ( $\text{\AA}^2 \times 10^3$ ) for barakol-3-hydroxybenzoic acid. $U_{eq}$ is defined as one third of the Trace of the orthogonalized $U_{ij}$ .....	73
D.2 Hydrogen-bond lengths ( $\text{\AA}$ ) for barakol- 3-hydroxybenzoic acid (BH).....	74

## LIST OF SCHEMES

Schemes	Page
1.1 The chemical structures of barakol, anhydrobarakol and anhydrobarakol hydrochloride.....	2
2.1 A flowchart for the steps involved in a crystal structure determination.....	10



สถาบันวิทยบริการ  
จุฬาลงกรณ์มหาวิทยาลัย

## LIST OF ABBREVIATIONS AND SYMBOLS

$\delta$	Chemical shift
$J$	Coupling constant
$^{\circ}\text{C}$	Degree Celsius
Equiv	Equivalent
Hz	Hertz
mp	Melting point
mmol	Millimol
ml	Mililiter
M	Molar
ppm	Part per million
s,d,t,m	Splitting patterns of $^1\text{H-NMR}$ (singlet, doublet, triplet and multiplet)
BA	Anhydrobarakol
BC	Anhydrobarakol hydrochloride
BP	Barakol-phthalate complex
BH	Barakol-3-hydroxybenzoic acid

สถาบันวิทยบริการ  
จุฬาลงกรณ์มหาวิทยาลัย

## CHAPTER I

### Introduction

#### 1.1 Barakol

*Cassia siamea* is a plant widely cultivated in Southeast Asia (Figure 1.1). The different parts of the plant have been used as Thai traditional medicines<sup>12-13</sup>, for example, for treatment of insomnia and various other medical conditions such as diabetes, hypertension, asthma, constipation and diuresis. *Cassia siamea* shows the physiological and pharmacological properties on the cardiovascular and central nervous systems<sup>4</sup>.

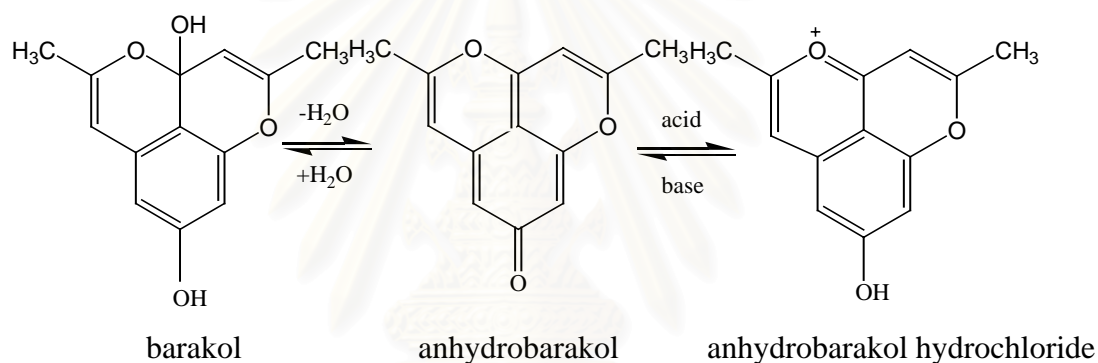
Barakol (3a,4-dihydro-3a,8-dihydroxy-2,5-dimethyl-1,4-dioxaphenalene or 2,5-dimethyl-3 $\alpha$ H-pyrano[2,3,4-de]-1-benzopyran-3a,8-diol) (Figure 1.2), major active constituent extracted from the leaves and flowers of *Cassia siamea*, was first extracted in 1969 by Hassanali-Walji *et al*<sup>5-6</sup>. It has been reported that barakol displays a non-sedative anxiolytic effect in the elevated plus-maze test, and reduced K<sup>+</sup>-stimulated release of endogenous dopamine<sup>7-9</sup> in striatal slice of the tested animals. However, Fiorino D. F. reported that barakol showed no evidence of its anxiolytic effects in either the plus-maze or the shock-probe test<sup>10-11</sup>. Furthermore, Bengsri *et al.* and Sukma *et al.* reported that barakol are not equivalent to the binding sites of 5-HT and GABA receptors<sup>12</sup>, which were in agreement with that reported by Fiorino D. F.



**Figure 1.1** Features of Khilek tree (*Cassia siamea*)

## 1.2 The Chemical Nature of Barakol and its derivatives

Barakol ( $C_{13}H_{12}O_4$ ) is a natural compound consists of a chromone hemiacetal (Figure 1.2), therefore barakol is unstable even in ambient conditions due to a hemiacetal group easily protonated, and then loses water from its molecule to become anhydrobarakol. Anhydrobarakol is the methylene quinone derivative; it decomposes at  $165^\circ\text{C}$ . In hydroxylic solvents or aqueous solutions, anhydrobarakol can be reversed to barakol. Barakol is very rapidly degraded by base. In acidic conditions, barakol and anhydrobarakol can be converted to a relatively stable anhydrobarakol salt, for example anhydrobarakol bromide<sup>5</sup> and anhydrobarakol chloride<sup>6</sup>. They are stable at room temperature and in dried condition.



**Scheme 1.1** Chemical structures of barakol, anhydrobarakol and anhydrobarakol hydrochloride<sup>6</sup>

## 1.3 Intermolecular interactions

Molecular structure and intermolecular interactions play important factors for studying biological activity of drugs. Examples of structural properties are conformation, flexibility, geometry and shape<sup>13</sup>. Examples of binding properties are electron distribution and intermolecular interactions, including electrostatic interactions (ion-ion, dipole-dipole and dipole-induce dipole interactions), hydrogen bonding, and  $\pi$ - $\pi$  interactions. The non-covalent interactions association of molecules is of central importance in biology and pharmacology. Very common are interactions of small molecules with proteins (ligand-receptor interactions) and protein-protein interactions. The relationships between the molecular structures and key-lock principle are important but they are not enough. Other properties, such as



electrostatics or hydrophobicity are of prime importance for intermolecular interaction. In other words, the 3D arrangement of dispersion, electrostatic and hydrophobic interaction, as well as hydrogen bonding, determines the strength of intermolecular interactions.

### 1.3.1 Hydrogen bonding

Hydrogen bonding is depicted as A-H---B where A and B are strongly electronegative, such as C, O or N (strong hydrogen bonding) or Cl, F, or S (weak hydrogen bonding). The B atom is usually a  $\sigma$  or  $\pi$  electron donor (Lewis base). The strength of a hydrogen bond is dependent on the electronegativity of A and B (acidity of the proton in HA and basicity of B), molecular geometry and steric effects<sup>14</sup>. Hydrogen bonds can be categorized as strong or weak according to properties such as bond distances, bond energy and bond angles. If H---B distances are between 1.2 to 1.5 Å, bond angles are about 180° and the bond energy is not less than 40 kJ mol<sup>-1</sup>, the hydrogen bond are classified as strong. There are many methods of studying hydrogen bonding, such as NMR, IR and X-ray diffraction techniques, but the most popular techniques is X-ray or neutron diffraction<sup>15</sup>. For a crystalline solid X-ray diffraction data provides the position and vibration of all atoms in the unit cell. From this knowledge, atomic distances, angles and molecular motion can be determined. If there is hydrogen bonding, A-H---B, the H---B distance should be less than the sum of the van der Waals radii of atoms H and B.

Possible hydrogen bond distance ranges in A-H---B system, (Å)

A-H---B	A---B ranges, Å	A-H---B	A---B ranges, Å
O-H---N	2.6-3.0	O-H---O	2.4-3.2
N-H---F	2.6-3.0	long	3.2-2.8
O-H---F	~2.7	medium	2.8-2.65
O-H---Cl	3.0-3.2	short	2.65-2.4

There are two main types of hydrogen bonding: intramolecular and intermolecular interactions<sup>16,17</sup>. Intramolecular interactions occurs when a proton donor and acceptor forms hydrogen bonding within a same molecule. Intermolecular hydrogen bonding leads to the formation of dimers, chains or three-dimensioned networks.

Intermolecular hydrogen bonding makes crystals more stable and is manifested as higher melting points, solubility and as frequency shifts in IR bands.

### 1.3.2 $\pi$ - $\pi$ interactions

$\pi$ - $\pi$  interactions play an important part in biological structures capable of molecular recognition and also in self-assembling macromolecules. They also feature in the packing of aromatic molecules in crystals, conformational preferences and binding properties of polyatomic macrocycles and complexation in many host-guest systems<sup>17-20</sup>. A simple model of the charge distribution in a  $\pi$ -system is used to explain the strong geometrical requirements for interactions between aromatic molecules. Strong attractive interactions between  $\pi$ -systems have been known for over half a century. They control such diverse phenomena as the vertical base-base interactions stabilize the double helical structure of DNA, the interaction of drugs into DNA, the packing of aromatic molecules in crystals and complexation in many host-guest systems.

Two main models are used to interpret  $\pi$ - $\pi$  interactions, namely charge transfer (CT) and polar/ $\pi$  (coulomb) effects :-

1. Charge transfer: When two  $\pi$  aromatic systems have different substituent group; one electron-withdrawing and the other electron donating, charge transfer effects dominate.
2. Coulomb effect: When both  $\pi$  systems contain electron withdrawing groups coulomb effects become most important. The  $\pi$ - $\pi$  interaction is stronger when  $\pi$ -electron density is lower as a result of a lower repulsion between the  $\pi$ -shells in a face-to-face geometry.

The geometry between interacting  $\pi$  systems and the dihedral angle between the phenyl moieties is an important factor in assisting or impeding  $\pi$ - $\pi$  interactions. Planar aromatic molecules are known to interact with one another in three possible ways; namely stack (face-to-face), offset stack and herring bone (T-shape or edge-to-face). The face-to-face overlap results in the closet C---C contact. Hunter *et al*<sup>21</sup>. used the 3.4 to 4.8 Å distances of two separated aromatic rings as a criterion for studying  $\pi$ - $\pi$  interactions.

#### 1.4 Barakol complexes

Heterocycles containing sulfur and/or nitrogen atoms or containing one oxygen atom have been widely studied. They are useful as components of functional materials, play an important role in biological functions and chemical reactions. However, heterocyclic systems containing two oxygen atoms are rarely studied. Barakol, a biologically active substance and consisting of dioxophenalene ring, is an interesting example for studying its physical and chemical properties including its crystal structure and intermolecular interactions.

The heterocycles containing oxygen atoms, since heteroatoms in their rings are helpful to stabilize ions or ion-radical species. In addition intermolecular interactions caused by heteroatom contacts can be expected to form novel molecule assemblies.

Interactions between aromatic rings play an important role in molecular complexes. A number of inter-ring geometries have been identified ranging from a parallel face-to-face, or stacking to perpendicular edge-to-face orientation in which positively charged H atoms on the upper ring interact with negatively charged regions on a lower ring.<sup>22</sup>

The phthalic acid and the phthalate ion are a small carboxylate ligand that has special relevance to environmental chemists and geochemists. Carboxylate groups are capable of binding a metal in either a monodentate, bidentate or bridging mode leading to both mono- and polynuclear molecular and polymeric structures. In addition, the orientation of carbonyl group in *o*-phthalic acid was interested in the carboxylate complexes<sup>16,17</sup>. In the known structures of phthalic acid, intramolecular and intermolecular hydrogen bond was occurred in the complexes. Moreover, the effects of delocalization in aromatic systems and in symmetrical molecular entities in which a lone pair of electrons are particularly evident the presence of an ion-pair complex.

The 3-hydroxybenzoic acid composes of hydroxy group and carboxylic group in *meta*-position. Moreover, the planar structure of 3-hydroxybenzoic acid help to stabilize the structure of barakol in the same way as phthalic acid. The role of good proton donor of 3-hydroxybenzoic acid is to co-crystallize with barakol.

In this work, new molecular complexes based on O-heterocycles such as barakol and carboxylic acid were co-crystalized, for examples, phthalic acid and 3-

hydroxybenzoic acid. The planar molecules of the both components usually take a crystal structure which stack along a certain direction.

### 1.5 Objective

The chemical, physical, and biological properties of barakol have been previously reported. However, these reports, including NMR and IR spectroscopic data, are inconsistent. Also, its crystal structure, the key information for understanding biological properties has never been reported. Therefore, to understand its pharmacological properties and to develop it to pharmaceutical products, we need more information about its molecular structure to find its functional role in a biological system and its physicochemical properties. The aim of this work is to determine the crystal structures and chemical-physical properties of anhydrobarakol and barakol hydrochloride and barakol complexes with carboxylic acid by synthesis, recrystallization and characterization using elemental analysis, UV-vis, FT-IR,  $^1\text{H}$ -NMR and X-ray crystallography.



## CHAPTER 2

### Introduction to X-ray crystallography

#### Single crystal X-ray diffraction.

X-ray diffraction from crystalline solids occurs as a result of the interaction of X-rays with the electron charge distribution in the crystal lattice. The ordered nature of the electron charge distribution, whereby most of the electrons are distributed around atomic nuclei which are regularly arranged with translational periodicity, means that superposition of the scattered X-ray amplitudes will give rise to regions of constructive and destructive interference producing a diffraction pattern<sup>23,24</sup>.

The pattern of scattered X-rays can be directly recorded, either on photographic film or on a variety of other X-rays sensitive detectors, then the recombination which is impossible physically can be performed mathematically, with the aid of computers. The components of the material which interact with the incident X-rays and scatter them. These are the electrons in the atoms. Concentrations of electron density in the image correspond to atoms, somewhat spread out by time averaged vibration, and the results are usually interpreted and presented as atomic positions.

The source of X-rays is an 'X-ray tube'. The most commonly used X-ray tube target materials are copper and molybdenum, which give characteristic X-rays of wavelengths 1.54184 and 0.71073 Å, respectively.

In principle, then, the process of crystal structure determination is simple. We record the diffraction pattern from a crystal. Measurement of the diffraction pattern geometry and symmetry tells us the unit cell geometry and gives some information about the symmetry of arrangement of the molecules in the unit cell. Then from the individual intensities of the diffraction pattern, The process of working out the atoms in the unit cell, adding together the individual waves with their correct relative amplitudes and phases. The phase problem was seen because the measured diffraction pattern provides directly only the amplitudes and not the required phases.<sup>25,26</sup>

The diffraction maxima are sometimes individually considered to be the result of diffraction of the incident X-rays beam of wavelength from crystal lattice planes, having Miller indices  $hkl$  and spacing  $d_{hkl}$ . Diffraction occurs at an angle of incidence equal to the Bragg angle  $\theta_B$ , i.e. Bragg's law is obeyed:

$$\lambda = 2d_{hkl} \sin \theta_B \quad \text{----- (1)}$$

The intensities of diffraction pattern and the arrangement of atoms in the unit cell of the crystal structure are related to each other by Fourier transformation: the diffraction pattern is the Fourier transform of the electron density, and the electron density is itself the Fourier transform of the diffraction pattern.

### The forward Fourier transform ( the diffraction experiment )

The diffraction pattern is the Fourier transform (FT) of the electron density. In mathematics:

$$F_{hkl} = \int_{\text{cell}} \rho(xyz) \cdot \exp [2\pi i (hx + ky + lz)] dV \quad \text{----- (2)}$$

The structure factor (amplitude and phase) for reflection hkl is given by taking the value of the electron density at each point in the unit cell,  $\rho(xyz)$ . Multiplying it by the complex number  $\exp [2\pi i (hx + ky + lz)]$  and adding up (integrating over the whole cell volume,  $\int_{\text{cell}} \dots dV$ ) these values. The variation of intensity with angle is called the atomic scattering factor,  $f(\theta)$ .

Atom in crystalline solids, however, are not stationary; they vibrate to an extent which depends on the temperature and this effectively spreads out the atomic electron density and increase the interference effects. For an atom which vibrates equally in all directions (isotropic vibration), the effect is to multiply the atomic scattering factor by a term containing an isotropic displacement parameter ( $U$ ).  $U$  has units  $\text{\AA}^2$ .

With discrete atoms instead of a continuous electron density function, the forward Fourier transform takes the form

$$F(hkl) = \sum_j f_j(\theta) \cdot \exp(-8\pi^2 U_j \sin^2 \theta / \lambda^2) \cdot \exp[2\pi i (hx_j + ky_j + lz_j)] \quad \text{-----}$$

(3) j

The summation is made over all the atoms in the unit cell, each of which has its appropriate atomic scattering factor  $f_j$  (a function of Bragg angle  $\theta$ ), a displacement parameter  $U_j$  and coordinates  $(x_j, y_j, z_j)$  relative to the unit cell origin..

### The reverse Fourier transform (the recombination calculation)

The electron density is the reverse Fourier transform ( $FT^{-1}$ ) of the diffraction pattern<sup>29</sup>.

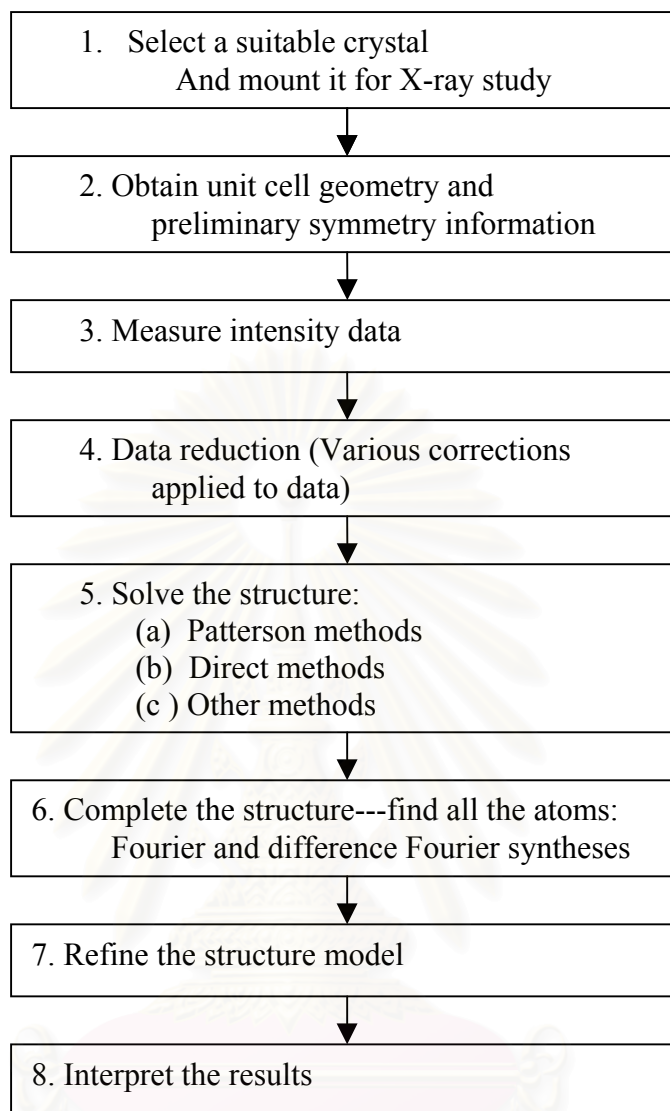
$$\rho(xyz) = \frac{1}{V} \sum_{hkl} F(hkl) \cdot \exp[-2\pi i (hx + ky + lz)] \quad \text{-----(4)}$$

Or

$$\rho(xyz) = \frac{1}{V} \sum_{hkl} |F(hkl)| \cdot \exp[i\phi(hkl)] \cdot \exp[-2\pi i (hx + ky + lz)] \quad \text{-----(5)}$$

1            2        3                    4                    5

$F(hkl)$  is a complex number, containing both amplitude and phase information. The image of the electron density (1), which originally generated the diffraction pattern, is obtained by adding together (2) all the diffracted beams, with their correct amplitudes (3) and phases (4, 5). ; the correct relative phases here include the intrinsic phases of the waves themselves, relative to the original incident beam (4), and an extra phase shift appropriate to each geometrical position in the image relative to the unit cell origin (5). The relative phase shifts can be calculated as required, but the intrinsic phases  $\phi(hkl)$  of the different reflections are unknown from the diffraction experiment. This means that it is not possible simply to calculate the reverse Fourier transform once the diffraction pattern has been measured.



**Scheme 2.1** A flowchart for the steps involved in a crystal structure determination.<sup>24</sup>

### The measurement of intensities

The data collection procedure include the maximum Bragg angle to be measured and whether to measure only the unique set of data.

The result of this process from whatever equipment is used, is a list of reflections, each with  $hkl$  indexed and a measured intensity. In addition, from diffractometer measurements, each intensity  $I$  has an associated standard uncertainty (s.u.,  $\sigma(I)$ ), which is calculated from the known statistical properties of the X-ray generation and diffraction processes, and is a measure of the position or reliability of the measurement.



### Data reduction

The intensity of an X-ray beam is proportional to the square of the wave amplitude ( $I(hkl) \propto |F(hkl)|^2$ ). The measured intensity is affected by applied. The conversion of intensities  $I$  to 'observed structure amplitudes'  $|F_o|$  ( $o = \text{observed}$ ) or  $F_o^2$  and correspondingly, of s.u.'s  $\sigma(I)$  to  $\sigma(F_o)$  or  $\sigma(F_o^2)$  is known as data reduction and has several components. There is also a correction needed because reflected radiation is partially polarized. These geometrical corrections, known as Lorenz-polarization factors, are well known and easily made.

Where absorption effects are significant a further correction must be made. Each reflection is affected differently by absorption, because the absorption depends on the path length of the X-rays through the crystal.

The data reduction process also includes the merging and averaging repeated and symmetry-equivalent measurements in order to produce unique, corrected and scaled set of data.<sup>28,29</sup>

At the same time, statistical analysis of the complete unique data set can provide an indication of the complete unique data set can provide an indication of the presence or absence of some symmetry elements, particularly whether the structure is centro symmetric or not, though this is not infallible, and the observed overall decay of intensity with increasing  $(\sin\theta/\lambda)$  gives an average atomic displacement parameter.

### Solving the structure

Having measure and appropriately corrected the diffraction data, we turn now to the solution of the structure; in which we obtain atomic positions in the unit cell from the data.

$$\rho(xyz) = \frac{1}{V} \sum_{hkl} |F(hkl)| \cdot \exp [ i\phi(hkl) ] \cdot \exp [ -2\pi i (hx + ky + lz) ] \quad \text{-----(6)}$$

The amplitudes  $|F(hkl)|$  have been measured, the final exponential term can be calculated for the contribution of each reflection  $hkl$  to each position  $xyz$ , but the

phases of the reflections are unfortunately unknown so the calculation cannot be carried out immediately. So the Fourier transform of the observed diffract beam amplitudes  $|F_o|$  gives the correct electron density, but it requires knowledge of the phases of all the reflections.

The two methods which seek to obtain approximate reflection phases are the Patterson method and direct methods

### The Patterson synthesis

The Patterson map looks rather like an electron density map. Patterson function is a map of vectors between pairs of atoms in the structure. In such cases it is usually possible to find a self-consistent set of atomic positions for the heavy atoms which explain the large Patterson peaks<sup>24</sup>.

### Direct methods

Direct method is method which seek to obtain approximate reflection phases from the measured intensities with no other information available.<sup>24</sup>.

The electron density is the Fourier transform of the diffraction pattern. This means we add together a set of waves in order to produce the electron density distribution. Direct method involve selecting the most important reflections, working out the probable relationships among their phases then trying different possible phases to see how well the probability relationships are satisfied. For the most promising combinations, Fourier transforms are calculated from the observed amplitudes and trial phases, and are examined for recognizable molecular features. So various methods are usually necessary to try many different sets of phases and use the relationships themselves to 'refine' or improve them.

### Completing the basic structure

Using the forward Fourier transform equation (the mathematical representation of the scattering process), we can calculate what the diffraction pattern would be if this model structure were, infact, the correct complete structure:

$$\text{Model structure} \xrightarrow{\text{FT}} \text{set of } F_c \text{ ----- (7)}$$

Where  $F_c$  are calculated structure factors, one corresponding to each observed structure factor  $F_o$ . The calculation provides values for the amplitudes and phases of  $F_c$  ( $|F_c|$  and  $\phi_c$ ) whereas we have only amplitudes for  $F_o$  ( $|F_o|$ , no  $\phi_o$ ). If the atoms of the model structure are approximately in the right positions, there should be at least some degree of resemblance between the calculated diffraction pattern and the observed one, i.e. between the sets of  $|F_c|$  and  $|F_o|$  values. The two sets of values can be compared in various ways. The most widely used assessment is a so-called residual factor or R-factor defined as

$$R = \frac{\sum | |F_o| - |F_c| |}{\sum |F_o|} \text{ ----- (8)}$$

Variation on this definition include using  $F^2$  values instead of  $|F|$  values, squaring the differences, and/or incorporating different weighting factors multiplying different reflections, based on their s.u.'s and hence incorporating information on the relative reliability of different measurements.

$$wR2 = \frac{\sum w (F_o^2 - F_c^2)^2}{(\sum w (F_o^2)^2)^{1/2}} \text{ ----- (9)}$$

$wR2$  is the conventional name for this residual factor. The  $w$  indicates that weights are included, and the 2 indicates that  $F^2$  values are used rather than  $F$  values.

Where each reflection has its own weight ( $w$ ). This is in many ways and certainly from a statistical viewpoint, more meaningful than the basic R factor. For a correct and complete crystal structure determined from well measured data, R is typically around 0.02 – 0.07; for an initial model structure it will be much higher, possibly 0.4-0.5 depending on the fraction of electron density so far found, and its decrease during the next stages is a measure of progress.

### Refining the structure

Once all the non-hydrogen atoms have been found, the model structure needs to be refined. This means varying the numerical parameters describing the structure to produce the ‘best’ agreement between the diffract pattern calculated from it by a Fourier transform and the observed diffraction pattern. The refinement process uses a well-established mathematical procedure called least-squares analysis, which defines the ‘best fit’ of two sets of data (here  $|F_o|$  and  $|F_c|$ ) to be that which minimizes one of the least-squares sums

$$\begin{aligned} & \Sigma w (|F_o| - |F_c|)^2 \\ \text{or } & \Sigma w (F_o^2 - F_c^2)^2 \end{aligned} \quad \text{----- (10)}$$

The least-squares refinement of crystal structure is similar, in principle, to finding a ‘best fit’ straight line through a set of points on a graph. Each least-squares calculation is approximate, not exact, giving an improvement to the model, but not the best possible fit; the calculation must be repeated several times until eventually the changes in the parameters are insignificant.

As well as providing a value for each refined parameter, the least-squares process also gives a standard uncertainty. These parameter s.u.’s depend on the s.u.’s of the data (a good structure requires good data).

WinGX is a MS-Windows system of programs for solving, refining and analysing single crystal X-ray diffraction data for small molecules<sup>27</sup>. WinGX uses SHELX format ASCII files. It has interfaces to other popular programs such as SHELXL-97<sup>28</sup> and SIR-97.

### SHELXS - Structure Solution.

SHELXS<sup>28</sup> is primarily designed for the solution of ‘small moiety’ (1-200 unique atoms) structures from single crystal at atomic resolution, but is also useful for the location of heavy atoms from macromolecular isomorphism or anomalous  $\Delta F$  data.

Before starting SHELXS, at least one file *-name.ins-* must have been prepared; it contains instructions, crystal and atom data etc. It will usually be necessary to prepare a *name.hkl* file as well which contains the reflection data; the format of this file is the same as for all versions of SHELX. After structure solution a file *name.res* is written; this contains crystal is written; this contains crystal data etc. as in the *name.ins* file, followed by potential atoms. It may be copied or edited to *name.ins* for structure refinement using SHELXL or partial structure expansion with SHELXS.

### SHELXL-Structure refinement

SHELXL<sup>31</sup> is a program for the refinement of crystal structures from diffraction data and is primarily intended for single crystal X-ray data of small moiety structures. To run SHELXL only two input files are required (atom/instructions and reflection data); since both these files and the output files are pure ASCII text files. The reflection data file (*name.hkl*) contains  $h, k, l$   $F^2$  and  $\sigma(F^2)$  in standard SHELX format. Crystal data, refinements and atom coordinates are all input as the file *name.ins*.

สถาบันวิทยบริการ  
จุฬาลงกรณ์มหาวิทยาลัย

## CHAPTER 3

### Experiments

#### 3.1 General procedures

##### 3.1.1 Analytical Instrument

###### 3.1.1.1 Nuclear magnetic resonance spectroscopy (NMR)

$^1\text{H}$ -NMR at 400 MHz and  $^{13}\text{C}$ -NMR spectra at 100 MHz were recorded on a Varian Mercury+ spectrometer. All chemical shifts were reported in part per million (ppm) using the residual proton or carbon signal in deuterated solvents as internal references.

###### 3.1.1.2 Ultraviolet and visible spectrophotometry (UV-VIS)

UV-visible spectra were recorded on a Varian CARY 50 Probe UV-visible spectrophotometer. Wavelength is in the range of 200-800 nm and cell width is 1 cm.

###### 3.1.1.3 Fourier transform infrared spectrometry (FT-IR)

Fourier transform infrared spectra were recorded on a Nicolet FT-IR Impact 410 Spectrophotometer. The solid samples were prepared by pressing the sample with KBr. Infrared spectra were recorded between  $400\text{ cm}^{-1}$  to  $4000\text{ cm}^{-1}$  in Transmittance mode.

###### 3.1.1.4 Mass spectrometry (MS)

Mass spectra were recorded on a Agilent 110 Series LC/MSD Electrospray mass spectrometer.

###### 3.1.1.5 Elemental analysis (EA)

Elemental analysis were recorded on CHNS/O ANALYZER (PERKIN ELMER PE2400 SERIES II).

### 3.1.2 Materials

#### 3.1.2.1 Plant Materials

Fresh young leaves of Khilek (*Cassia siamea* Lamk.) were obtained from Dontum farm in Nakhonpathom province, Thailand in November 2002.

#### 3.1.2.2 Solvents and chemicals

All materials and solvents used in this research were standard analytical grade, purchased from Aldrich and Merck. They were used without further purification. Chloroform and methanol were distilled under reduced pressure.

### 3.2 Extraction of Barakol<sup>29</sup>

The barakol extraction and purification procedures of *Cassia siamea* Lamk are presented in Figure 3.1. Two kilograms of fresh young leaves and flowers of *Cassia siamea* Lamk. were sliced into small pieces, boiled with 4 liters of 0.5 % (v/v) aqueous sulfuric acid for 1 hour. It was then cooled to room temperature and filtered. The marc was re-boiled with 2 liters of 0.5 % (v/v) aqueous sulfuric acid, cooled and filtered. The filtrates were combined and basified with sodium hydrogen carbonate to pH 8-9. The basic solution was extracted with chloroform (300 ml) three times. The combined chloroform extracts were concentrated under reduced pressure until the volume was one-fourth of the starting volume, and mixed with the equal volume of distilled water. The mixture was shaken strongly by hand to allow precipitation of the yellow lemon needle crystals, then left the solution in a refrigerator overnight for complete precipitation. The yield was approximately 5 g. The mixture of chloroform and methanol (9:1) was employed as a solvent system in the TLC analysis. The crystals were recrystallized in 15% (v/v) methanol. The final yield of presumably barakol was approximately 3 g.

Barakol was dissolved in a minimum amount of methanol and the concentrated hydrochloric acid was later added. The presumed anhydrobarakol hydrochloride was slowly crystallized in yellow needle form.

The chemical structures of barakol and anhydrobarakol hydrochloride were characterized by spectroscopic study such as IR, UV-visible,  $^1\text{H-NMR}$ , MS.

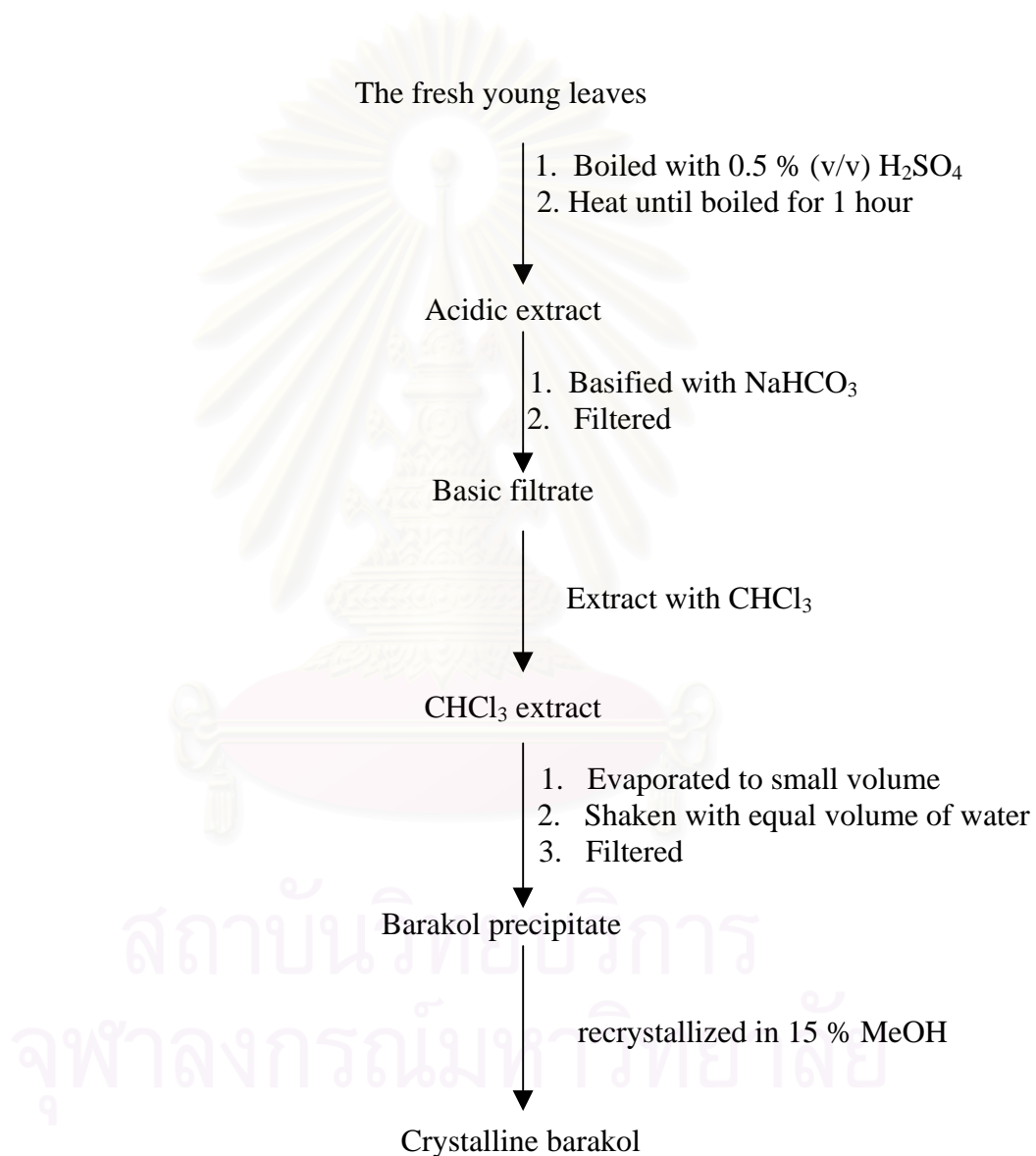


**Figure 3.1** The Barakol extraction and purification procedures<sup>29</sup>



### 3.3 Preparations of barakol complexes.

#### 3.3.1 Barakol - salicylic acid complex

The barakol (0.1 mmol) was added in the saturated solution of salicylic acid (0.5 mmol dissolved in 5 ml of hot absolute methanol). The yellow crystal was crystallized from methanol by slow evaporation<sup>30</sup>.

#### 3.3.2 Barakol - phthalic acid complex (BP)

The barakol (0.1 mmol) was added in the saturated solution of phthalic acid (0.5 mmol dissolved in 5 ml of hot absolute methanol). The yellow crystal was crystallized from methanol by slow evaporation<sup>30</sup>.

NMR titration: A solution of 0.005 M of barakol in  $\text{CDCl}_3$  and  $\text{CD}_3\text{OD}$  was prepared in an NMR tube. A solution of 0.005 M of phthalic acid in  $\text{CDCl}_3$  and  $\text{CD}_3\text{OD}$  was prepared in a vial. The solution of phthalic acid was added directly to the NMR tube by a microsyringe to have barakol : phthalic ratios (1:0, 0:1, 1:0.25, 1:0.5, 1:1 v/v).  $^1\text{H-NMR}$  spectras were recorded after each addition.

#### 3.3.3 Barakol - 3-hydroxybenzoic acid complex (BH)

The barakol (0.1 mmol) was added in the saturated solution of 3-hydroxybenzoic acid (0.5 mmol dissolved in 5 ml of hot absolute methanol). The yellow crystal was crystallized from methanol by slow evaporation<sup>30</sup>.

# CHAPTER 4

## Results and Discussion

### 4.1 Barakol

The extraction of shredded fresh young leaves and flowers of *Cassia siamea* Lamk. with 0.5% sulphuric acid followed by alkalization with sodium hydrogen carbonate gave 0.15% yield of pale lemon-yellow crystalline solid compound, presumably barakol.

The structure of yellow crystalline compound, presumably barakol (Figure 4.1) was characterized by TLC, UV-vis, FT-IR, NMR, mass spectroscopic data as following:

The R<sub>f</sub> value was 0.32, and 0.53 when using an aluminum plate as the absorbent and mixtures of chloroform and methanol (9:1) and chloroform and acetone (6:4) as solvent systems, respectively.

The UV-vis spectrum of extracted barakol (yellow crystalline compound) in ethanol (Figure A.1) showed the absorption bands at 242 (4.15), 250 (4.15) and 379 (3.76) nm. The numbers in parenthesis are log  $\epsilon$  (mol<sup>-1</sup>.cm<sup>-1</sup>.L)

The IR spectrum of extracted barakol (yellow crystalline compound) is shown in Figure.A.2 and the details of absorption peaks are given in Table 4.1. The spectrum showed broad absorption bands at 3295 and 3444 cm<sup>-1</sup> corresponding to an O-H stretching with the strong hydrogen bonding. The peak at 1676 cm<sup>-1</sup> was assigned to the  $\nu$ (C=O) stretching, indicating barakol is unstable and can be converted to anhydrobarakol (Figure 4.1).

**Table 4.1** IR absorption bands of extracted barakol (Figure A.2)

Compound	IR data (cm <sup>-1</sup> )		
	$\nu$ (O-H)	$\nu$ (C-O)	$\nu$ (C=O)
Barakol	3444 (s,b)	1188 (m)	1676(s)
	3295 (s,b)	1267 (m)	

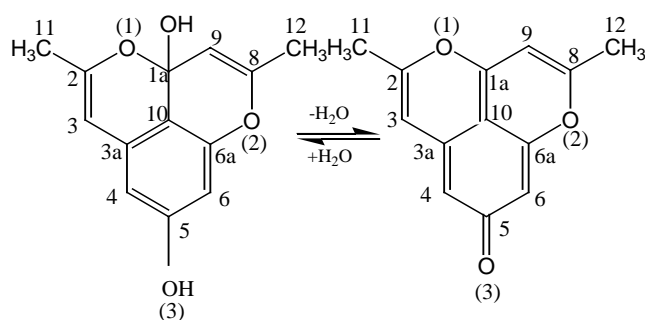


**Figure 4.1** Chemical structures of barakol and anhydrobarakol with atomic numbering.<sup>31-32</sup>

The  $^1\text{H-NMR}$  spectrum of extracted barakol (Table 4.2) indicated two methoxy groups attached to aromatic carbons (C2 and C8) at  $\delta_{\text{H}}$  2.23 and 2.38 ppm, four protons on aromatic ring (H3, H4, H6 and H9) at  $\delta_{\text{H}}$  6.33(1H), 6.33(1H), 6.44 (1H) and 6.11(1H) ppm, respectively.

**Table 4.2** NMR chemical shifts (ppm) of barakol (1) and barakol (2) reported by Bycroft<sup>6</sup> (Figure A.3, A.4)

Position	$^1\text{H-NMR}$ (ppm)		$^{13}\text{C-NMR}$ (ppm)
	1 <sup>a</sup>	2 <sup>a</sup>	1 <sup>a</sup>
2	-	-	154.6
3	6.33 (1H, s)	6.03 (1H, s*)	108
4	6.33 (1H, s)	6.07 (1H, s)	113.8
5	-	-	183.7
6	6.44 (1H, s)	6.17 (1H, s)	106.2
8	-	-	168.2
9	6.11 (1H, s)	5.77 (1H, s)	105.1
10	-	-	99.2
1a	-	-	161.8
3a	-	-	132
6a	-	-	159
2-Me	2.23 (3H, s)	2.05 (3H, s)	19.6
8-Me	2.38 (3H, s)	2.16 (3H, s)	21.2

<sup>a</sup> In  $\text{CDCl}_3$

\* s = singlet

**Table 4.3** Mass spectrum data of extracted barakol and barakol reported by Bycroft<sup>6</sup> (Figure A.5)

Compound	MS, m/z (rel)
barakol	M <sup>+</sup> 232(2), 215(100), 184(22), 158(10), 146(12), 106(5)
barakol (Bycroft,1970)	M <sup>+</sup> 232(1.5), 214(100), 186(59), 158(23), 143(6), 128(6), 110(17), 105(15), 93(10), 89(8), 51(3)

Mass spectrum of extracted barakol (yellow crystalline compound) indicated a molecular ion at  $m/z$  232 ( $C_{13}H_{12}O_4$ , 2.0%) which was consistent to that of barakol reported by Bycroft.<sup>6</sup> The prominent ion at  $m/z$  215 ( $C_{13}H_{11}O_3$ , 100%) indicated to barakol salt, while anhydrobarakol ( $m/z$  at 214 ( $C_{13}H_{10}O_3$ ), 100%) is the major molecular ion presented in the mass spectrum reported by Bycroft.<sup>6</sup>

From UV-vis, IR, NMR and MS spectrum data, which are consistent with previously reported data by Bycroft<sup>6</sup>, the pale-yellow crystals obtained from the extraction of *Cassia siamea* Lamk. is considered to be The mixture of barakol and anhydrobarakol.

## 4.2 Barakol-Salicylic acid (BA)

The reaction of barakol and salicylic acid in hot methanol gave a mixture of greenish yellow needle and colourless prism crystals. The greenish yellow crystals (BA) were isolated and characterized by UV-vis, FT-IR, NMR and X-ray analysis.

### 4.2.1 Crystallographic study of BA

Suitable single crystals of BA for X-ray analysis was recrystallized as greenish yellow needles from methanol by slow evaporation, mp. 160°C (Found: C 51.0%, H 6.42% calculated for  $C_{13}O_7H_{18}$ : C 54.50%, H 6.29%).

X-ray diffraction data were collected at room temperature on Enraf-Nonius<sup>33</sup> Kappa CCD area detector. The collected data were reduced using Denzo and Scalepak (Otwinowski & Minor, 1997)<sup>34</sup>. Accurate lattice parameters were determined from least squares refinements of well-centered reflections in the ranges  $2.91 \leq \theta \leq 23.26$ . A total of 3565 reflections were measured, of which 1935 reflections ( $R_{(int)}=0.0153$ )

were unique. All diagrams and calculations were performed using maXus (Bruker Nonius, Delft & MacScience, Japan). The structure was solved by direct methods using SIR 97 and refined by full matrix least-squares using the SHELX-97 package for PC<sup>28</sup>. The displacement factors of non-hydrogen atoms were refined with anisotropic thermal parameters. The hydrogen atoms were found from different Fourier maps, and were included in a refinement with isotropic displacement parameters. The final refinement gave  $R_1 = 0.0421$  and  $wR_2 = 0.1360$  [ $I > 2\sigma(I)$ ].

The crystal structure of anhydrobarakol was crystallized in a monoclinic crystal system, space group  $P2_1/c$  with the unit cell dimensions of  $a = 13.228(7)$  Å,  $b = 6.873(2)$  Å,  $c = 19.7879(9)$  Å,  $\beta = 127.013(2)$  Å<sup>3</sup>,  $Z = 1$ . The crystallographic and experimental data are summarized in Table 4.4. An ORTEP<sup>35</sup> drawing of BA with atomic labeling is shown in Figure 4.3. Atomic coordinates and equivalent isotropic displacement parameter are listed in Table A.1. Bond lengths and angles are given in Table 4.5. The asymmetric unit of BA comprises of one anhydrobarakol and four solvated water molecules. The dioxaphenalene ring is perfect planar with 0.0118 Å deviated from the mean plane of all atoms in the ring. The C5=O3 distance of 1.285 (3) Å is slightly longer than the normal C=O distance (1.22 Å), and shorter than the typical C(*sp*<sup>2</sup>)-OH distance (1.44 Å). It is probably due to the C5=O3 group forming intermolecular hydrogen bonding with a solvated water molecule, resulting in the elongation of C5=O [O3...O1W, 2.885(3) Å]. The C-C and C=C bond distances within the rings are in the range of 1.325(4) Å to 1.375(3) Å. The C-O bond distances in the ring are 1.352(3) Å and 1.384(3) Å for O1, and 1.364(3) and 1.374(3) for O2. The C-O1-C and C-O2-C bond angles are 118.8(1) and 120.8(1), respectively, indicating C-O partial double bond characteristics.

The molecular packing diagram of BA is shown in Figure. 4.4. The molecules of anhydrobarakol are stacked in parallel, forming a columnar structure along the *a*-axis. The separation distance between these two molecular planes of anhydrobarakol is 3.36 Å, indicating a strong  $\pi$ - $\pi$  interactions. The shortest intermolecular contacts are C11...C5 (-x+1,-y+1,-z+1); 3.362(2) Å and C7...C3 (-x+1,-y+1,-z+1; 3.370(2) Å. In order to reduce steric effects of the methoxyl groups, the methyl groups and carbonyl groups are stacked face-to-face with an inversion. There are two heterocyclic oxygen atoms within the dioxaphenalene ring. One of them (O2) is located directly above to the aromatic carbon atoms, participating  $\pi$ - $\pi$  interactions.

The other (O1) has only van der waal contact to the neighboring atoms. The solvated water molecules are located between the two stacked molecular columns and form networks of intermolecular hydrogen bonds. The oxygen carbonyl atom is participated in the hydrogen bonds to O2w and O3w (Figure 4.4). The geometric details of hydrogen bonds are given in Table A.2.

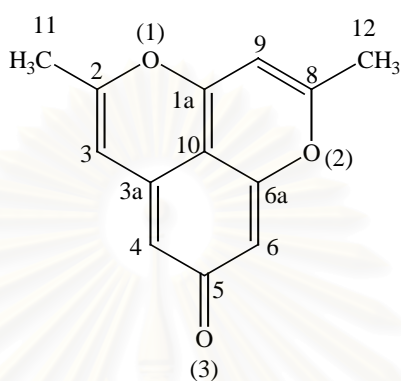


**Figure 4.2** Chemical structure of anhydrobarakol (BA) with atomic numbering<sup>31-32</sup>

สถาบันวิทยบริการ  
จุฬาลงกรณ์มหาวิทยาลัย

**Table 4.4** Crystal and experimental data of BA

Formula	$C_{13}H_{10}O_3 \cdot 4H_2O$
Formula weight	286.22
X-rays	Mo $K_{\alpha}$
Wavelength, (Å)	0.71073
Crystal system	monoclinic
Space group	$P2_1/c$
Z	1
$a$ , (Å)	13.2280(7)
$b$ , (Å)	6.8738(2)
$c$ , (Å)	19.7879(9)
$\beta$ , (°)	127.013(2)
$V$ , (Å <sup>3</sup> )	1436.74(10)
$D_{cal}$ , (g/cm <sup>3</sup> )	1.282
Absorption coefficient ( $\mu$ ), (mm <sup>-1</sup> )	0.107
Crystal size, (mm)	0.30x0.45x0.27
reflections collected/unique	3565/1935 [ $R(int)$ = 0.0153]
Refinement method	Full-matrix least-squares on $F^2$
Goodness-of-fit on $F^2$	1.215
Final $R$ indices [ $I > 2\sigma(I)$ ]	$R_1 = 0.0421$ , $wR_2 = 0.1360$
$R$ indices(all data)	$R_1 = 0.0482$ , $wR_2 = 0.1436$

สถาบันวิทยบริการ  
จุฬาลงกรณ์มหาวิทยาลัย

**Table 4.5** Bond lengths (Å) and angles (°) of BA

C(1A)-O(1)	1.355(3)	C(4)-C(5)	1.428(3)
C(1A)-C(10)	1.371(3)	C(5)-O(3)	1.285(3)
C(1A)-C(9)	1.408(4)	C(5)-C(6)	1.428(4)
C(2)-C(3)	1.325(4)	C(6)-C(6A)	1.361(4)
C(2)-O(1)	1.383(3)	C(6A)-O(2)	1.373(3)
C(2)-C(11)	1.489(4)	C(6A)-C(10)	1.415(3)
C(3)-C(3A)	1.440(3)	C(8)-C(9)	1.347(4)
C(3A)-C(4)	1.375(3)	C(8)-O(2)	1.363(3)
C(3A)-C(10)	1.420(3)	C(8)-C(12)	1.492(4)
O(1)-C(1A)-C(10)	121.1(2)	C(6A)-C(6)-C(5)	120.0(2)
O(1)-C(1A)-C(9)	117.8(2)	C(6)-C(6A)-O(2)	119.6(2)
C(10)-C(1A)-C(9)	121.1(2)	C(6)-C(6A)-C(10)	121.4(2)
C(3)-C(2)-O(1)	122.0(2)	O(2)-C(6A)-C(10)	119.0(2)
C(3)-C(2)-C(11)	127.2(3)	C(9)-C(8)-O(2)	122.3(2)
O(1)-C(2)-C(11)	110.8(2)	C(9)-C(8)-C(12)	125.8(3)
C(2)-C(3)-C(3A)	121.9(2)	O(2)-C(8)-C(12)	112.0(2)
C(4)-C(3A)-C(10)	119.4(2)	C(8)-C(9)-C(1A)	118.2(2)
C(4)-C(3A)-C(3)	126.2(2)	C(1A)-C(10)-C(6A)	118.8(2)
C(10)-C(3A)-C(3)	114.4(2)	C(1A)-C(10)-C(3A)	121.8(2)
C(3A)-C(4)-C(5)	121.3(2)	C(6A)-C(10)-C(3A)	119.4(2)
O(3)-C(5)-C(6)	120.5(2)	C(1A)-O(1)-C(2)	118.92(19)
O(3)-C(5)-C(4)	121.1(2)	C(8)-O(2)-C(6A)	120.59(19)
C(6)-C(5)-C(4)	118.5(2)		



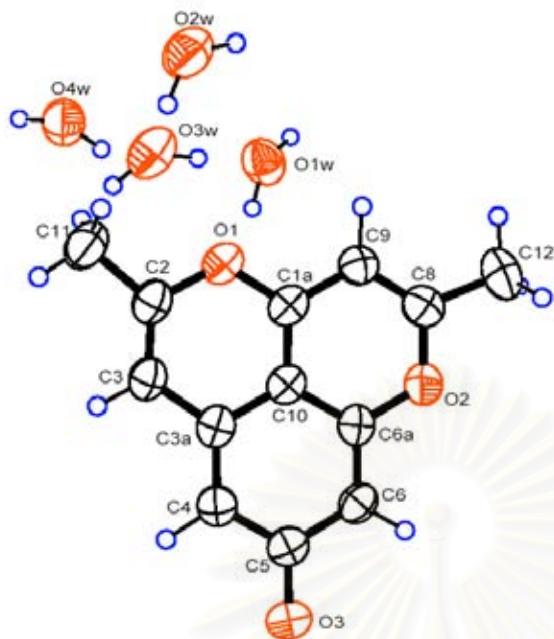
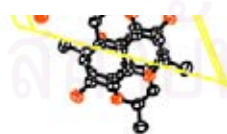
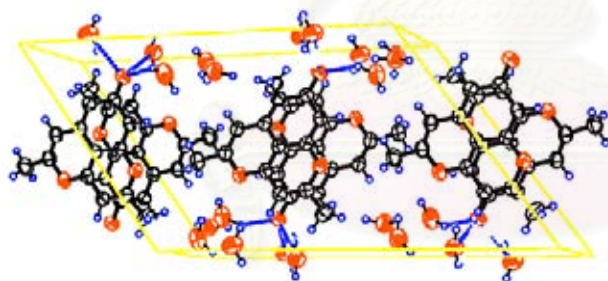


**Figure 4.3** An ORTEP drawing of BA, showing 50 % probability displacement ellipsoids



(a)

(b)

**Figure 4.4** (a) Crystal packing diagram of anhydrobarakol (BA), viewed along  $a$ -axis, hydrogen atoms were omitted for clarity (b) hydrogen bonding of BA with water.

#### 4.2.2 Spectroscopic studies of BA

The UV-vis spectrum of BA in ethanol shows the absorption bands at 242 (4.15), 250 (4.15) and 379 (3.76) nm. (Figure B.1).

The IR-spectra of crystalline anhydrobarakol in KBr pellet (Figure B.2) is in an excellent agreement with the crystal structure analysis. The spectrum shows broad absorption bands at 3400-2800  $\text{cm}^{-1}$  range corresponding to the O-H vibrations relative to the networks intermolecular hydrogen bonding between water molecules, or the hydroxyl group in BA and water molecules. The strong absorption band of C=O stretching at 1676  $\text{cm}^{-1}$  was red shifted from a typical C=O stretching frequency at about 1710  $\text{cm}^{-1}$  of a ketone or carboxylic group. It is probably because the C=O group exists in a keto-enol form, or probably due to the conjugation of C=O with C=C.

The existence of the keto-enol forms (Figure 4.5) might be indicated by the intensive absorption band that was observed at 3439 and 836  $\text{cm}^{-1}$ , assigned to the stretching and bending of a hydroxide group (Figure B.2). Moreover, the difference in bond distances between C1A-O1 (1.353(3) Å) and O1-C2 (1.383(3) Å); 0.030 Å, is higher than that of between the bonds around O2; 0.010 Å, indicating that the O1=C bond is a partial double bond.

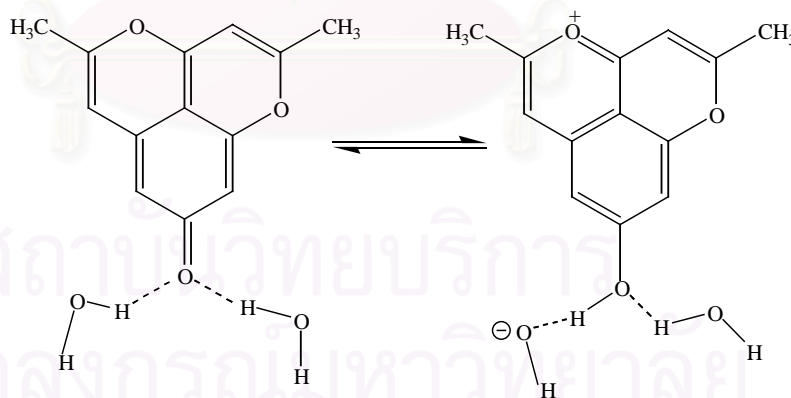


**Figure 4.5** Keto-enol form of anhydrobarakol

**Table 4.6** IR data of anhydrobarakol (Figure B.2)

Compound	IR data (cm <sup>-1</sup> )		
	v(O-H)	v(C-O)	v(C=O)
Anhydrobarakol	3439 (s,b)	1192 (m)	1676(s)
	3289 (s,b)	1267 (m)	

The <sup>1</sup>H-NMR spectrum of the BA in CDCl<sub>3</sub>, Figure B.3, was similar to that of barakol in section 4.1, indicated two methoxy groups attached to aromatic carbons (C2 and C8) at δ<sub>H</sub> 2.23 and 2.38 ppm, four protons on aromatic ring (H4, H3, H6 and H9) at δ<sub>H</sub> 6.38, 6.38, 6.48, 6.18 ppm, respectively. (Table 4.7).

The comparison of <sup>1</sup>H-NMR spectra between the extracted barakol, salicylic acid and the mixture of barakol-salicylic acid is shown in Figure 4.6. The chemical shifts of the barakol in the mixture are slightly downfield shifted compared to that of the free barakol. The <sup>1</sup>H chemical shifts of salicylic acid in the mixture are unchanged when compared to the free salicylic acid. As a result from <sup>1</sup>H-NMR, it can be explained that barakol shows less participation of intermolecular interactions to salicylic acid, resulting in separating recrystallization between the crystals of BA and the crystals of salicylic acid.

สถาบันวิทยบริการ  
จุฬาลงกรณ์มหาวิทยาลัย

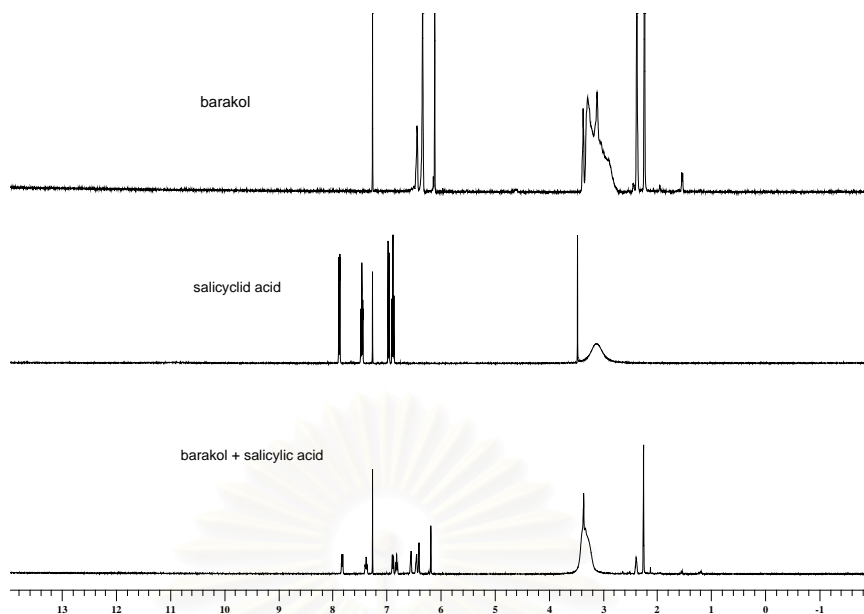


**Figure 4.6**  $^1\text{H-NMR}$  spectra of barakol, salicylic acid and barakol-salicylic acid mixture

**Table 4.7** NMR spectral data ( $\delta$  ppm) for Anhydrobarakol (Figure B.3)

Position	$^1\text{H-NMR}$ (ppm)	
	BA <sup>a</sup>	Extracted barakol <sup>b</sup>
3	6.38 (1H,s)	-
4	6.38 (1H,s)	6.33 (2H,s)
6	6.48 (1H,s)	6.48 (1H,s)
9	6.18 (1H,s)	6.11 (1H,s)
2-Me	2.23 (3H,s)	2.23 (3H,s)
8-Me	2.38 (3H,s)	2.38 (3H,s)

<sup>a</sup> In  $\text{CDCl}_3 + \text{MeOH-d}_4$

\* s = singlet

<sup>b</sup> In  $\text{CDCl}_3$

### 4.3 Anhydrobarakol hydrochloride (BC)

Anhydrobarakol hydrochloride was prepared by adding concentrated hydrochloric acid into barakol dissolved in a minimum amount of methanol until the anhydrobarakol hydrochloride was precipitated as yellow crystalline solid. The  $R_f$  value showed at 0.35 and 0.53 with an aluminium plate as the absorbent and mixtures of chloroform:methanol (9:1) and chloroform:acetone (6:4) as solvent systems. [mp. 212°C (Found: C 58.0%, H 5.94%, calculated for C<sub>13</sub>H<sub>13</sub>O<sub>4</sub>Cl : C 58.10%, H 4.84%)]

#### 4.3.1 Crystallographic study of anhydrobarakol hydrochloride (BC)

Suitable single crystals of BC for X-ray analysis were kindly provided by Dr. Chaiyo Chaichantipyuth.

X-ray diffraction data were collected at room temperature using a Bruker SMART CCD area detector. The collected data were reduced using SAINT<sup>36</sup> and empirical absorption correction was performed using SADABS<sup>37</sup>. Accurate lattice parameters were determined from least squares refinements of well-centered reflections in the range of  $2.13 \leq \theta \leq 30.72$ . A total of 9083 reflections were measured, of which 3647 reflections ( $R_{(int)}=0.0197$ ) were unique. The structure was solved by direct methods and refined with anisotropic displacement parameters for all non hydrogen atoms by full matrix least-squares using the SHELX-97 package for PC<sup>28</sup>. The hydrogen atoms were found from difference Fourier maps, and were included in a refinement with isotropic displacement parameters. The final refinement gave  $R_1 = 0.0410$  and  $wR_2 = 0.1071$  [ $I > 2\sigma(I)$ ].

The crystal of anhydrobarakol hydrochloride is crystallized in a monoclinic crystal system, space group  $P2_1/n$  with unit cell dimensions of  $a = 12.2547(2)$  Å,  $b = 8.051(2)$  Å,  $c = 12.8133(2)$  Å,  $\beta = 99.514(1)$  Å<sup>3</sup>,  $Z = 4$ . The crystallographic and experimental data are summarized in Table 4.8. An ORTEP drawing<sup>35</sup> of BC with atomic labeling is shown in Figure 4.8. Bond lengths and angles are given in Table 4.9. Atomic coordinates and equivalent isotropic displacement are listed in Table B.1.

The crystal structure of BC is similar to that of BA (anhydrobarakol), except that the oxygen atom in the dioxophenalene ring (barakol ring) is oxonium cation. The asymmetric unit consists of barakol cation, chloride anion and one solvated water molecule. The 1.3351(16) Å of C5-O3 bond distance in BC is longer than that of

1.288(3) Å in BA (which is significantly longer than the normal C=O distance (1.22 Å), indicating a single bond C( $sp^2$ )-O characteristic. The hydrogen atom bound to O3 was found from difference Fourier maps. Therefore, the functional group of O3 is a hydroxyl group. The Cl<sup>-</sup> anion participates in the strong and weak electrostatic interactions with oxygen atoms in the dioxophene ring; Cl<sup>-</sup>...O1, 3.33 Å; Cl<sup>-</sup>...O2, 3.73 Å, respectively. This suggests that positive charges are localized within the ring between these two oxygen atoms, and O1 is more positive than O2 based on this intermolecular distance.

In comparison of BA and BC, the differences between the C-O bond distances of the carbon atoms bound to the same oxygen atom within the ring, ( $\Delta d$  (Om-n); where m is the oxygen position; n is BA or BC). In table 4.9,  $\Delta d$  (O1-BC) = 0.061(17) Å is higher than  $\Delta d$  (O1-BA) = 0.028(3) Å in table 4.5. This indicated that O1 in BC is more positive charged than O1 in BA.

The C-C bond distances within the rings are in the range of 1.330(2) Å and 1.434(3) Å. The molecular packing diagram of BC is shown in Figure. 4.9. The barakol cation moieties are stacked in parallel, forming a columnar packing along the *b*-axis with the separation distance between the planes of 3.46 Å. The crystal packing is organized around the chloride anion. The chloride ion forms a hydrogen bonding to two water molecules, one hydroxyl group in the barakol ring, and participate an electrostatic interaction with oxonium of barakol. The geometric details of hydrogen bonds are given in Table B.2.

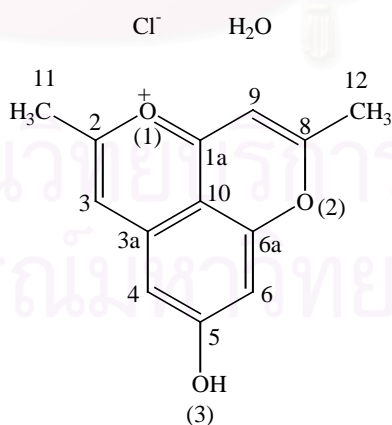


**Figure 4.7** Chemical structure of anhydrobarakol hydrochloride • H<sub>2</sub>O with atomic numbering<sup>31-32</sup>

**Table 4.8** Crystal and experimental data of BC

Formula	$C_{13}H_{11}O_3 \cdot Cl \cdot H_2O$
Formula weight	268.58
X-rays	Mo $K\alpha$
Wavelength, ( $\text{\AA}$ )	0.71073
Crystal system	monoclinic
Space group	$P2_1/n$
Z	4
a, ( $\text{\AA}$ )	12.2547(2)
b, ( $\text{\AA}$ )	8.051(2)
c, ( $\text{\AA}$ )	12.8133(2)
$\beta$ , ( $^\circ$ )	99.514(1)
V, ( $\text{\AA}^3$ )	1246.79(3)
$D_{cal}$ , ( $\text{g/cm}^3$ )	1.426
Absorption coefficient ( $\mu$ ), ( $\text{mm}^{-1}$ )	0.310
Crystal size, (mm)	0.1x0.2x0.1
reflections collected/unique	9083/3647 [ $R(int) = 0.0197$ ]
Refinement method	Full-matrix least-squares on $F^2$
Goodness-of-fit on $F^2$	1.017
Final R indices [ $I > 2\sigma(I)$ ]	$R_1 = 0.0410$ , $wR_2 = 0.1071$
R indices(all data)	$R_1 = 0.0582$ , $wR_2 = 0.1188$

สถาบันวิทยบริการ  
จุฬาลงกรณ์มหาวิทยาลัย

**Table 4.9** Bond lengths (Å) and angles (°) of BC

C(1A)-O(1)	1.330(17)	C(4)-C(5)	1.398(2)
C(1A)-C(10)	1.383(18)	C(5)-O(3)	1.335(16)
C(1A)-C(9)	1.397(19)	C(5)-C(6)	1.394(18)
C(2)-C(3)	1.330(2)	C(6)-C(6A)	1.368(18)
C(2)-O(1)	1.391(17)	C(6A)-O(2)	1.360(15)
C(2)-C(11)	1.478(2)	C(6A)-C(10)	1.399(18)
C(3)-C(3A)	1.432(2)	C(8)-C(9)	1.348(2)
C(3A)-C(4)	1.378(19)	C(8)-O(2)	1.352(16)
C(3A)-C(10)	1.415(17)	C(8)-C(12)	1.475(2)
O(1)-C(1A)-C(10)	120.94(12)	C(6A)-C(6)-C(5)	117.66(13)
O(1)-C(1A)-C(9)	117.8(2)	C(6)-C(6A)-O(2)	118.60(12)
C(10)-C(1A)-C(9)	120.19(2)	C(6)-C(6A)-C(10)	121.87(11)
C(3)-C(2)-O(1)	121.41(13)	O(2)-C(6A)-C(10)	119.54(11)
C(3)-C(2)-C(11)	127.75(15)	C(9)-C(8)-O(2)	122.29(12)
O(1)-C(2)-C(11)	110.8(2)	C(9)-C(8)-C(12)	126.58(14)
C(2)-C(3)-C(3A)	121.52(13)	O(2)-C(8)-C(12)	111.13(14)
C(4)-C(3A)-C(10)	118.83(13)	C(8)-C(9)-C(1A)	118.53(13)
C(4)-C(3A)-C(3)	126.11(12)	C(1A)-C(10)-C(6A)	118.92(11)
C(10)-C(3A)-C(3)	115.06(12)	C(1A)-C(10)-C(3A)	121.35(12)
C(3A)-C(4)-C(5)	119.75(12)	C(6A)-C(10)-C(3A)	119.73(12)
O(3)-C(5)-C(6)	121.14(13)	C(1A)-O(1)-C(2)	119.71(11)
O(3)-C(5)-C(4)	116.70(12)	C(8)-O(2)-C(6A)	120.52(11)
C(6)-C(5)-C(4)	122.16(12)		



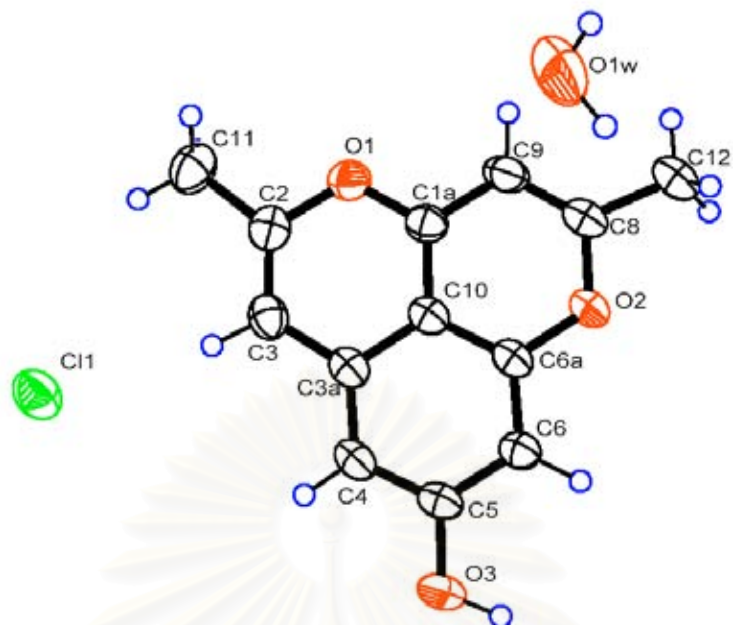


**Figure 4.8** An ORTEP drawing of BC, showing 50 % probability displacement ellipsoids

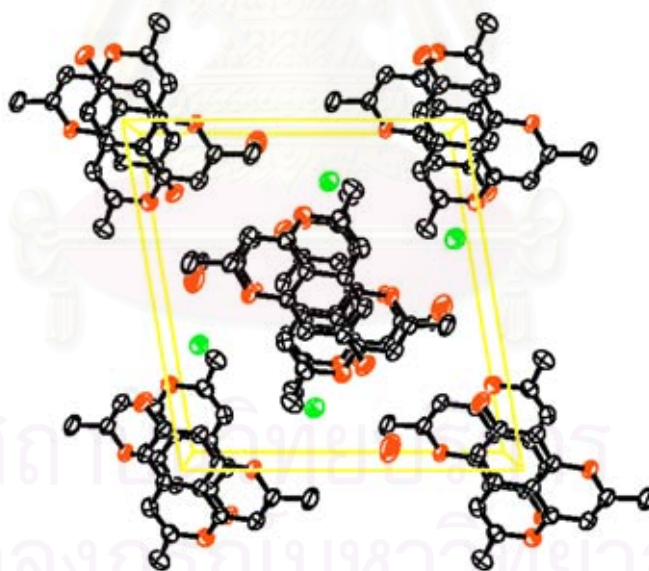


**Figure 4.9** Crystal packing diagram of anhydrobarakol hydrochloride (BC), viewed along *b*-axis, hydrogen atoms were omitted for clarity.

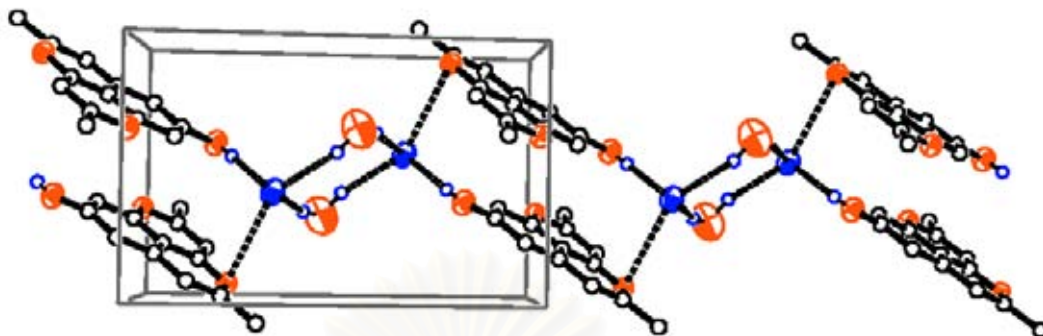


**Figure 4.10** Infinite chain of hydrogen bonding in anhydrobarakol hydrochloride

### 4.3.2 Spectroscopic studies of BC

The UV-vis spectrum of BC in ethanol (Figure C.1), shows the absorption bands at 215, 240, 330, 380 nm. The comparison of UV-vis absorption data between BC and anhydrobarakol hydrochloride reported by Bycroft<sup>6</sup> are given in Table 4.10.

The <sup>1</sup>H-NMR spectrum of the BC in CDCl<sub>3</sub>, Figure C.3, was similar to that of barakol in section 4.1, indicated two methoxy groups attached to aromatic carbons (C2 and C8) at  $\delta_{\text{H}}$  2.40 and 2.65 ppm, four protons on aromatic ring (H3, H4, H6 and H9) at  $\delta_{\text{H}}$  6.76, 6.81, 6.91, 6.74 ppm, respectively. (Table 4.12)

Interestingly, the IR spectrum of BC showed sharp intensive bands of  $\nu(\text{OH})$  stretching at 3516 and 3444  $\text{cm}^{-1}$  instead of broad absorption. It is probably due to isolated hydrogen bonding. The small quantity of a compound contains a number of individual molecules, and each of these may be hydrogen bonded to a slightly different extent, then the extended hydrogen bonding is prevented through the lack of molecular contact. Therefore, in these situations the broad O-H peak of water molecule is replaced by a sharp peak around 3510  $\text{cm}^{-1}$  and the O-H stretching band of barakol appears at 3444  $\text{cm}^{-1}$  (anhydrobarakol hydrochloride contains the hydroxyl group. It is possible to acquire IR spectra of OH<sup>-</sup> - containing compounds without seeing the broad signal.). The peaks around 2500 to 3000  $\text{cm}^{-1}$  were assigned to the C-H stretching which are less sterically hindered from the frequency of OH stretching. The  $\nu(\text{C}=\text{O})$  at 1671  $\text{cm}^{-1}$  reveals that barakol exists in a keto-enol form.

**Table 4.10** UV-Vis data of anhydrobarakol hydrochloride (BC) in ethanol (Figure C.1) and anhydrobarakol hydrochloride Bycroft<sup>6</sup> in ethanol.

Compound	$\lambda$ ,nm (log $\epsilon$ )
Anhydrobarakol hydrochloride (BC)	215 (4.56), 240 (4.95), 330 (4.00), 380 (4.32)
Anhydrobarakol hydrochloride (Bycroft) <sup>6</sup>	241 (4.56), 242 (4.54), 372 (4.15)

**Table 4.11** IR data of anhydrobarakol hydrochloride (BC) (Figure C.2) and anhydrobarakol hydrochloride (Bycroft)<sup>6</sup>.

Compound	IR data (cm <sup>-1</sup> )		
	$\nu$ (O-H)	$\nu$ (C-O)	$\nu$ (C=O)
Anhydrobarakol hydrochloride	3516 (m,sh) 3444 (m,sh)	1268 (s,sh)	1671(s,sh)
Barakol hydrochloride (Bycroft) <sup>6</sup>	3500 (broad) 3440	-	1660 1620

**Table 4.12**  $^1\text{H-NMR}$  chemical shifts ( $\delta$  ppm) of anhydrobarakol hydrochloride, (BC) and anhydrobarakol hydrochloride (Bycroft<sup>6</sup> at 200 MHz) (2) (Figure C.3, C.4)

Position	$^1\text{H-NMR}$ (ppm)		$^{13}\text{C-NMR}$ (ppm)
	BC <sup>a</sup>	2 <sup>a</sup>	1 <sup>a</sup>
2	-	-	158.2
3	6.76 (1H,s)	-	109.0
4	6.81 (1H,s)	-	110.0
5	-	-	175.8
6	6.91 (1H,s)	6.90 (4x1H)	108.2
8	-	-	171.8
9	6.74 (1H,s)	-	102.4
10	-	-	103.0
1a	-	-	168.0
3a	-	-	134.6
6a	-	-	159.0
2-Me	2.40 (3H,s)	2.48 (3H,s)	19.4
8-Me	2.65 (3H,s)	2.70 (3H,s)	21.8

<sup>a</sup> In  $\text{CDCl}_3$  \* s = singlet

#### 4.4 Barakol-Phthalic acid (BP)

The reaction of barakol and phthalic acid in hot methanol gave yellow needle crystals. [mp. 212°C (Found: C 59.43%, H 5.39%, calculated for C<sub>21</sub>H<sub>22</sub>O<sub>10</sub> : C 58.06%, H 5.707%)]

The obtained yellow crystals (BP) were characterized by UV-vis, FT-IR, NMR and X-ray analysis.

##### 4.3.3 Crystallographic study of barakol phthalic acid complex (BP)

Suitable single crystals of BP were recrystallized from methanol. X-ray diffraction data were collected at room temperature using a Bruker SMART CCD area detector. The collected data were reduced using SAINT<sup>36</sup> and empirical absorption correction was performed using SADABS<sup>37</sup>. Accurate lattice parameters were determined from least squares refinements of well-centered reflections in the ranges  $1.68 \leq \theta \leq 28.03$ . A total of 11796 reflections were measured, of which 4674 reflections ( $R_{(int)}=0.0476$ ) were unique. The crystallographic data are presented in Table 4.6. The structure was solved by direct methods and refined with anisotropic displacement parameters for all non hydrogen atoms by full matrix least-squares using the SHELX-97 package for PC<sup>28</sup>. The hydrogen atoms were found from difference Fourier maps, and were included in a refinement with isotropic displacement parameters. The final refinement gave  $R_1 = 0.0879$  and  $wR_2 = 0.1772$  [ $I > 2\sigma(I)$ ]. The crystal structure of barakol is crystallized in a triclinic crystal system, space group  $P(-1)$  with the unit cell dimensions of  $a = 7.3721(8)$  Å,  $b = 11.3144(2)$  Å,  $c = 12.4748(14)$  Å,  $\alpha = 103.765(2)^\circ$ ,  $\beta = 91.893(2)^\circ$ ,  $\gamma = 96.752(2)^\circ$ ,  $V = 101.63(19)$  Å<sup>3</sup>,  $Z = 2$ . An ORTEP<sup>35</sup> drawing with atomic labeling is shown in Figure 4.11. Bond lengths and angles are given in Table 4.14. Atomic coordinates and equivalent isotropic displacement parameter are listed in Table C.1.

The crystal structure of barakol-phthalate (BP) was determined by X-ray analysis in order to study the electrostatic effect from a counter ion. The X-ray crystallographic analysis showed that the asymmetric unit of BP comprises of barakol molecule, hydrogen phthalate and three water molecules (Figure 4.12). The hydrogen atom bound to O3 was found from the difference Fourier maps, indicating that the O3 is a hydroxyl group. Therefore, the barakol molecule in BP exists as barakol cation.

The BP complex is an 1:1 ion pair complex between barakol cation and hydrogen phthalate. Therefore, the formation of barakol-phthalate (BP) complex is stabilized by the combination of electrostatic interactions,  $\pi$ - $\pi$  stacking and hydrogen bonding.

The molecular packing diagram of BP (Figure. 4.13) shows that the molecules of barakol and phthalate alternatively stacked in parallel along *a*-axis, forming a one-dimensional molecular packing columnar. The hydrogen phthalate molecules are located between the molecular planes of barakol. The ring B of barakol molecule is superimposed on the pseudo-ring E of the phthalate molecule. The interplanar distance between barakol planes and hydrogen phthalate is 3.34 Å, as illustrated by the top and side views (Figure 4.14). The centre of phthalate ring D is located above and below the quinol ring C of barakol, participating  $\pi$ - $\pi$  interactions. The hydroxyl hydrogen atom in the hydrogen phthalate forms a symmetric intramolecular hydrogen bonding to O2b and O3a (O2a---H23---O3a). The O2a-H23 and O3a-H23 distances are 1.18(6) Å and 1.22(6) Å. The O1a=C7a and O4a=C8a bond distances of the carboxylate groups in the hydrogen phthalate are 1.216(5) Å and 1.220(5) Å, indicating a typical C=O bond characteristic of carboxylic group (1.220 Å). Therefore, the C=O bonds of the hydrogen phthalate are not involved in conjugative resonance of  $\pi$  electron over the carboxylate groups. The water molecules participate in hydrogen bonding to the phthalate and barakol molecules, forming a two dimensional hydrogen bonding network plane along *bc*-planes. The barakol hydroxyl group (O3-H33) forms strong hydrogen bonding to the nearest water molecule [O3...O1w, 2.528(4) Å]. The O1 and O2 in the barakol ring do not involve in any hydrogen bonding.

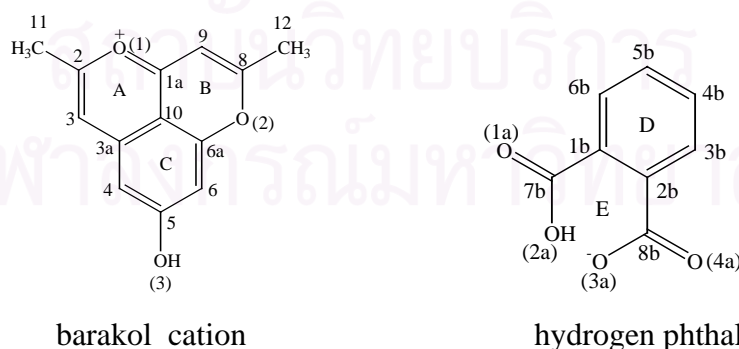


**Figure 4.11** Chemical structure of barakol cation<sup>31-32</sup> and phthalate (BP), with atomic numbering

**Table 4.13** Crystal and experimental data of BP

Formula	$C_{13}H_{11}O_3 \cdot C_8H_5O_4 \cdot 3H_2O$
Formula weight	439.38
X-rays	Mo $K_{\alpha}$
Wavelength, (Å)	0.71073
Crystal system	triclinic
Space group	$P(-1)$
Z	2
$a$ , (Å)	7.3721(8)
$b$ , (Å)	11.3144(2)
$c$ , (Å)	12.4748(14)
$\alpha$ , (°)	103.765(2)
$\beta$ , (°)	91.893(2)
$\gamma$ , (°)	96.752(2)
$V$ , Å <sup>3</sup>	1001.63(19)
$D_{cal}$ , (g/cm <sup>3</sup> )	1.440
Absorption coefficient ( $\mu$ ), (mm <sup>-1</sup> )	0.116
Crystal size, (mm)	0.20x0.40x0.32
reflections collected/unique	11796/4674 [ $R(int) = 0.0476$ ]
Refinement method	Full-matrix least-squares on $F^2$
Goodness-of-fit on $F^2$	1.084
Final $R$ indices [ $I > 2\sigma(I)$ ]	$R_1 = 0.0879$ , $wR_2 = 0.1772$
$R$ indices(all data)	$R_1 = 0.1572$ , $wR_2 = 0.2052$

**Table 4.14** Bond lengths (Å) and angles (°) for BP

C(1A)-O(1)	1.364(4)	C(8)-O(2)	1.359(4)
C(1A)-C(9)	1.364(5)	C(8)-C(12)	1.478(5)
C(1A)-C(10)	1.377(5)	C(1B)-C(6B)	1.385(5)
C(2)-C(3)	1.313(5)	C(1B)-C(2B)	1.418(4)
C(2)-O(1)	1.397(4)	C(1B)-C(7B)	1.517(5)
C(2)-C(11)	1.476(5)	C(2B)-C(3B)	1.391(5)
C(3)-C(3A)	1.396(5)	C(2B)-C(8B)	1.516(5)
C(3A)-C(4)	1.363(5)	C(3B)-C(4B)	1.375(6)
C(3A)-C(10)	1.420(5)	C(4B)-C(5B)	1.377(6)
C(4)-C(5)	1.397(5)	C(5B)-C(6B)	1.358(6)
C(5)-O(3)	1.332(4)	C(7B)-O(1A)	1.219(4)
C(5)-C(6)	1.399(5)	C(7B)-O(2A)	1.265(5)
C(6)-C(6A)	1.357(5)	C(8B)-O(4A)	1.219(5)
C(6A)-O(2)	1.390(4)	C(8B)-O(3A)	1.260(5)
C(6A)-C(10)	1.405(4)		
C(8)-C(9)	1.334(5)		
O(1)-C(1A)-C(9)	119.2(3)	C(6A)-C(10)-C(3A)	118.9(3)
O(1)-C(1A)-C(10)	120.6(3)	C(1A)-O(1)-C(2)	118.8(3)
C(9)-C(1A)-C(10)	120.2(3)	C(8)-O(2)-C(6A)	121.2(3)
C(3)-C(2)-O(1)	120.1(3)	C(6B)-C(1B)-C(2B)	117.8(3)
C(3)-C(2)-C(11)	126.2(4)	C(6B)-C(1B)-C(7B)	114.0(3)
O(1)-C(2)-C(11)	113.7(4)	C(2B)-C(1B)-C(7B)	128.1(3)
C(2)-C(3)-C(3A)	124.8(4)	C(3B)-C(2B)-C(1B)	117.5(3)
C(4)-C(3A)-C(3)	126.0(3)	C(3B)-C(2B)-C(8B)	113.9(3)
C(4)-C(3A)-C(10)	119.7(3)	C(1B)-C(2B)-C(8B)	128.6(3)
C(3)-C(3A)-C(10)	114.3(3)	C(4B)-C(3B)-C(2B)	123.2(4)
C(3A)-C(4)-C(5)	119.7(3)	C(3B)-C(4B)-C(5B)	118.3(4)
O(3)-C(5)-C(4)	116.7(3)	C(6B)-C(5B)-C(4B)	120.0(4)
O(3)-C(5)-C(6)	121.9(3)	C(5B)-C(6B)-C(1B)	123.1(4)
C(4)-C(5)-C(6)	121.5(3)	O(1A)-C(7B)-O(2A)	121.2(4)
C(6A)-C(6)-C(5)	118.5(3)	O(1A)-C(7B)-C(1B)	118.2(4)
C(6)-C(6A)-O(2)	120.9(3)	O(2A)-C(7B)-C(1B)	120.6(3)
C(6)-C(6A)-C(10)	121.6(3)	O(4A)-C(8B)-O(3A)	120.9(4)
O(2)-C(6A)-C(10)	117.4(3)	O(4A)-C(8B)-C(2B)	118.4(4)
C(9)-C(8)-O(2)	120.5(3)	O(3A)-C(8B)-C(2B)	120.6(4)
C(9)-C(8)-C(12)	122.8(4)		
O(2)-C(8)-C(12)	116.7(3)		
C(8)-C(9)-C(1A)	121.0(4)		
C(1A)-C(10)-C(6A)	119.6(3)		
C(1A)-C(10)-C(3A)	121.4(3)		



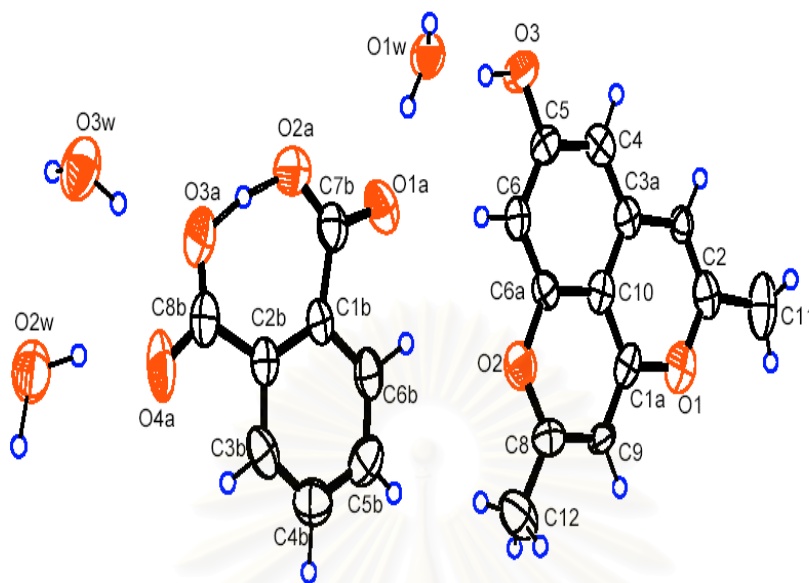


**Figure 4.12** An ORTEP drawing of BP, showing 50 % probability displacement ellipsoids

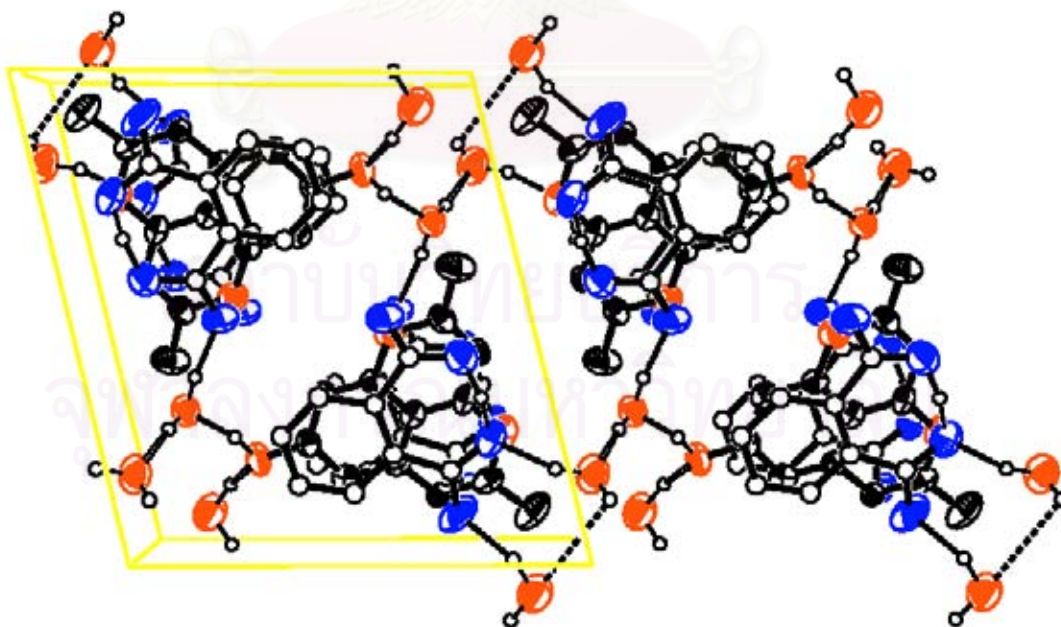


**Figure 4.13** Crystal packing diagram of barakol phthalate (BP), viewed along *a*-axis, hydrogen atoms were omitted for clarity.

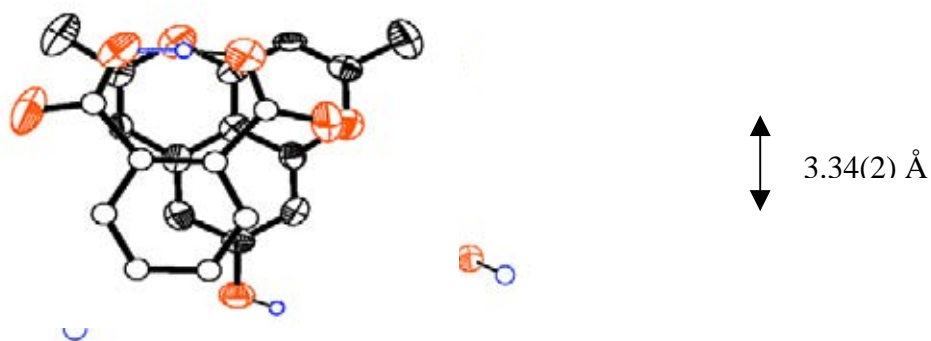


**Figure 4.14**  $\pi$ - $\pi$  interactions of barakol-phthalate (BP)

#### 4.4.2 Spectroscopic studies of BP

The UV-vis spectrum of BP in ethanol (Figure 4.15), shows the absorption bands at 205, 240, 281, 378 nm. The UV-vis absorption data of BP in ethanol are given in Table 4.15. The spectrum of BP shows that the  $\pi$ - $\pi^*$  absorption band of barakol was blue shifted from 379 to 378 nm due to barakol became a barakol cation. The absorption band of phthalic acid at 286 nm was blue shifted to 281 nm because phthalic acid was protonated to be hydrogen phthalate. Therefore, BP exists in an ion-pair complex consistent with the X-ray analysis.

**Table 4.15** UV-Vis data of barakol , phthalic acid and BP in ethanol (Figure 4.13)

Compound	$\lambda$ , nm (log $\epsilon$ .)
barakol	242 (4.15) , 250 (4.50) , 379 (3.76)
phthalic acid	204 (4.24) , 234 (3.64) , 286 (3.00)
BP complex	205 (4.34) , 240 (4.24) , 281 (3.70) , 378 (3.60)

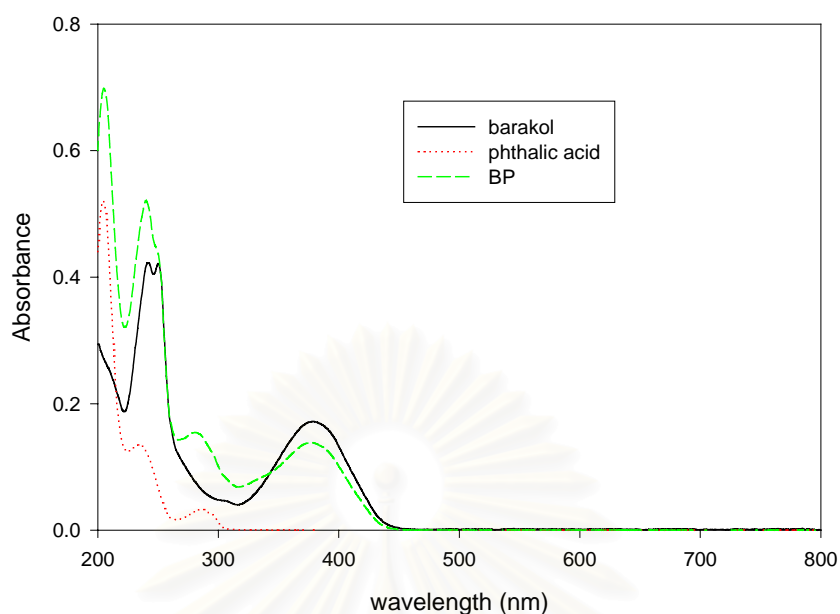


**Figure 4.15** UV-Spectrum of anhydrobarakol, phthalic acid and BP complex

The formation of BP complex was confirmed by both IR and  $^1\text{H-NMR}$  spectroscopic techniques.

**Table.4.16** Selected IR and  $^1\text{H-NMR}$  data for barakol (cation), phthalic acid and BP complex

Compound	IR data ( $\text{cm}^{-1}$ )			NMR data (ppm)
	$\nu(\text{O-H})$	$\nu(\text{C-O})$	$\nu(\text{C=O})$	
Barakol	3444 (s,b)	1188 (m)	1676 (s)	2.28,2.32 (s,6H)
	3295 (s,b)	1267 (m)		6.42,6.35 (s,2H) 6.34, 6.15 (s,2H)
Phthalic acid	3439 (s,b)	1278 (m)	1670 (s)	7.70,7.49 (q,4H)
BP complexe	3250 (s,b)	1071 (s)	1689 (s)	2.36,2.59 (s,6H)
	3010 (s,b)	1282 (m)		6.99,6.88 (s,2H) 6.65, 6.48 (s,2H)
				8.07, 7.45 (q,4H)

The IR-spectrum of crystalline BP in KBr pellet (Figure.D.1) is in an excellent agreement with the crystal structure analysis. The spectrum showed broad absorption bands at 3000-2800  $\text{cm}^{-1}$  range corresponding to the hydrogen bonding O-H vibrations. The strong absorption band of C=O stretching at 1689  $\text{cm}^{-1}$  was red shifted from a C=O stretching frequency at about 1670 and 1676  $\text{cm}^{-1}$  of a carboxylic group in phthalic acid and a carbonyl group in barakol, respectively. It is probably because the C=O group exists in a carboxylate.

The  $^1\text{H-NMR}$  spectrum of BP in  $\text{CDCl}_3+\text{CD}_3\text{OD}$  (Figure. 4.16) were displayed the chemical shifts corresponding to barakol and phthalic acid. For barakol resonances, two methoxy groups attached to aromatic carbons (C2 and C8) at  $\delta_{\text{H}}$  2.36 and 2.59 ppm, four protons on aromatic ring (H3, H4, H6 and H9) at  $\delta_{\text{H}}$  6.65, 6.88, 6.99 and 6.48 ppm, respectively.

The methyl protons of free barakol at 2.28, 2.32 ppm downfield shifted to 2.36, 2.59 ppm in BP. Four protons on aromatic rings of free barakol at 6.15, 6.34, 6.35, 6.42 ppm split as four separated peaks in BP and shifted to downfield at 6.48, 6.65, 6.88, 6.98 ppm.

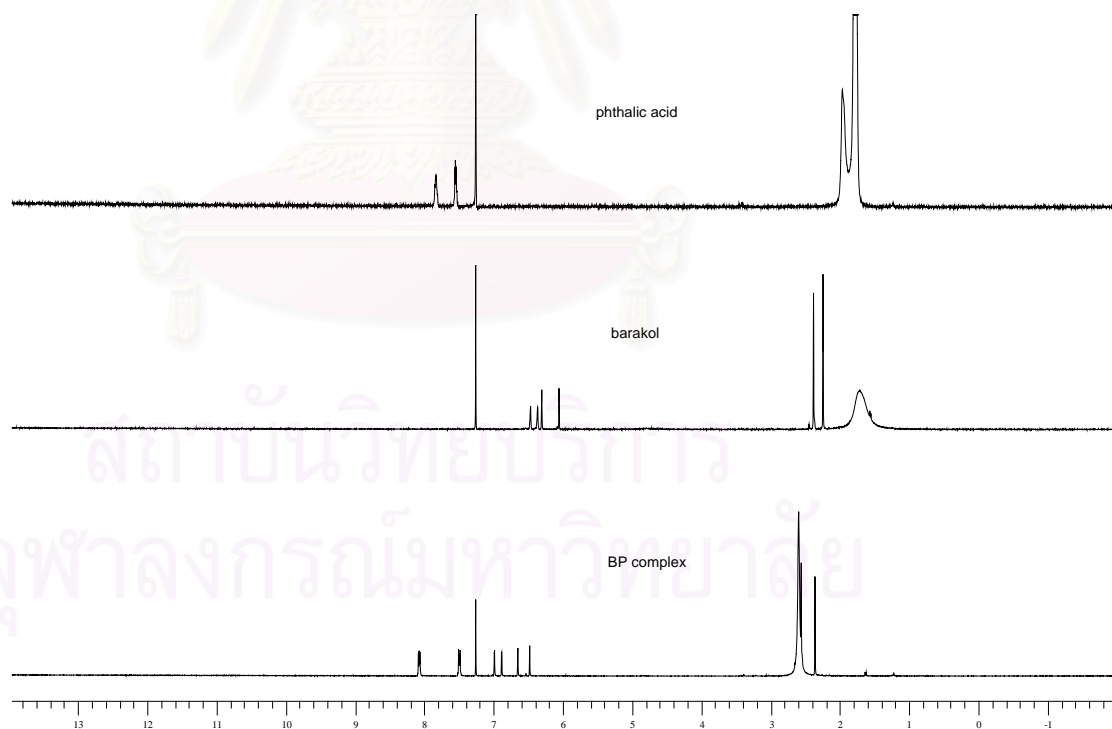


**Figure 4.16**  $^1\text{H-NMR}$  spectra of barakol, phthalic acid and BP

The chemical shift of aromatic proton at 7.70 ppm (free phthalic acid) was shifted to downfield at 8.07 ppm (phthalate) ( $\Delta\delta_{\text{H}} = 0.37$  ppm). In contrast, the aromatic proton at 7.49 ppm (free phthalic acid) shifted upfield to 7.45 ppm (phthalate) due to anisotropic effects, arising from the stacking of phthalic acid and barakol in the BP complex. The  $^1\text{H-NMR}$  titration was used to observe the changing of chemical shifts of barakol and phthalic acid.

In  $^1\text{H-NMR}$  titration, barakol was protonated by phthalic acid and converted to barakol salt, and then co-crystallized with phthalate forming a stacking dimer, resulting in anisotropic effects at the aromatic protons of both components. Therefore, the chemical shifts of all protons in barakol and phthalate were shifted to downfield. However, the chemical shifts of barakol further shifted downfield as more phthalic acid was added until the mole ratio of phthalic acid and barakol is 1:1. This ratio is the same as the ratio of the 1:1 ion-pair co-crystallized complex of barakol and phthalic acid.

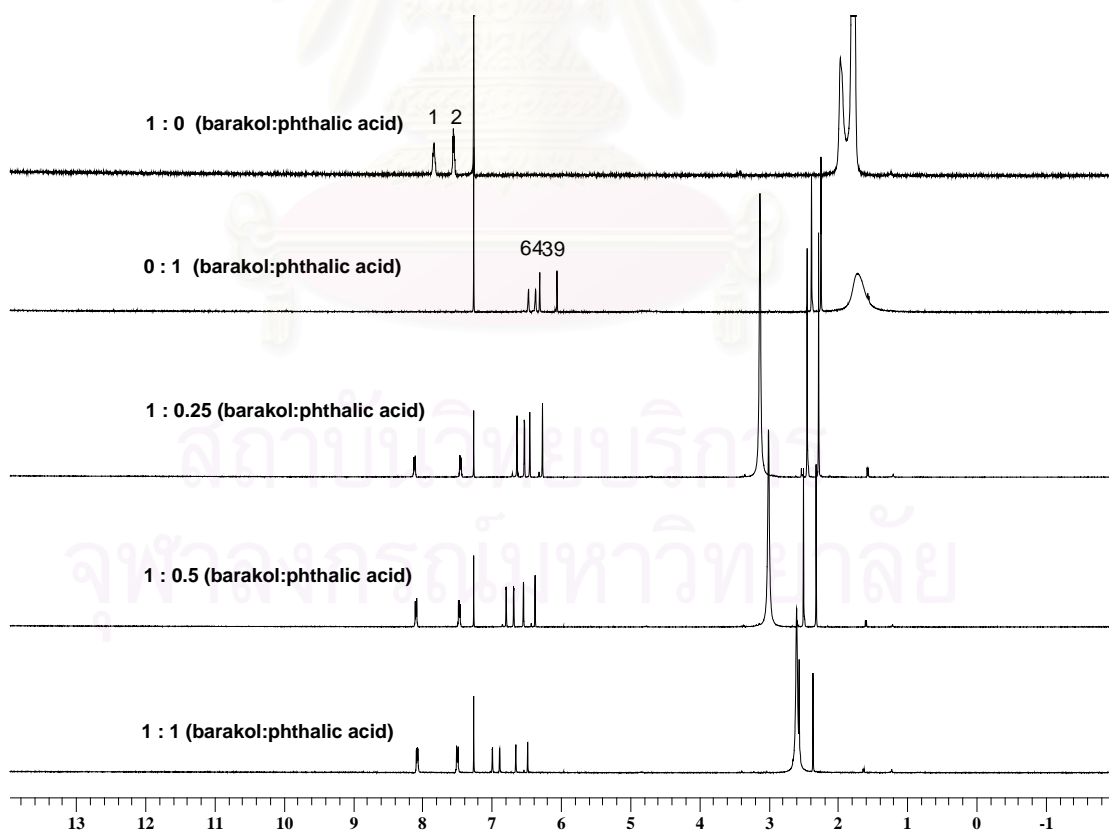


**Figure 4.17**  $^1\text{H-NMR}$  titration of the mixture of barakol and phthalic acid at various mole ratios

The aromatic protons at H4 and H6 in barakol were deshielded by the aromatic ring of phthalate. The chemical shifts at H4 and H6 were clearly shifted to downfield due to decreasing of electron density and anisotropic effects. The aromatic proton at H3 in barakol was deshield because the position is close to a carbonyl group of phthalate. The aromatic proton at H9 and methyl proton in barakol was not changed significantly due to the less influence of the  $\pi$ - $\pi$  stacking.



สถาบันวิทยบริการ  
จุฬาลงกรณ์มหาวิทยาลัย

#### 4.5 Barakol-3-hydroxybenzoic acid (BH)

The reaction of barakol and 3-hydroxybenzoic acid in hot methanol gave yellow needle crystals. mp 212°C (Found: C 62.82%, H 4.92%, calculated for C<sub>22</sub>H<sub>24</sub>O<sub>8</sub> : C 63.46%, H 5.77%)

The obtained yellow crystals (BH) were characterized by UV-vis, FT-IR, NMR and X-ray analysis.

##### 4.3.4 Crystallographic study of barakol-3-hydroxybenzoic acid (BH)

Suitable single crystals of BH were recrystallized from methanol by slow evaporation. X-ray diffraction data were collected at room temperature on Enraf-Nonius Kappa CCD area detector<sup>33</sup>. The collected data were reduced using Denzo and Scalepak<sup>34</sup>. Accurate lattice parameters were determined from least squares refinements of well-centered reflections in the ranges  $3.24 \leq \theta \leq 26.36$ . A total of 2289 reflections were measured, of which 2156 reflections ( $R_{(int)}=0.0322$ ) were unique. The crystallographic data are presented in Table 4.17. The structure was solved by direct methods and refined with anisotropic displacement parameters for all non hydrogen atoms by full matrix least-squares using the SHELX-97 package for PC<sup>28</sup>. The hydrogen atoms were found from different Fourier maps, and were included in a refinement with isotropic displacement parameters. The final refinement gave  $R_1 = 0.1043$  and  $wR_2 = 0.3013$  [ $I > 2\sigma(I)$ ]. The R factors are high probably due to the disorder of methanol solvent molecules. The crystal structure of BH is crystallized in a orthorhombic crystal system, space group *Pnn2* with the unit cell dimensions of  $a = 16.9520(3)$  Å,  $b = 17.0560(11)$  Å,  $c = 6.7610(11)$  Å,  $Z = 4$ . An ORTEP<sup>35</sup> drawing with atomic labeling is shown in Figure 4.19. Bond lengths and angles are given in Table 4.18. Atomic coordinates and equivalent isotropic displacement parameter are listed in Table D.1.

The X-ray analysis shows that the crystal structure of barakol and 3-hydroxybenzoic acid (BH) comprises of one barakol ring, one 3-hydroxybenzoic acid and two methanol molecules. For barakol molecule, no hydrogen atom connected to O3 in barakol found from the difference Fourier maps, therefore, the functional group of C5-O3 is carbonyl group. Consequently, the barakol moiety is anhydrobarakol, thus BH is 1:1 pi-pi molecular complex. However, the C5-O3 distance of 1.295(5) Å

is slightly longer than that of BA (1.285 Å), longer than the normal C=O distance (1.22Å), and shorter than the typical C(*sp*<sup>2</sup>)-OH distance (1.44Å). It is probably due to the C5=O3 forming strong intermolecular hydrogen bonding with the hydroxyl group of 3-hydroxybenzoic acid, resulting in the elongation of C5=O [O3...O2a, 2.559 (5)Å]. The details of hydrogen bonding geometry are given in Table A.6. The formation of BH is solely stabilized by  $\pi$ - $\pi$  interactions between the  $\pi$ -delocalized electrons within the rings of anhydrobarakol and 3-hydroxybenzoic acid. The molecular packing of BH (Figure 4.20) shows that the acid molecule are located between the barakol planes with the interplanar distances of 3.42 Å, forming a mixed stack columnar. The methanol molecules are disorder. They are located in the large cavity from by the molecular stack columnars.

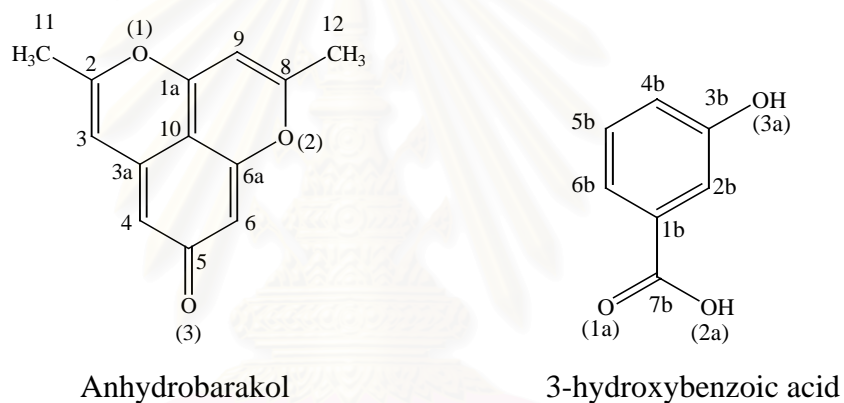


**Figure 4.18** Chemical structures of anhydrobarakol<sup>31-32</sup> and 3-hydroxybenzoic acid, with atomic numbering

สถาบันวิทยบริการ  
จุฬาลงกรณ์มหาวิทยาลัย



**Table 4.17** Crystal and experimental data of BH

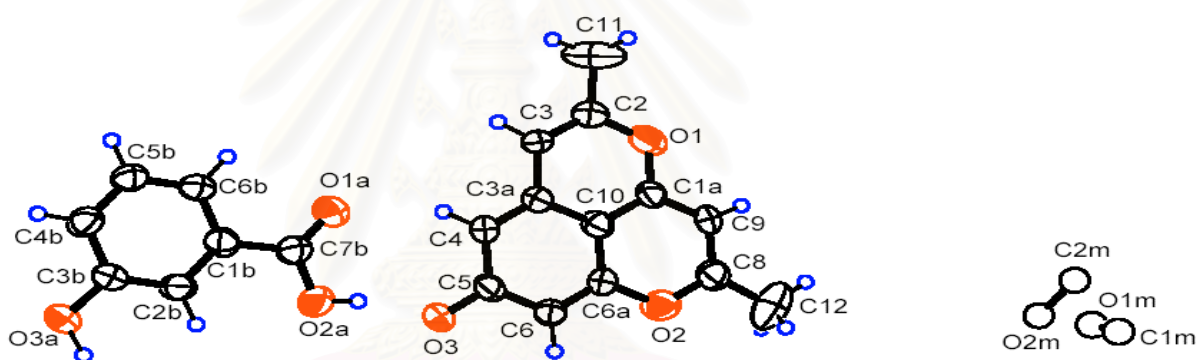
Formula	$C_{13}H_{10}O_3 \cdot C_7H_6O_3 \cdot 2CH_3OH$
Formula weight	416.34
X-rays	Mo $K_{\alpha}$
Wavelength, (Å)	0.71073
Crystal system	orthorhombic
Space group	$Pnn2$
Z	4
a, (Å)	16.9520(3)
b, (Å)	17.0560(11)
c, (Å)	6.7610(11)
V, (Å <sup>3</sup> )	1954.8(3)
$D_{cal}$ , (g/cm <sup>3</sup> )	1.330
Absorption coefficient ( $\mu$ ), (mm <sup>-1</sup> )	0.102
Crystal size, (mm)	0.27 x 0.32 x 0.41
reflections collected/unique	2289/2156 [ $R(int) = 0.03$ ]
Refinement method	Full-matrix least-squares on $F^2$
Goodness-of-fit on $F^2$	1.365
Final R indices [ $I > 2\sigma(I)$ ]	$R_1 = 0.1043$ , $wR_2 = 0.3013$
R indices(all data)	$R_1 = 0.1274$ , $wR_2 = 0.3356$

**Table 4.18** Bond lengths (Å) and angles (°) for BH.

C(1A)-O(1)	1.352(6)	C(3A)-C(10)	1.397(6)
C(1A)-C(9)	1.368(7)	C(3B)-O(3A)	1.359(5)
C(1A)-C(10)	1.394(6)	C(3B)-C(4B)	1.391(6)
C(1B)-C(2B)	1.393(6)	C(4)-C(5)	1.433(6)
C(1B)-C(6B)	1.397(6)	C(4B)-C(5B)	1.376(7)
C(1B)-C(7B)	1.481(6)	C(5)-O(3)	1.295(5)
C(2)-C(3)	1.352(7)	C(5)-C(6)	1.405(7)
C(2)-O(1)	1.372(7)	C(5B)-C(6B)	1.373(7)
C(2)-C(11)	1.476(7)	C(6)-C(6A)	1.362(6)
C(2B)-C(3B)	1.375(7)	C(6A)-O(2)	1.367(6)
C(2M)-O(2M)	1.29(5)	C(6A)-C(10)	1.425(6)
C(3)-C(3A)	1.428(6)	C(7B)-O(1A)	1.203(6)
C(3A)-C(4)	1.353(6)	C(7B)-O(2A)	1.307(5)
O(1)-C(1A)-C(9)	118.8(4)	C(5B)-C(4B)-C(3B)	119.9(4)
O(1)-C(1A)-C(10)	120.2(4)	O(3)-C(5)-C(6)	120.8(4)
C(9)-C(1A)-C(10)	121.0(4)	O(3)-C(5)-C(4)	120.5(4)
C(2B)-C(1B)-C(6B)	120.2(4)	C(6)-C(5)-C(4)	118.6(4)
C(2B)-C(1B)-C(7B)	122.9(4)	C(6B)-C(5B)-C(4B)	121.0(4)
C(6B)-C(1B)-C(7B)	116.9(4)	C(6A)-C(6)-C(5)	121.0(4)
C(3)-C(2)-O(1)	121.5(4)	C(6)-C(6A)-O(2)	121.4(4)
C(3)-C(2)-C(11)	125.0(5)	C(6)-C(6A)-C(10)	119.9(4)
O(1)-C(2)-C(11)	113.4(5)	O(2)-C(6A)-C(10)	118.6(4)
C(3B)-C(2B)-C(1B)	119.7(4)	C(5B)-C(6B)-C(1B)	119.1(4)
C(2)-C(3)-C(3A)	121.6(4)	O(1A)-C(7B)-O(2A)	121.7(4)
C(4)-C(3A)-C(10)	121.4(4)	O(1A)-C(7B)-C(1B)	122.4(4)
C(4)-C(3A)-C(3)	123.7(4)	O(2A)-C(7B)-C(1B)	115.9(4)
C(10)-C(3A)-C(3)	114.8(4)	O(2)-C(8)-C(9)	120.4(4)
O(3A)-C(3B)-C(2B)	123.5(4)	O(2)-C(8)-C(12)	115.1(5)
O(3A)-C(3B)-C(4B)	116.4(4)	C(9)-C(8)-C(12)	124.3(5)
C(2B)-C(3B)-C(4B)	120.0(4)	C(1A)-C(9)-C(8)	119.4(4)

**Table 4.18** (continuous) Bond lengths (Å) and angles (°) for BH.

C(3A)-C(4)-C(5)	119.9(4)	C(3A)-C(10)-C(6A)	119.0(4)
C(3A)-C(4)-H(4)	120.7	C(1A)-O(1)-C(2)	119.4(4)
C(5)-C(4)-H(4)	119.3	C(8)-O(2)-C(6A)	121.7(4)
C(1A)-C(10)-C(3A)	122.3(4)		
C(1A)-C(10)-C(6A)	118.7(4)		



สถาบันวิทยบริการ  
จุฬาลงกรณ์มหาวิทยาลัย

**Figure 4.19** An ORTEP drawing of BH, showing 50 % probability displacement ellipsoids

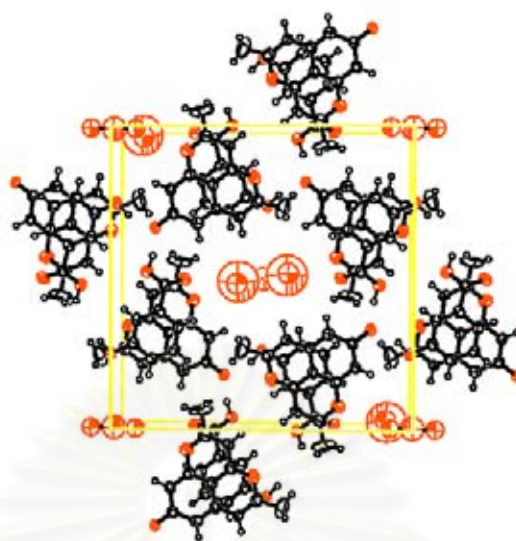


**Figure 4.20** Crystal packing diagram of barakol and 3-hydroxybenzoic acid (BH), viewed along  $a$ -axis, hydrogen atoms were omitted for clarity.



**Figure 4.21**  $\pi$ - $\pi$  interactions of barakol-3-hydroxybenzoic acid (BH)

#### 4.5.2 Spectroscopic studies of BH

The BH complex was characterized by UV-vis,  $^1\text{H-NMR}$  and IR spectroscopic techniques.

The UV-vis absorption data of BH in ethanol are given in Table 4.19. The UV-vis spectrum of BH in ethanol shows the absorption bands at 202, 240, 286, 376 nm. The molecular absorptivities ( $\log \epsilon$ ) of BH are in range of 3.34-4.17, were assigned to  $\pi$ - $\pi^*$  transition. In BH the  $\pi$ - $\pi^*$  absorption bands of barakol and 3-hydroxybenzoic acid in BH were blue shifted from 379 (free barakol) to 376, and 289 (free 3-hydroxybenzoic acid) to 286 nm, respectively. This is probably due to  $\pi$ - $\pi$

interaction between barakol and 3-hydroxybenzoic acid, consistent with the result from X-ray analysis.

The  $^1\text{H-NMR}$  spectra of the BH in  $\text{CDCl}_3+\text{CD}_3\text{OD}$  in Figure 4.23. The chemical shifts corresponding barakol slightly downfield shifted at about 0.3 ppm in relative to free compound The chemical shifts corresponding to 3-hydroxybenzoic acid are slightly upfield shifted at about 0.08 ppm in relative to free compound ( $\Delta\delta_{\text{H}} = 0.06\text{-}0.08$  ppm). This is probably because of anisotropic effects

The IR-spectra of crystalline BH in KBr pellet (Figure E.1) is in an excellent agreement with the crystal structure analysis. The spectrum showed broad absorption bands at  $3300\text{-}2800\text{ cm}^{-1}$  range corresponding to the O-H vibrations relative to the network of intermolecular hydrogen bonds.

**Table 4.19** UV-Vis absorption data of barakol, 3-hydroxybenzoic acid and BH in ethanol (Figure 4.22)

Compound	$\lambda$ , nm (log $\epsilon$ .)
Barakol	242 (4.15) , 250 (4.50) , 379 (3.76)
3-hydroxybenzoic acid	202 (4.15) , 230 (3.36) , 289 (2.84)
BH complex	202 (4.17) ,240 (4.17) ,286 (3.34) , 376 (3.58)

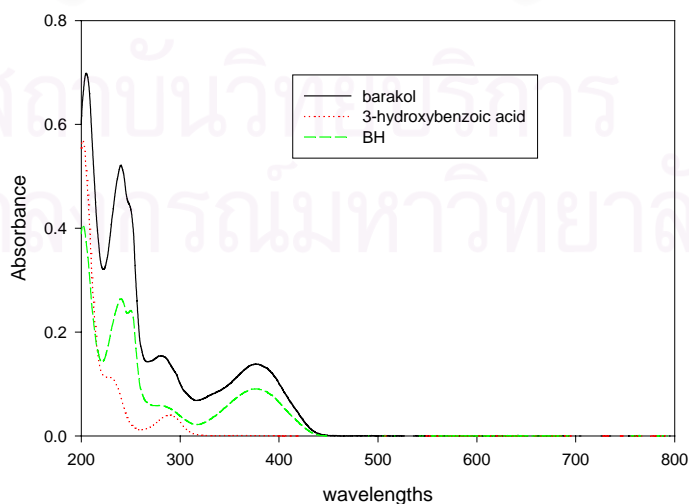


**Figure 4.22** UV-Spectrum of barakol, 3-hydroxybenzoic acid and BH.

**Table.4.20** Selected IR and <sup>1</sup>H-NMR data for barakol, 3-hydroxybenzoic acid and BH

Compound	IR data (cm <sup>-1</sup> )			NMR data (ppm)
	v(O-H)	v(C-O)	v(C=O)	
Barakol	3444 (s,b)	1267 (m)	1670 (s)	2.28,2.32(s,6H)
	3295 (s,b)	1188		6.42,6.35 (s,2x1H) 6.34,6.15 (s,2x1H)
3-hydroxybenzoic	3275 (s,b)	1257 (s)	1699 (s)	7.53(d,1H)
				7.45 (s)
				7.26 (t,1H)
				7.03(d,1H)
BH complexes	3335 (m,b)	1235 (s)	1695 (s)	Barakol
				2.32,2.50 (s,6H)
	3064 (m,b)			6.77,6.70 (s,2H)
				6.62,6.45 (s,2H)
				3-hydroxybenzoic
				7.45 (d,1H)
				7.39 (s)
				7.20(t,2H)
				6.95(d,1H)

สถาบันวิทยบริการ  
จุฬาลงกรณ์มหาวิทยาลัย

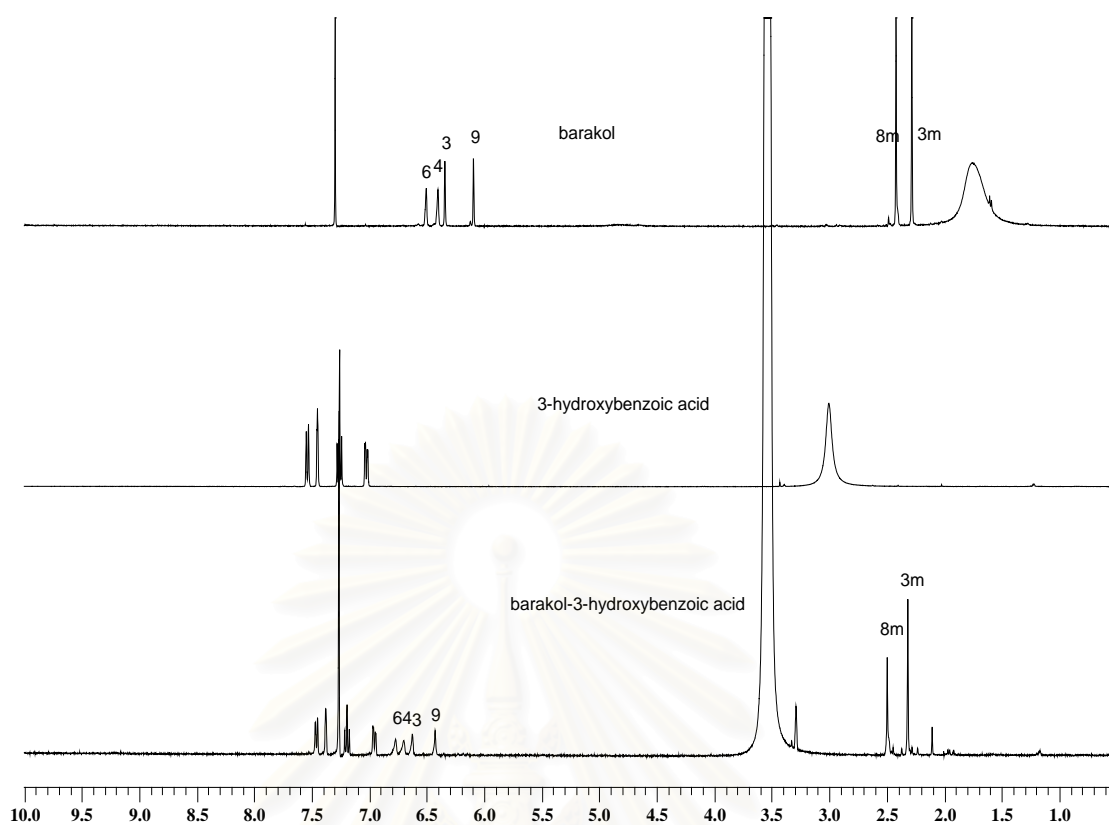


**Figure 4.23** Compared  $^1\text{H-NMR}$  spectra of barakol, 3-hydroxybenzoic acid and BH.

สถาบันวิทยบริการ  
จุฬาลงกรณ์มหาวิทยาลัย

## CHAPTER 5

### Conclusion

A yellow crystalline substance was extracted from young KhiLek leaves and flowers giving 0.15% yield of barakol. The extracted substance was characterized and it was identical to barakol.<sup>6</sup>

This thesis presents the first successful X-ray single crystal analysis of anhydrobarakol and barakol complexes. The novel 1:1 molecular complexes of barakol and carboxylic acid (salicylic acid, phthalic acid and 3-hydroxybenzoic acid) were prepared and characterized by spectroscopic and X-ray diffraction techniques. The suitable single crystals for all complexes were recrystallized from methanol by slow evaporation. The chemical and physical properties including molecular structure, electron distribution of barakol moiety were influenced by the counter anion (acid strength, pKa) and the types of solvents. Table 5.1 shows the summarized X-ray crystallographic results of anhydrobarakol, barakol chloride, the complexes of barakol with phthalic acid and 3-hydroxybenzoic acid. The ORTEP structures of anhydrobarakol, barakol hydrochloride, barakol-phthalic acid (BP) and barakol-3-hydroxybenzoic acid (BH) are given in Figure 5.1.

The X-ray crystallographic studies revealed that barakol ( $C_{13}H_{12}O_4$ ) contains a hemiacetal dioxaphenalene ring structure. This is an unstable form which is easily converted to anhydrobarakol ( $C_{13}H_{10}O_3$ ), a more stable form, by losing a water molecule.

Single crystals of anhydrobarakol (BA) can be obtained by recrystallization of the resulting product of the reaction between barakol and salicylic acid. The crystal structure of anhydrobarakol was then determined. Its molecular structure showed the elongated C=O bond distance of 1.285 (3) Å. It is longer than a normal carbonyl bond (C=O, 1.22 Å), due to the formation of strong hydrogen bonding with water molecules. Therefore, the  $\nu(C=O)$  of the carbonyl group in the IR spectrum of anhydrobarakol ( $1676\text{ cm}^{-1}$ ) is red shifted from that of a typical  $\nu(C=O)$  of aromatic quinone ( $1700\text{ cm}^{-1}$ ).



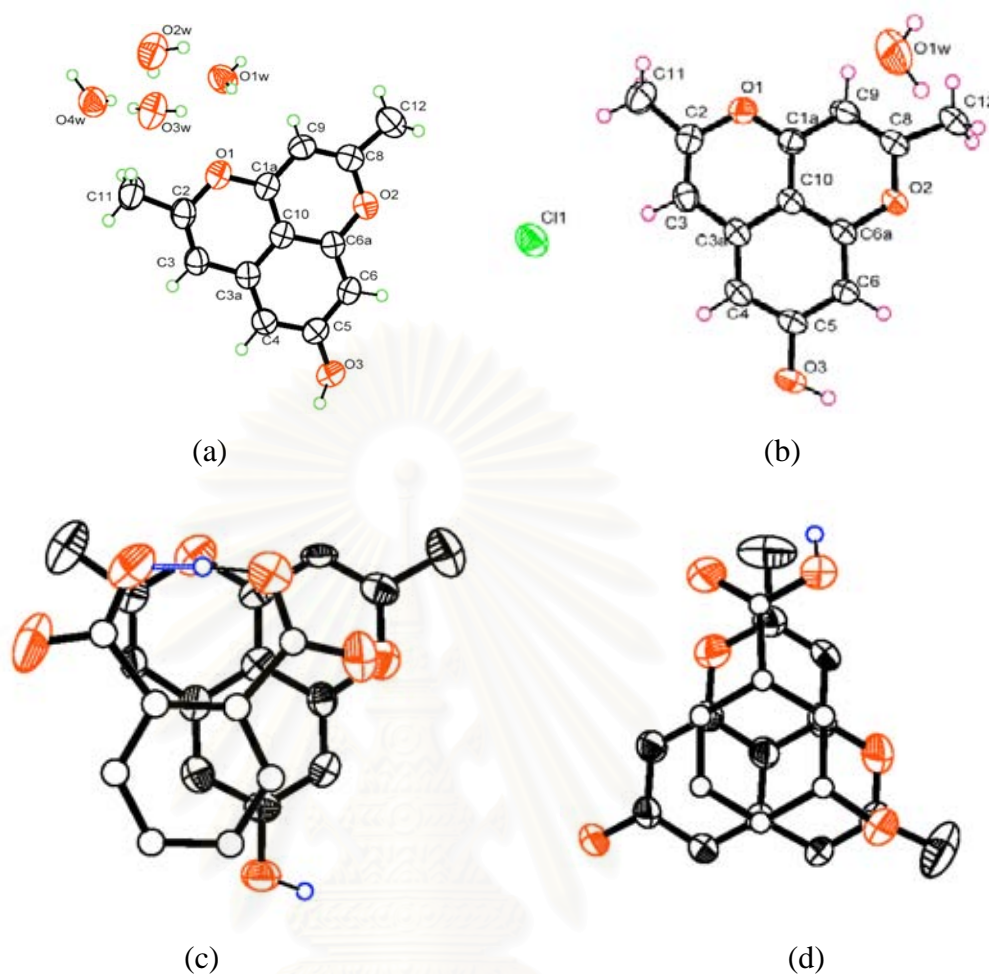


**Figure 5.1** ORTEP structures of (a) anhydrobarakol (b) anhydrobarakol hydrochloride (c) barakol-phthalic acid (BP) (d) barakol-3-hydroxybenzoic acid (BH).

Barakol hydrochloride (BC) is a stable salt form of barakol. Barakol hydrochloride was prepared by adding concentrated hydrochloric acid into barakol dissolved in a minimum amount of methanol. The crystal structure of BC composes of one barakol cation, one chloride anion and one water molecule. The moiety of barakol cation is similar to the barakol cation in barakol-phthalate (BP). The chloride anion participates in an electrostatic interaction with the O1 in the barakol ring [O1...Cl<sup>-</sup>, 3.33(2) Å]. In order to study the electron delocalization within the barakol molecule, the molecular structures, bond lengths and angles of anhydrobarakol (BA) and barakol cation in (BC) are compared. The bond distances of O1-C1a, C10-C3a, C4-C5 are

shorten, and C1a-C10, C3a-C4, C5-O3 are elongated. The rest of bond distances within the ring are comparable to each other.

The reaction of barakol and phthalic acid gave a 1:1 ion-pair complex of barakol cation-hydrogen phthalate (BP). The formation of the BP ion-pair complex was stabilized by the combination of electrostatic and  $\pi$ - $\pi$  interactions.

By contrast, the reaction between barakol and 3-hydroxybenzoic acid (BH) gave a molecular complex of anhydrobarakol-3-hydroxybenzoic acid. The formation of the BH molecular complex was solely stabilized by  $\pi$ - $\pi$  interactions.

As a result, the reactions between barakol and carboxylic acids gave different types of the barakol complexes, depending on the acid being used. The comparison of acid strengths between these three acids (Table 5.2) shows that the acid strength of phthalic acid is the strongest (2.89). Barakol was protonated into barakol cation and then formed an ion-pair complex, giving the same result as when strong acid, such as hydrochloric acid, was used.

**Table 5.1** Comparison of acid strengths ( $pK_a$ ), barakol complexes and types of barakol ring.

Acid	$pK_a$	Complex	Type of barakol ring
HCl	-	Barakol <sup>+</sup> Cl <sup>-</sup>	Barakol cation
Phthalic acid	2.89, 5.51	Barakol-Phthalate	Barakol cation
Salicylic acid	2.97, 13.40	Anhydrobarakol	Anhydrobarakol
3-hydroxybenzoic acid	4.06, 9.92	Anhydrobarakol-3-hydroxybenzoic acid	Anhydrobarakol

The spectroscopic and X-ray crystallographic studies show that the physical properties of barakol, such as <sup>1</sup>H-NMR, IR, and its molecular structures including electron delocalization within the aromatic rings are affected by intermolecular interactions between barakol and the co-complex molecules.

**Table 5.1** Summarized X-ray crystallographic results of anhydrobarakol, barakol chloride, the complexes of barakol with phthalic acid and 3-hydroxybenzoic acid.

	BA	BC	BP	BH
Formula	C <sub>13</sub> H <sub>10</sub> O <sub>7</sub> •4H <sub>2</sub> O	C <sub>13</sub> H <sub>11</sub> O <sub>3</sub> Cl•H <sub>2</sub> O	C <sub>13</sub> H <sub>11</sub> O <sub>3</sub> •C <sub>8</sub> H <sub>5</sub> O <sub>4</sub> •3H <sub>2</sub> O	C <sub>13</sub> H <sub>10</sub> O <sub>3</sub> •C <sub>7</sub> O <sub>3</sub> H <sub>6</sub> •2CH <sub>3</sub> OH
Formula weight	286.22	268.58	434.39	416.34
Crystal system	monoclinic	monoclinic	triclinic	orthrorhombic
Space group	<i>P2<sub>1</sub>/c</i>	<i>P2<sub>1</sub>/n</i>	<i>P(-1)</i>	<i>Pnn2</i>
Z	4	4	2	4
<i>a</i>	13.2280(7) Å	12.2547(2) Å	7.3721(8) Å	16.9520(3) Å
<i>b</i>	6.8738(2) Å	8.051(2) Å	11.3144(2) Å	17.0560(11) Å
<i>c</i>	19.7879(9) Å	12.8133(2) Å	12.4748(14) Å	6.7610(11) Å
$\alpha$	90°	90°	103.765(2)°	90°
$\beta$	127.013(2)°	99.514(1)°	91.893(2)°	90°
$\gamma$	90°	90°	96.752(2)°	90°
<i>V</i>	1436.74(10) Å <sup>3</sup>	1246.79(3) Å <sup>3</sup>	1001.63(19) Å <sup>3</sup>	1954.79(3) Å <sup>3</sup>
<i>D</i> <sub>cal</sub>	1.282 g/cm <sup>3</sup>	1.426 g/cm <sup>3</sup>	1.440 g/cm <sup>3</sup>	1.330 g/cm <sup>3</sup>
Absorption coefficient ( $\mu$ )	0.107 mm <sup>-1</sup>	0.310 mm <sup>-1</sup>	0.116 mm <sup>-1</sup>	0.102 mm <sup>-1</sup>
Crystal size	0.300x0.450x0.275 mm	0.150x0.230x0.325 mm	0.20x0.40x0.32 mm	0.27x0.32x0.41 mm
reflections collected/unique	3565/1935 [R(int) = 0.0153]	9083/3647 [R(int) = 0.0197]	11799/4674 [R(int) = 0.0476]	2289/2156 [R(int) = 0.030]
Goodness-of-fit on F <sup>2</sup>	1.215	1.017	1.084	1.017
Final R indices [I>2 $\sigma$ (I)]	R <sub>1</sub> = 0.0619, wR <sub>2</sub> = 0.1770	R <sub>1</sub> = 0.0410, wR <sub>2</sub> = 0.1071	R <sub>1</sub> = 0.0879, wR <sub>2</sub> = 0.1772	R <sub>1</sub> = 0.1043, wR <sub>2</sub> = 0.3013
R indices(all data)	R <sub>1</sub> = 0.0681, wR <sub>2</sub> = 0.1836	R <sub>1</sub> = 0.0582, wR <sub>2</sub> = 0.1188	R <sub>1</sub> = 0.1572, wR <sub>2</sub> = 0.2052	R <sub>1</sub> = 0.1234, wR <sub>2</sub> = 0.3356

### Further work

The studies in this thesis show many interesting characteristics of barakol. Therefore, there are many possibilities for further research on this substance and its complexes. For examples,

1. The N-heterocyclic series of molecules are interested to cocrystallize with barakol for observing the behavior of charge transfer salt.
2. The calculation of electron distribution by XD package help to consider the electron delocalization of barakol salt.



สถาบันวิทยบริการ  
จุฬาลงกรณ์มหาวิทยาลัย

## References

1. Satyavati, G.V.; Raona, M.K. and Sharmam. **Medicinal Plants of India (Indian Council of Medicinal Research)**. New Delhi, **1979**.
2. Mokasmit, M. **Hypertensive effects of Thai medicinal plants**. *Newslett. Natl. Res. Council Thailand*. **1981**; 22, 3-4.
3. Arunlakshana, O. **Pharmacological study of the leaves of Cassia siamea**. *Siriraj Hosp Gaz*. **1949**; 1, 434-444.
4. Chantarayotha. **Effect of barakol on central nervous system**. Master thesis (M.Sc in pharm.), Department of Physiology, Graduate School, Chulalongkorn University. **1987**.
5. Hassanali-Walji, A.; King, T.J.; Wallwork, S.C. **Barakol, A novel dioxaphenalene derivative from Cassia siamea**. *J. Chem. Soc. Chem. Commum*. **1969**; 12, 678.
6. Bycroft, B.W.; Hassanali-walju A.; Johnson, A.W. and King, J.J. **The structure and synthesis of barakol : a novel dioxaphenalene derivative from Cassia siamea**. *J. Chem. Soc.* **1970**; 12, 1686-1689.
7. Thongsaard, W.; Deachapunya, C.; Pongsakorn, S.; Boyd, E.A.; Bennett, G.W.; Marsden, C.A. **The dioxaphenalene derivative barakol extracted from Cassia siamea : A natural anxiolytic**. *J. Pharmacol* **1995**; 114, 284.
8. Thongsaard, W.; Pongsakorn, S.; Sudsuang, R.; Bennett, G.W.; Kendall, D.A.; Marsden, C.A. **Barakol, a natural anxiolytic inhibits striatal dopamine release but not uptake in vitro**. *Eur. J. Pharmacol.* **1997**; 319, 157-164.
9. Thongsaard, W.; Chainakul, S.; Bennett, G.W.; Marsden, C.A. **Determination of Barakol extracted from Cassia siamea by HPLC with electrochemical detection**. *J. Pharm. Biomed. Anal.* **2001**; 25, 853-859.

10. Colpaert, F.C.; Meert T.F. and Janssen P.A.J. **Behaviour and 5-HT antagonist effects of ritanserin : a pure and selective antagonist of LSD discrimination in rat.** *Psychopharmacology*. **1985**; 86, 45-54.
11. Haefely, W. **The role of GABA in anxiolytic/antidepressant drug action.** Chichester : John Wiley; **1992** : 151-168.
12. Tongroach, P.; Jantarayota, P.; Tantisira, B.; Kanluan, P.; Tongroach, C.; Chaichantipyuth, C. **Barakol, a neuroactive compound from Cassia siamea Proceedings of the first JSPS-NRCT Joint Seminar in Pharmaceutical Sciences : Advances in Research on Pharmacologically active substances from Natural Sources.** Chiangmai, Thailand, **1992** : OP21.
13. Schultz, T.W.; Cronin, M.T.D.; Walder, J.D.; Aptula A.O. **Quantitative structure-activity relationships (QSARS) in toxicology : a historical perspective.** *J. Mol. Struct – (Theochem)*. **2003**; 622, 1-22.
14. Jeffrey G.A. **An Introduction to hydrogen bonding.** New York : Oxford University Press; **1997**.
15. Coppens, P. **X-ray charge densities and chemical bonding.** IUCR texts on crystallography 4. Oxford U.K.: Oxford University Press, **1992**.
16. Jin, Z.M.; Pan, Y.J.; He, L.; Guang, Z.L.; Yu, K.B. **Crystal structure of the 1:2:2 adduct of Piperazine, o-phthalic acid and water.** *Anal. Sci.* **2003**; 19, 336-334.
17. Loring, J.S.; Karlsson, M.; Fawcett, W.R.; Casey, W.H. **Infrared spectra of phthalic acid, the hydrogen phthalate ion, and the phthalate ion in aqueous solution.** *Spectrochim. Acta A.* **2001**; 57, 1635-1642.

18. Rosenfeld, S.M.; Lawler, R.G.; Ward, H.R. **Electron transfer in a New Highly Conducting Donor-Acceptor Complex**. *J. Am. Chem. Soc.* **1973**, February 7, 948-949.
19. Muehldork, A.V.; Engen, D.V.; Warner, J.C. and Hamilton, A.D. **Aromatic-Aromatic Interactions in Molecular Recognition : A family of Artificial Receptors for Thymine That shows both Face-to-Face and Edge-to-Face Orientations**. *J. Am. Chem. Soc.* **1988**; 110, 6561-6562.
20. Kuznetsov A.M. and Ulstrup, J. **Electron Transfer in Chemistry and Biology. An introduction to the theory**. Chichester : Wiley, **1999**.
21. Christopher, A.; Hunter and Jerrmy, K.M. and Sanders. **The Nature of  $\pi$ - $\pi$  interactions**. *J. Am. Chem. Soc.* **1990**; 112, 5525-5534.
22. Tomura, M.; Yamashita, Y. **One-dimensional zigzag chain structures with Intermolecular C-H - -  $\pi$  and C-H - - O Interaction consisted of phthalic acid and pyridine derivatives**. *Chem. Lett.* **2001**; 532.
23. Giacovazzo, C.(ed). **Fundamentals of crystallography**. IUCR texts on crystallography 2. Oxford U.K.: Oxford University Press, **1992**.
24. Clegg, W. **Crystal structure Determination**. Oxford New York. : Yokyo Oxford University Press, **1998**.
25. Weiss, R.J. **X-ray Determination of electron distribution**. Amstersdam : North Holland Publishing Co., **1996**.
26. Koritsanszky, T.S.; Coppens P. **Chemical Applications of X-ray Charge-Density Analysis**. *Chem. Rev.* **2001**; 101, 1583-1627.
27. Farrugia, L.J. **WinGX package**. *J. Appl. Cryst.* **1999**; 32, 837-838
28. Sheldrick, G.M. **SHELX-97**. Germany: University of Gottingen, **1997**.

29. Chaichantipyuth, C. **A phytochemical study of the leaves of *Cassia siamea* Lamk. and *Cassia spectabilis* DC.** Master's Thesis, Chulalongkorn University. **1978.**
30. Jones P.G. **Crystal growing.** *Chem in Brist.* **1981**; 17, 222-225.
31. Teeyapant, R.; Srikun, O.; Wray, V. and Witte, L. **Chemical investigation of anhydrobarakol from *Cassia*.** *Fititerapia.* **1998**; 69, 475-476.
32. Subhadhirasakul, S.; Khomfang, P. **Screening of barakol from *Cassia* plants and some of its biological activites.** *J.Sci.Technol.* **2000**; 22(4), Oct-Dec.
33. Mackay, s.; Gilmore, C.J.; Edwards, C.; Stewart, N. & Shankland, K. **maXus Computer Progeam for the Solution and Refinement of Crystal Structures.** Buker Nonius, The Netherlands, Macscience, Japan & The university of Glasgow. **1990.**
34. Otwinowski, Z. and Minor, W. **In Methods in Enzymology, 276, edited by C.W. Carter, Jr. & R.M.Sweet .** Now York : Academic Press. **1997**; 307-326.
35. Johnson, C.K. and Bernett, M.N. **ORTEP-3 for windows U.K. :** University of Glasgow, **1996.**
36. SAINT. **Data Integration Software, Version 4.0.** Madison, Wisconsin, USA : Bruker AXS, Inc. **1997.**
37. Sheldrick, G.M. **SADABS, Program for Empirical Absorption Correction of Area detector Data.** Germany: University of Gottingen, **1996.**





APPENDIX

สถาบันวิทยบริการ  
จุฬาลงกรณ์มหาวิทยาลัย

**Table A.1** Fractional atomic coordinates ( $\times 10^4$ ) and equivalent isotropic displacement parameters ( $\text{\AA}^2 \times 10^3$ ) for Anhydrobarakol.  $U_{\text{eq}}$  is defined as one third of the trace of the orthogonalized  $U_{ij}$  tensor.

	x	y	z	$U_{\text{eq}}$
C(1A)	3695(2)	2125(3)	4018(2)	44(1)
C(2)	4588(3)	2244(4)	3285(2)	52(1)
C(3)	5731(3)	2590(4)	3993(2)	49(1)
C(3A)	5956(2)	2744(3)	4800(2)	43(1)
C(4)	7101(2)	3102(4)	5566(2)	47(1)
C(5)	7215(2)	3187(3)	6330(2)	45(1)
C(6)	6105(2)	2905(3)	6283(2)	46(1)
C(6A)	4970(2)	2573(3)	5521(2)	41(1)
C(8)	2762(2)	1965(4)	4727(2)	50(1)
C(9)	2618(2)	1867(3)	3993(2)	46(1)
C(10)	4861(2)	2475(3)	4766(1)	41(1)
C(11)	4231(3)	2032(5)	2418(2)	72(1)
C(12)	1737(3)	1714(5)	4826(2)	75(1)
O(1)	3542(2)	2018(3)	3277(1)	53(1)
O(2)	3907(2)	2311(3)	5482(1)	51(1)
O(1W)	247(2)	9911(4)	2108(2)	79(1)
O(3)	8289(2)	3515(3)	7046(1)	58(1)
O(2W)	611(3)	1758(4)	1052(1)	82(1)
O(3W)	1798(2)	5315(3)	1648(1)	81(1)
O(4W)	1443(2)	8470(3)	646(1)	75(1)

**Table A.2** Hydrogen-bond lengths (Å) for Anhydrobarakol (BA)

D-H...A	d(D-H)	d(H...A)	d(D...A)	<(DHA)
O(2W)-H(2WB)...O(1)	0.93(8)	2.96(2)	3.727(19)	167.61(3)
O(2W)-H(2WB)...O(3W)	0.95(5)	2.21(5)	2.765(8)	155.33(4)
O(3W)-H(3WB)...O(4W)	0.94(5)	2.49(8)	2.781(5)	97.94(6)
O(3W)-H(3WA)...O3#1	0.98(5)	1.92(8)	2.774(4)	145.27(3)
O(2W)-H(2WA)...O(1W)#2	0.96(5)	2.29(5)	2.727(5)	105.83(5)
O(1W)-H(1WA)...O1#3	0.96(5)	2.83(8)	3.782(5)	156.46(5)
O(1W)-H(1WB)...O3#4	0.98(2)	1.80(5)	2.741(6)	160.14(5)

Symmetry transformations used to generate equivalent atoms:

#1  $-x+1, -y+1, -z+1$  #2  $x,+y-1,+z$  #3  $x, +y+1, +z$  #4  $x-1, -y+1/2, +z-1/2$

สถาบันวิทยบริการ  
จุฬาลงกรณ์มหาวิทยาลัย

**Table B.1** Fractional atomic coordinates ( $\times 10^4$ ) and equivalent isotropic displacement parameters ( $\text{\AA}^2 \times 10^3$ ) for anhydrobarakol hydrochloride (BC).  $U_{\text{eq}}$  is defined as one third of the trace of the orthogonalized  $U_{ij}$  tensor.

	x	y	z	$U_{\text{eq}}$
C(1A)	4218(1)	-1552(2)	6535(1)	36(1)
C(2)	5901(1)	-195(2)	7155(1)	41(1)
C(3)	6350(1)	-742(2)	6343(1)	40(1)
C(3A)	5741(1)	-1759(2)	5533(1)	35(1)
C(4)	6122(1)	-2369(2)	4654(1)	39(1)
C(5)	5425(1)	-3336(2)	3920(1)	37(1)
C(6)	4341(1)	-3705(2)	4038(1)	36(1)
C(6A)	3973(1)	-3105(2)	4917(1)	33(1)
C(8)	2530(1)	-2916(2)	5917(1)	41(1)
C(9)	3138(1)	-1957(2)	6658(1)	43(1)
C(10)	4647(1)	-2138(2)	5671(1)	33(1)
C(12)	1387(1)	-3495(3)	5915(2)	58(1)
C(11)	6421(2)	858(2)	8045(2)	53(1)
O(3)	5850(1)	-3904(2)	3095(1)	49(1)
O(1)	4819(1)	-592(1)	7256(1)	41(1)
O(2)	2926(1)	-3481(1)	5059(1)	39(1)
Cl(1)	9189(1)	804(1)	6613(1)	57(1)
O(1W)	1267(2)	1667(3)	5465(2)	103(1)

**Table B.2** Hydrogen-bond lengths ( $\text{\AA}$ ) for anhydrobarakol hydrochloride(BC)

D-H...A	d(D-H)	d(H...A)	d(D...A)	$\angle(\text{DHA})$
O(1W)-H(1WA)...Cl(1)#1	0.80(3)	2.43(3)	3.2210(19)	168.2(3)
O(1W)-H(1WB)...Cl(1)#2	0.97(5)	2.33(5)	3.296(2)	177.6(4)
O3-H(-3)...Cl(1)#3	0.94(2)	2.03(2)	2.969(2)	175.8(5)

Symmetry transformations used to generate equivalent atoms:

#1  $x-1, y, z$  #2  $-x+1, -y, -z+1$  #3  $x-1/2, -y-1/2, +z-1/2$

**Table C.1** Fractional atomic coordinates ( $\times 10^4$ ) and equivalent isotropic displacement parameters ( $\text{\AA}^2 \times 10^3$ ) for barakol-phthalate (BP)  $U_{\text{eq}}$  is defined as one third of the trace of the orthogonalized  $U_{ij}$  tensor.

	x	y	z	$U_{\text{eq}}$
O(1W)	3637(4)	8237(3)	6991(3)	56(1)
O(2W)	-1604(5)	8583(3)	-669(3)	84(1)
O(3W)	-1225(5)	10497(3)	1789(3)	80(1)
C(1A)	4410(4)	1968(3)	6781(3)	42(1)
C(2)	5714(5)	1905(4)	8531(3)	47(1)
C(3)	5946(5)	3109(4)	8827(4)	36(1)
C(3A)	5437(4)	3868(3)	8167(3)	37(1)
C(4)	5641(5)	5119(3)	8459(3)	42(1)
C(5)	5025(4)	5762(3)	7720(3)	40(1)
C(6)	4251(5)	5152(3)	6666(3)	42(1)
C(6A)	4069(4)	3907(3)	6376(3)	36(1)
C(8)	3062(5)	2006(3)	5060(3)	45(1)
C(9)	3634(6)	1378(4)	5757(4)	40(1)
C(10)	4639(4)	3230(3)	7105(3)	38(1)
C(11)	6202(7)	1076(5)	9214(4)	82(2)
C(12)	2145(6)	1404(4)	3961(3)	72(1)
O(1)	4929(4)	1293(2)	7482(2)	62(1)
O(2)	3274(3)	3253(2)	5348(2)	54(1)
O(3)	5219(4)	6980(2)	8069(2)	56(1)
C(1B)	640(4)	6154(3)	3272(3)	38(1)
C(2B)	-116(4)	6269(3)	2247(3)	39(1)
C(3B)	-672(5)	5194(4)	1439(3)	53(1)
C(4B)	-543(5)	4044(4)	1596(4)	58(1)
C(5B)	131(5)	3951(4)	2611(4)	57(1)
C(6B)	706(5)	4982(4)	3415(3)	47(1)
C(7B)	1453(5)	7169(4)	4255(3)	48(1)
C(8B)	-442(5)	7426(4)	1899(3)	52(1)
O(1A)	2133(5)	6880(3)	5044(2)	80(1)
O(2A)	1448(4)	8284(3)	4244(3)	73(1)
O(3A)	-8(5)	8466(3)	2551(3)	76(1)
O(4A)	-1178(5)	7325(3)	987(3)	96(1)

**Table C.2** Hydrogen-bond lengths (Å) for barakol-phthalate(BP)

D-H...A	d(D-H)	d(H...A)	d(D...A)	<(DHA)
O(3W)-H(3WB)...O(2W)#1	0.86(7)	1.94(7)	2.786(5)	168(6)
O(3W)-H(3WA)...O(3A)	1.00(6)	1.95(6)	2.908(5)	161(4)
O(3W)-H(3WA)...O(4A)	1.00(6)	2.63(5)	3.494(5)	145(4)
O(2A)-H(23)...O(3A)	1.18(6)	1.22(6)	2.400(4)	174(5)
O(3)-H(33)...O(1W)	0.99(5)	1.56(5)	2.528(4)	165(4)
O(1W)-H(1WA)...O(1A)	0.96(5)	1.73(5)	2.671(4)	166(4)
O(1W)-H(1WB)...O(3W)#2	0.84(6)	1.86(6)	2.696(5)	178(6)
O(2W)-H(2WA)...O(4A)	0.98(6)	1.85(6)	2.803(5)	162(5)
O(2W)-H(2WB)...O(3)#3	1.29(9)	1.68(9)	2.941(4)	166(6)

Symmetry transformations used to generate equivalent atoms:

#1 -x,-y+2,-z #2 -x,-y+2,-z+1 #3 x-1, y, z-1

สถาบันวิทยบริการ  
จุฬาลงกรณ์มหาวิทยาลัย

**Table D.1** Fractional atomic coordinates ( $\times 10^4$ ) and equivalent isotropic displacement parameters ( $\text{\AA}^2 \times 10^3$ ) for barakol-3-hydroxybenzoic acid (BH).  $U_{\text{eq}}$  is defined as one third of the trace of the orthogonalized  $U_{ij}$  tensor.

	x	y	z	$U_{\text{eq}}$
C(1A)	3967(2)	3644(3)	376(11)	46(1)
C(1B)	1538(3)	-1102(3)	385(12)	48(1)
C(1M)	4031(6)	9989(19)	9920(80)	990(160)
C(2)	4825(3)	2560(3)	420(15)	53(1)
C(2B)	769(3)	-1389(3)	394(12)	49(1)
C(2M)	5000	10000	4840(20)	57(9)
C(3)	4212(2)	2054(3)	359(12)	46(1)
C(3A)	3414(2)	2320(3)	387(11)	45(1)
C(3B)	640(2)	-2184(3)	333(13)	50(1)
C(4)	2782(3)	1835(3)	380(15)	51(1)
C(4B)	1275(3)	-2699(3)	377(14)	56(1)
C(5)	2000(2)	2155(3)	386(14)	50(1)
C(5B)	2033(3)	-2412(3)	346(14)	55(1)
C(6)	1910(2)	2974(3)	369(14)	49(1)
C(6A)	2549(3)	3458(2)	403(13)	45(1)
C(6B)	2176(3)	-1620(3)	365(13)	50(1)
C(7B)	1725(3)	-253(3)	378(14)	54(1)
C(8)	3103(3)	4742(3)	313(14)	55(1)
C(9)	3861(2)	4439(3)	369(12)	48(1)
C(10)	3324(2)	3135(3)	393(13)	45(1)
C(11)	5664(3)	2333(5)	375(18)	101(3)
C(12)	2915(6)	5584(4)	288(19)	100(2)
O(1)	4710(2)	3357(2)	391(10)	66(1)
O(1A)	2391(2)	-11(2)	377(17)	90(2)
O(1M)	4112(10)	9823(8)	11160(60)	351(19)
O(2)	2466(2)	4255(2)	392(11)	65(1)
O(2A)	1119(2)	220(2)	359(11)	67(1)
O(2M)	4390(30)	9860(30)	5910(90)	240(30)
O(3)	1391(2)	1697(2)	357(12)	63(1)
O(3A)	-91(2)	-2512(2)	371(16)	74(1)
O(3M)	4314(18)	10050(20)	5020(50)	65(19)

**Table D.2** Hydrogen-bond lengths (Å) for barakol-3-hydroxybenzoic acid (BH)

D-H...A	d(D-H)	d(H...A)	d(D...A)	<(DHA)
O(2A)-H(2A)...O(3)	0.85	1.8	2.559(5)	148.4
O(3A)-H(3A)...O(3)#2	0.98	1.71	2.606(5)	150.2

Symmetry transformations used to generate equivalent atoms:

#1 -x+1, -y+2, z #2 -x, -y, z



สถาบันวิทยบริการ  
จุฬาลงกรณ์มหาวิทยาลัย



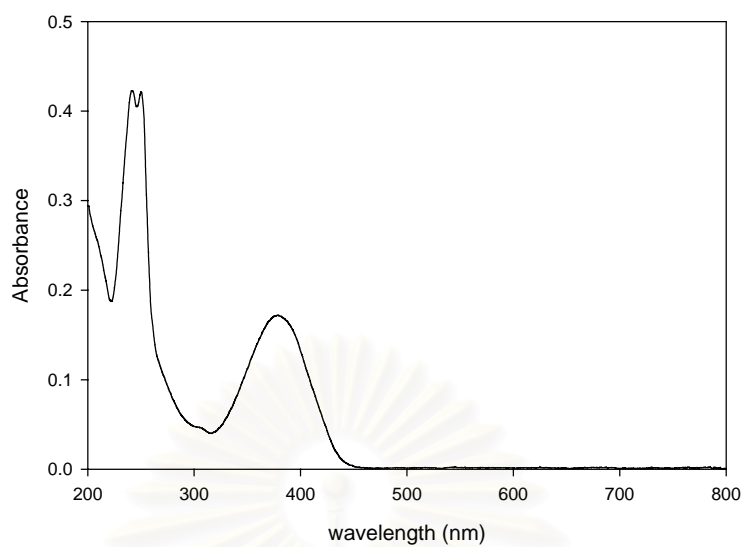


Figure A.1 The UV spectrum of extracted barakol in ethanol

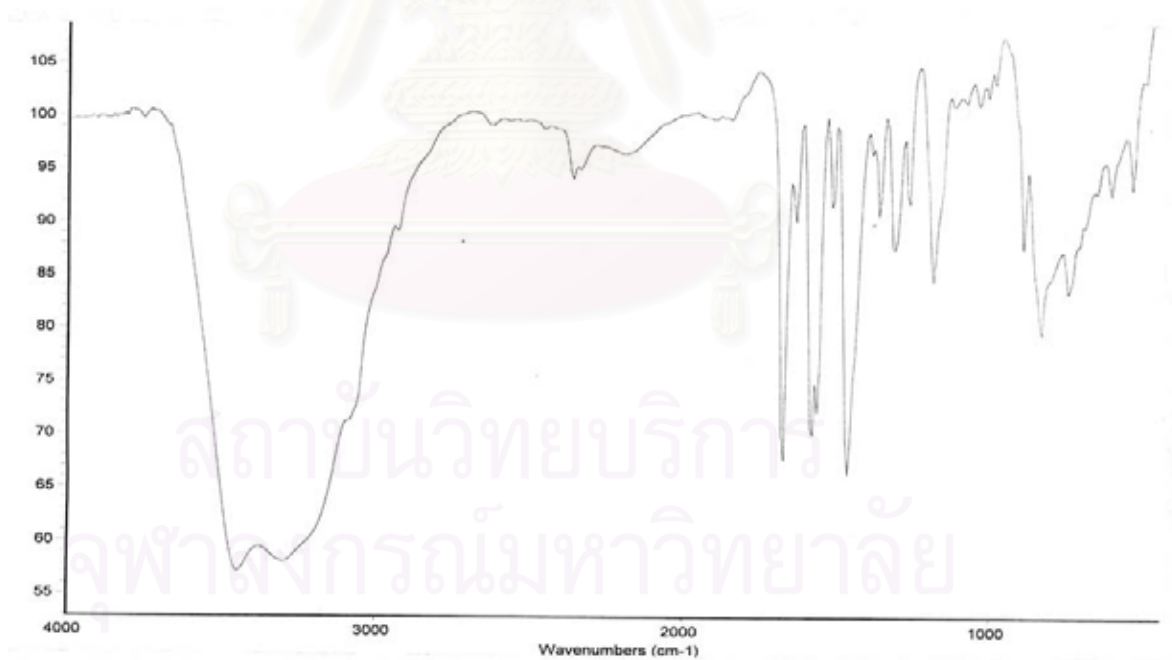


Figure A.2 The IR spectrum of barakol in KBr

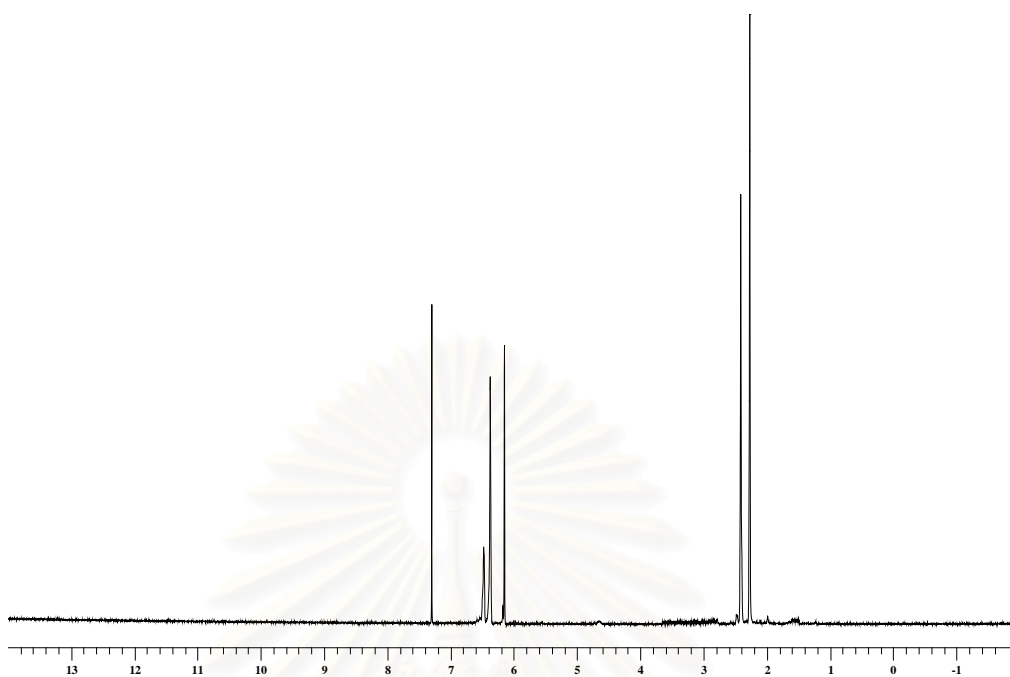


Figure A.3 The  $^1\text{H}$ -NMR spectrum of extracted barakol in  $\text{CDCl}_3$

```
=====
Archive directory: /export/home/vmruser/vmrsgs/data
Sample directory: ms84_2153-65-27
F110: CARBON

Pulse Sequence: szpul
Solvent: CDCl3
Temp: 18.3 C / 291.2 K
Relax. delay 1.000 sec
Pulse 45.3 degrees
Acq. time 1.119 sec
Width 25125.6 Hz
312 repetitions
OBSERVE F1, 101.5486226 MHz
DECOUPLE H1, 399.8464144 MHz
Power 28 dB
continuously on
WALTZ-16 modulated
Line Broadening 1.0 Hz
FT size 65536
Total time 19 min
```

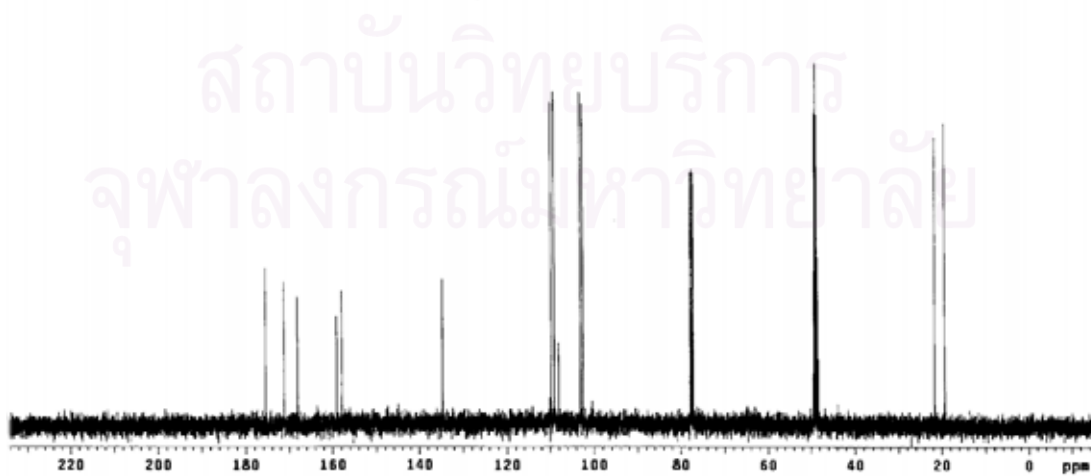


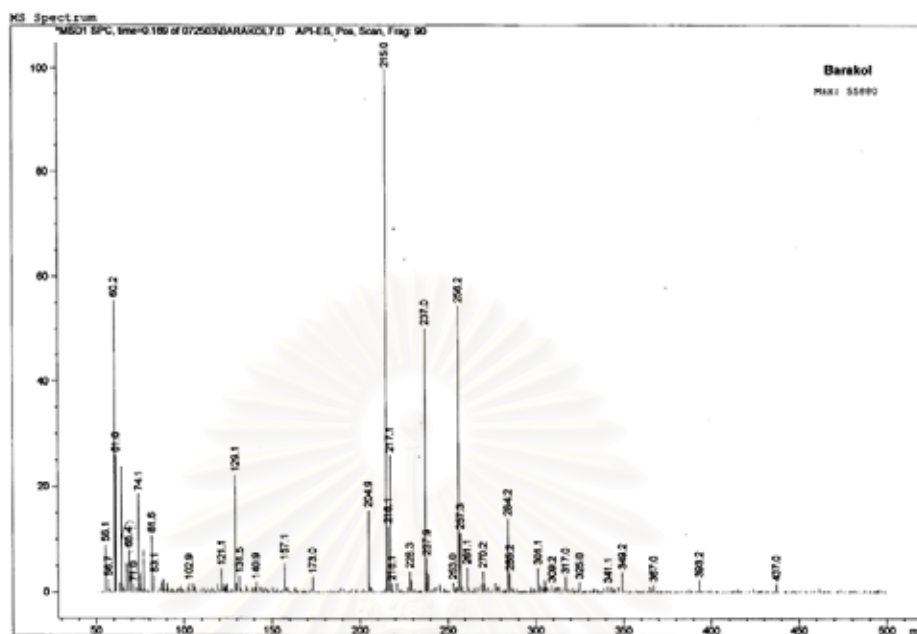
Figure A.4 The  $^{13}\text{C}$ -NMR of extracted barakol in  $\text{CDCl}_3$ 

Figure A.5 The Mass spectrum of extracted barakol

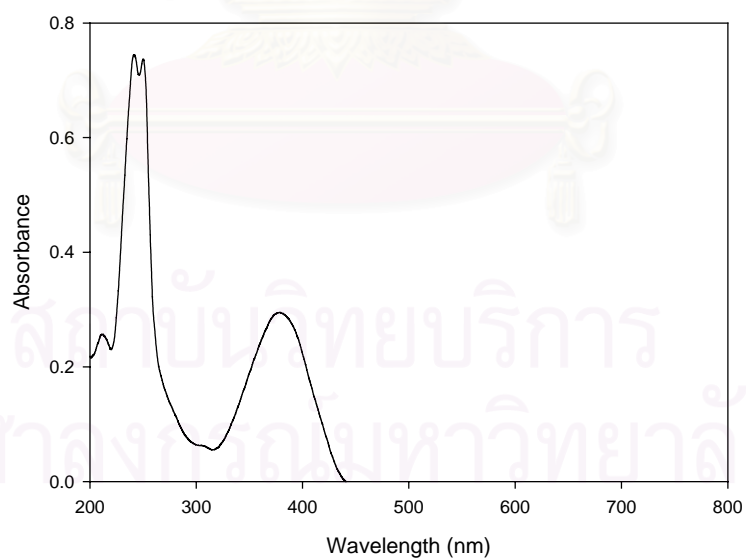


Figure B.1 The UV spectrum of anhydrobarakol (BA) in ethanol

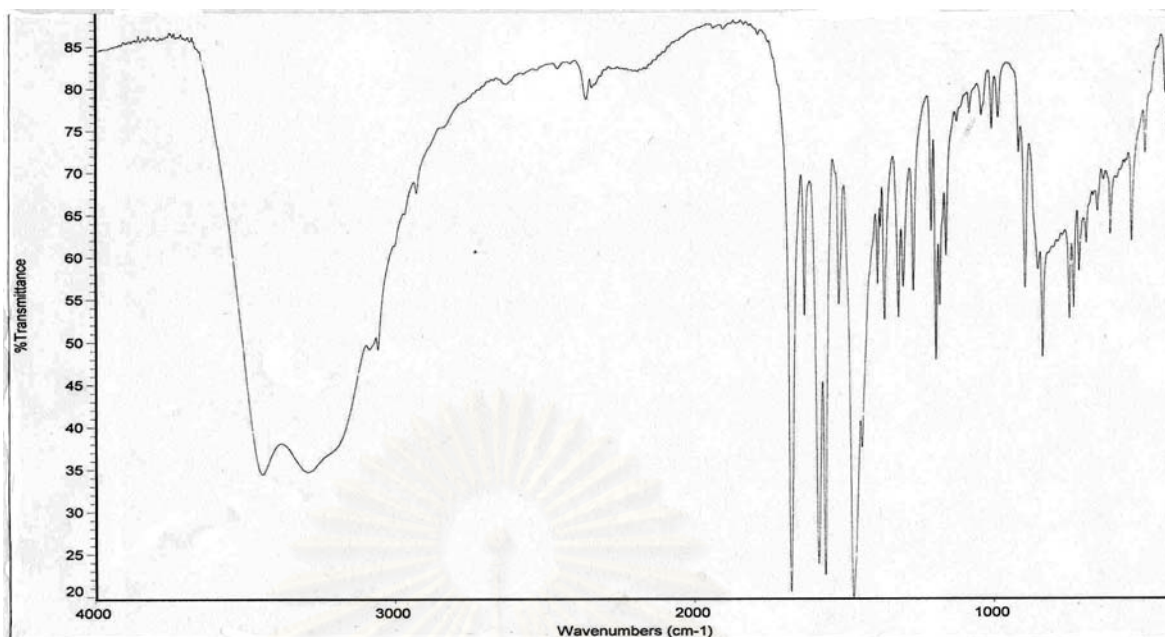


Figure B.2 The IR spectrum of anhydrobarakol in KBr

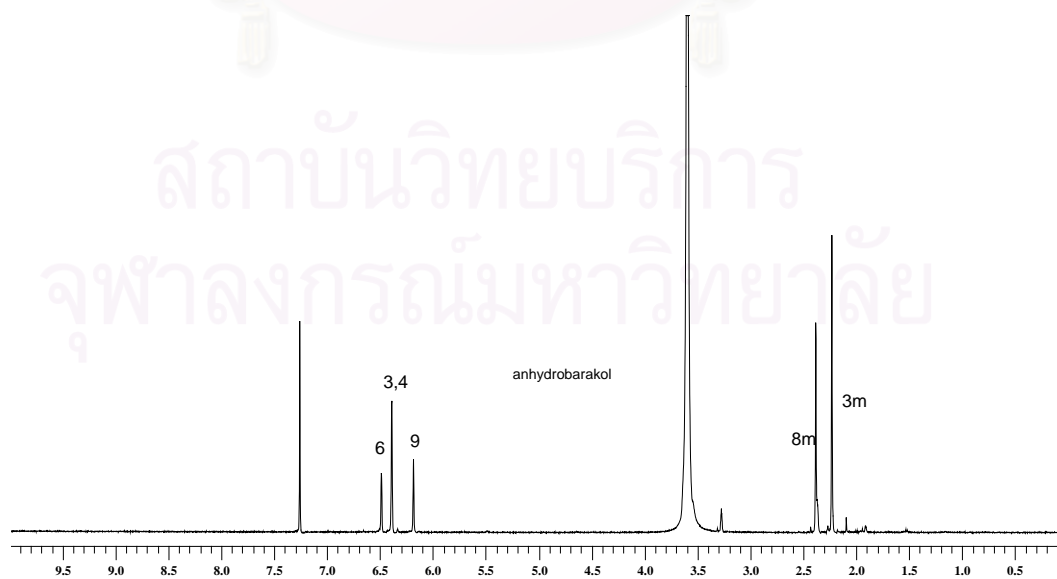


Figure B.3 The  $^1\text{H}$ -NMR spectrum of anhydrobarakol in  $\text{CDCl}_3 + \text{CDCl}_3$

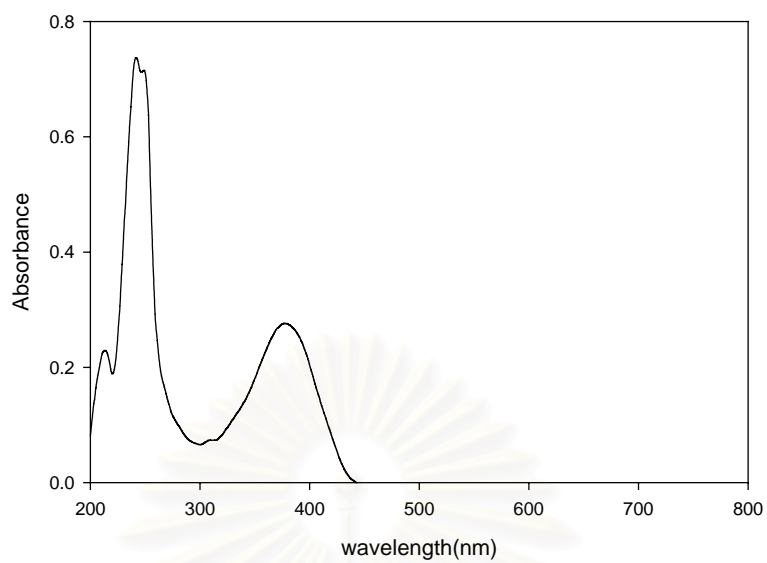


Figure C.1 The UV spectrum of anhydrobarakol hydrochloride (BC) in ethanol

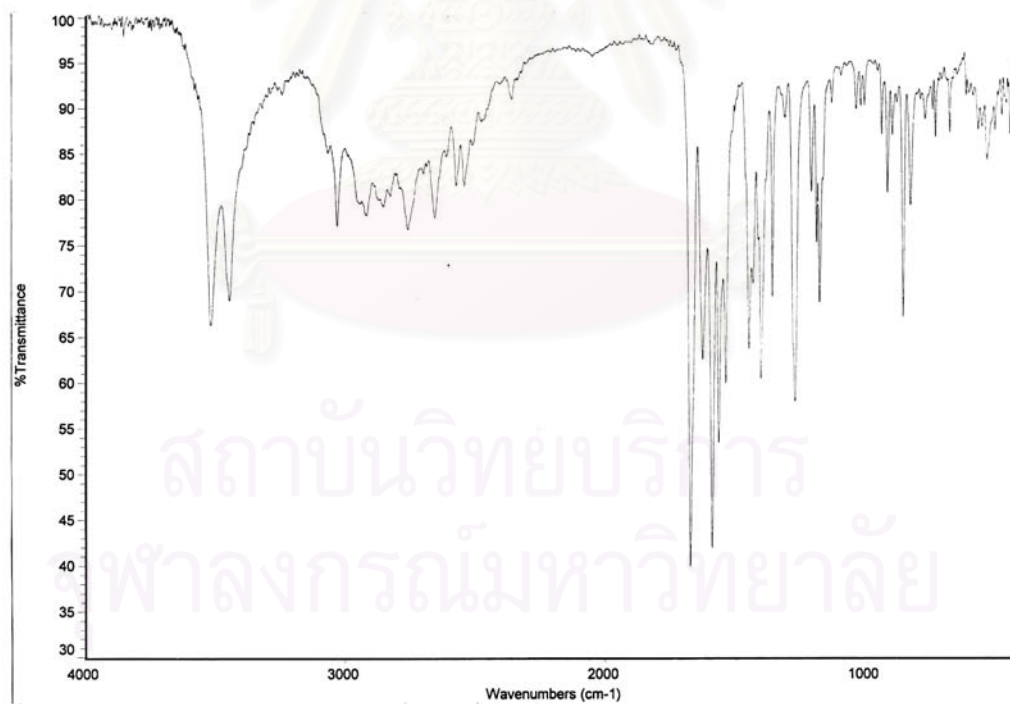


Figure C.2 The IR spectrum of anhydrobarakol hydrochloride in KBr

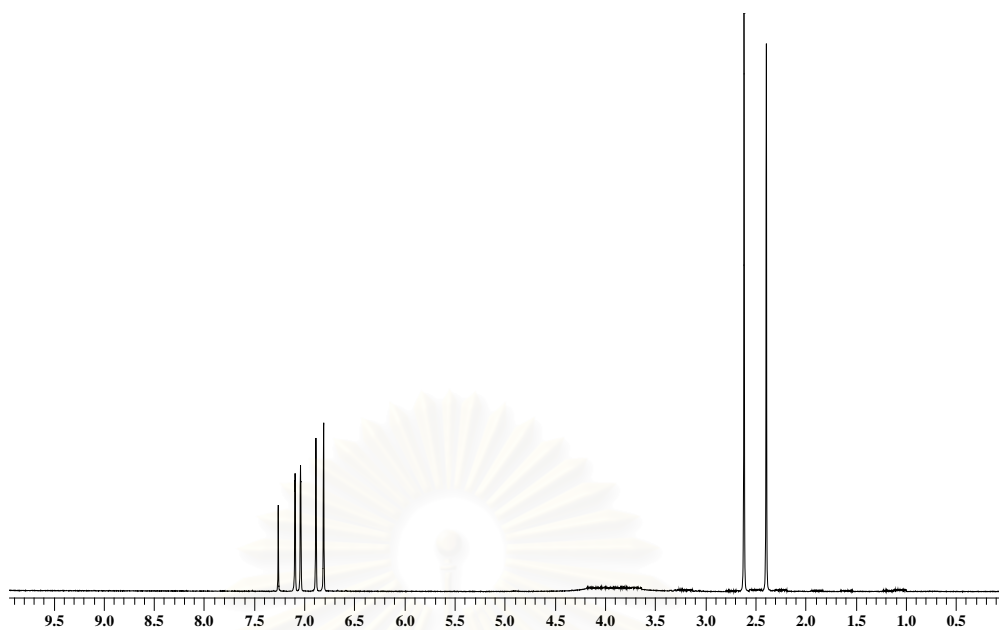


Figure C.3 The  $^1\text{H}$ -NMR spectrum of anhydrobarakol hydrochloride in  $\text{CDCl}_3$

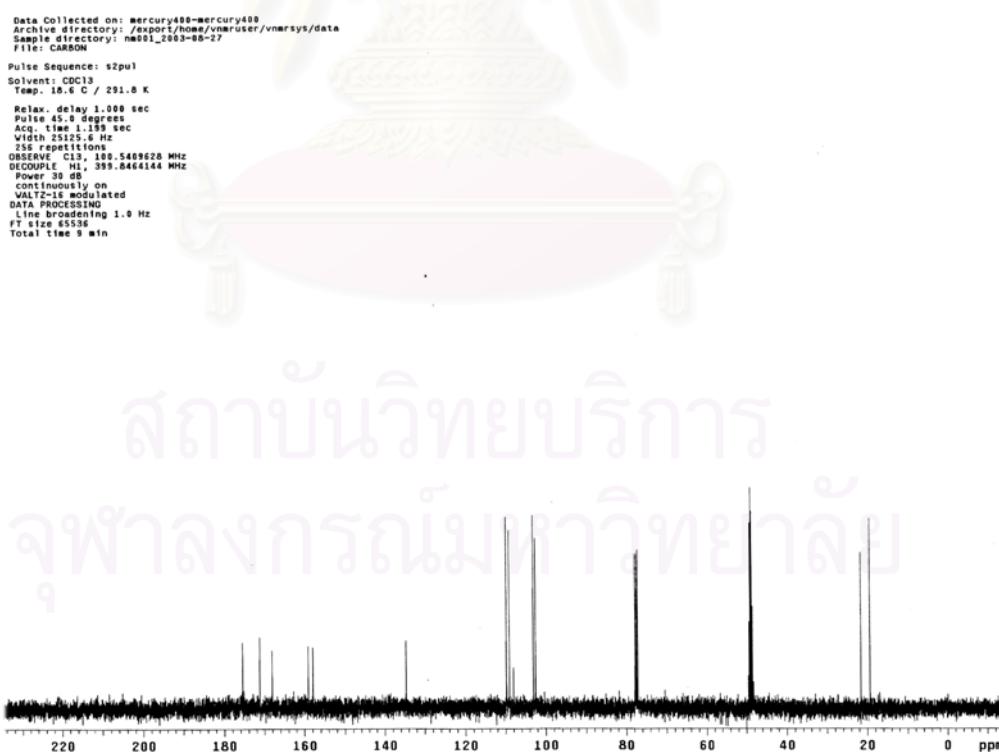


Figure C.4 The  $^{13}\text{C}$ -NMR of barakol hydrochloride in  $\text{CDCl}_3$

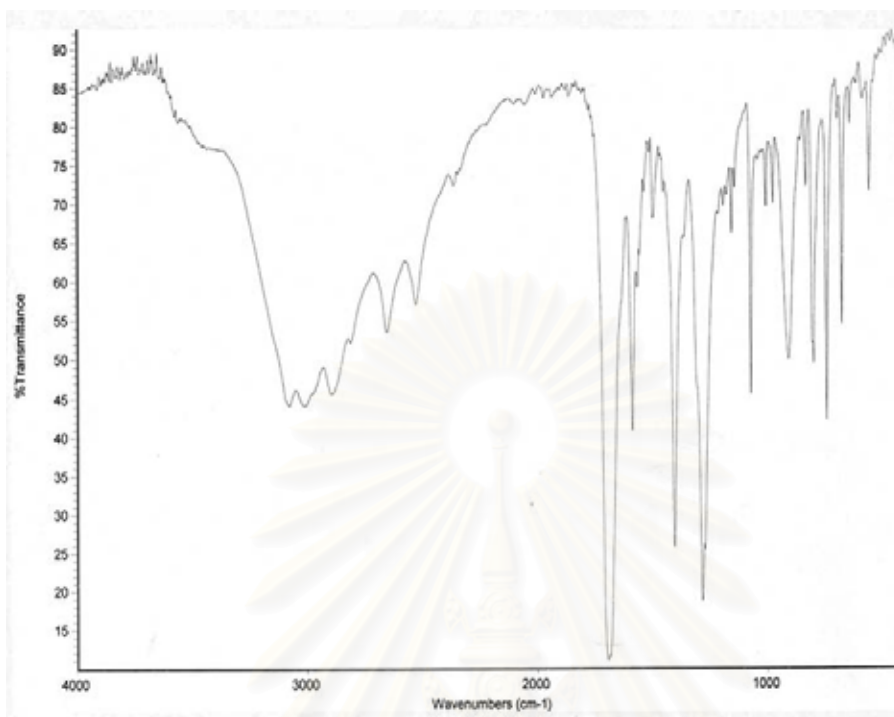


Figure D.1 The IR spectrum of barakol-phthalic acid (BP) in KBr

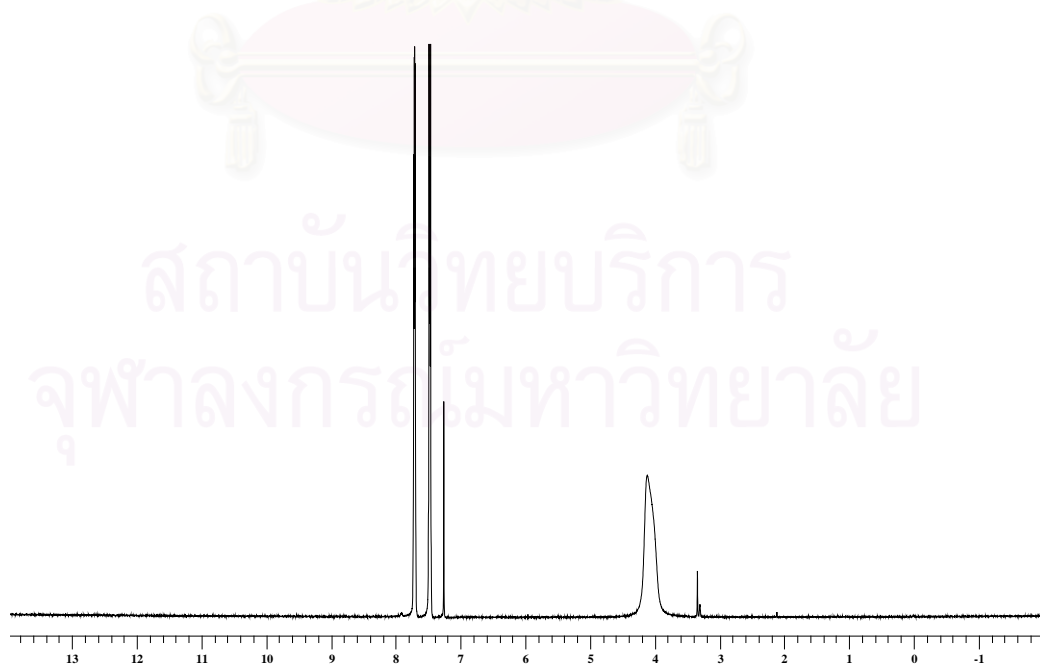


Figure D.2 The  $^1\text{H}$ -NMR spectrum of phthalic acid in  $\text{CDCl}_3 + \text{CDCl}_3$

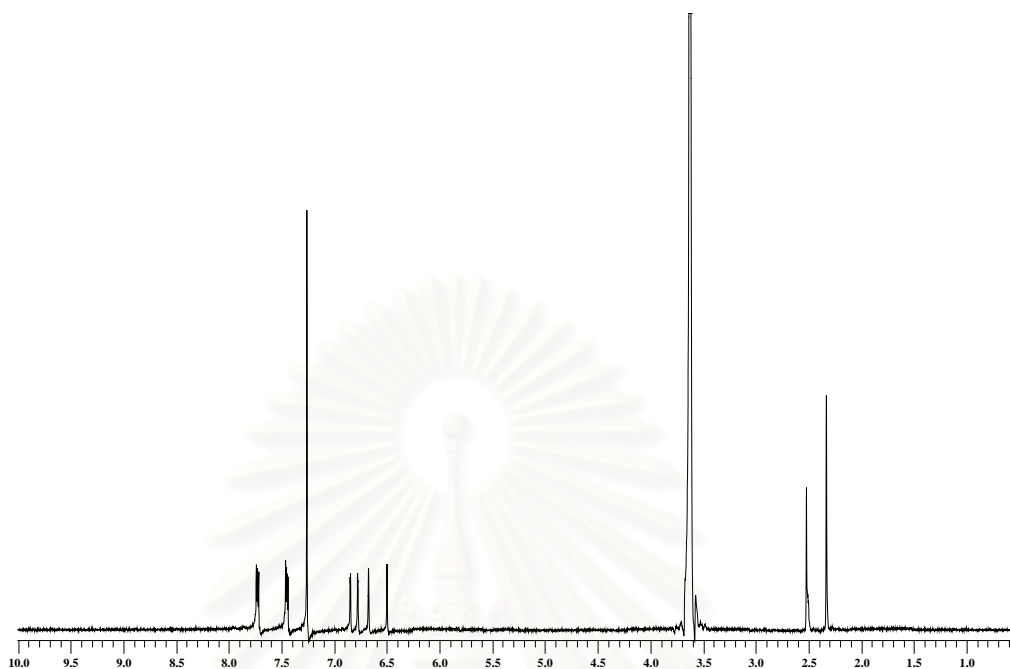


Figure D.3 The  $^1\text{H-NMR}$  spectrum of barakol-phthalic acid (BP) in  $\text{CDCl}_3+\text{CDCl}_3$

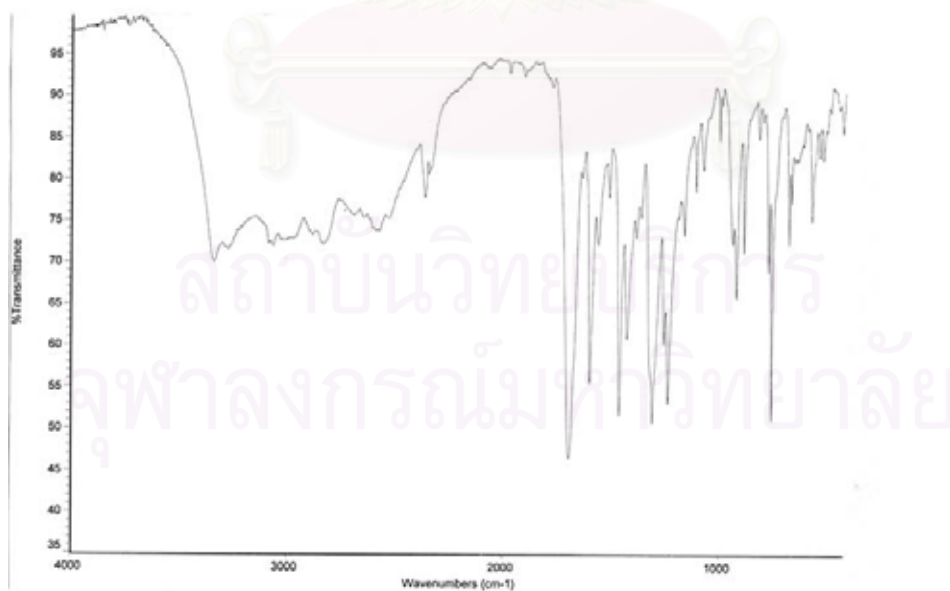


Figure E.1 The IR spectrum of barakol-3-hydroxybenzoic acid (BH) in KBr



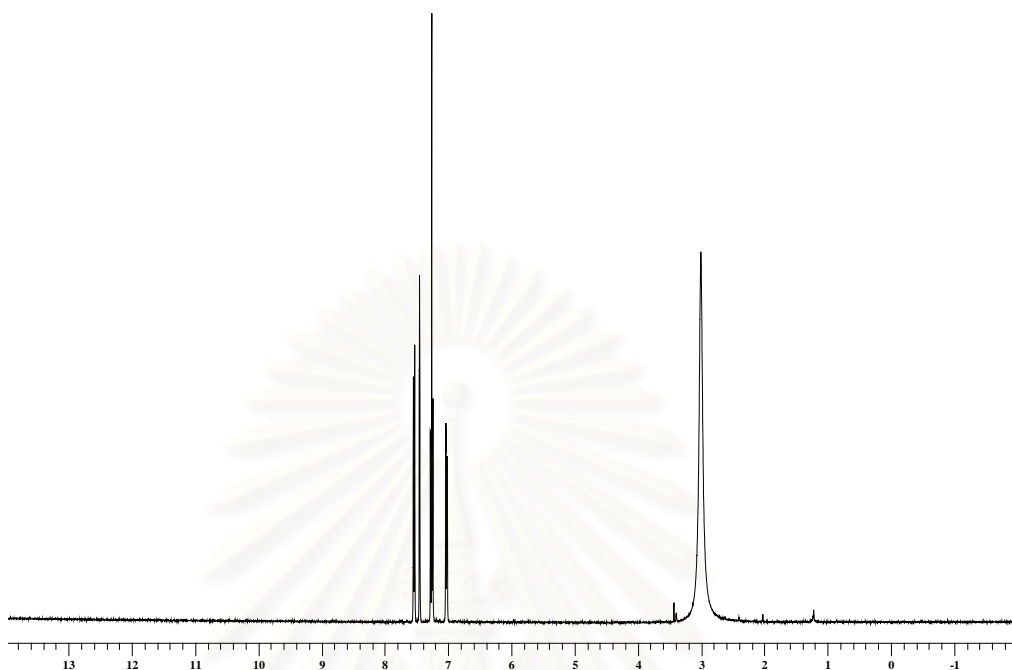


Figure E.2 The  $^1\text{H-NMR}$  spectrum of 3-hydroxybenzoic acid in  $\text{CDCl}_3+\text{CDCl}_3$

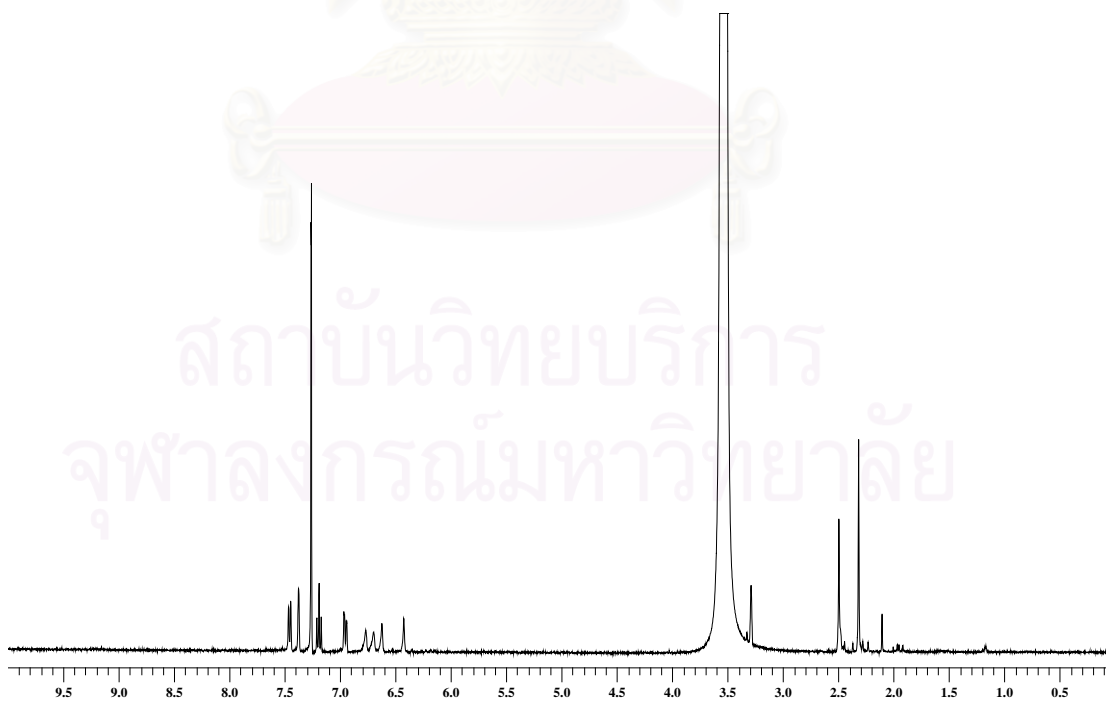


Figure E.3 The  $^1\text{H-NMR}$  spectrum of barakol-3-hydroxybenzoic acid (BH) in  $\text{CDCl}_3+\text{CDCl}_3$

## VITA

Miss Pitiporn Chimsook was born on March 18, 1979 in Nakornsawan. Her address is 125 Saengsawannuea Road, Chumsaeng, Nakornsawan, Thailand, 60120. She received a Bachelor's Degree of Science, from Department of Chemistry, Chiangmai University, Chiangmai, in 2001. In the same year she was admitted to the Master's Degree program, Department of Chemistry, Faculty of Science, Chulalongkorn University Bangkok



สถาบันวิทยบริการ  
จุฬาลงกรณ์มหาวิทยาลัย